6-1-2014

Towards the characterization of a novel thermohalophilic antioxidant Thioredoxin from the metagenome of the Red Sea; LCL of Atlantis II Brine pool

Mohamed Mohamed Gamal Abdelwahed

The American University in Cairo
School of Sciences and Engineering

Towards the Characterization of a Novel Thermohalophilic Antioxidant Thioredoxin from the Metagenome of the Red Sea; LCL of Atlantis II Brine Pool

A Thesis Submitted to
The Biotechnology Graduate Program

May 2014

in partial fulfillment of the requirements for
the degree of Master of Science

By
Mohamed M. Gamal Abdel-Wahed

Under the supervision of

Professor Hamza Dorry (Advisor)
Associate Professor Ahmed Sayed (Co-Advisor)

The American University in Cairo

Towards the Characterization of a Novel Thermohalophilic Antioxidant Thioredoxin from the Metagenome of the Red Sea; LCL of Atlantis II Brine Pool

A Thesis Submitted by

Mohamed M. Gamal Abdel-Wahed

To the Biotechnology Graduate Program

May 2014

In partial fulfillment of the requirements for
The degree of Master of Science
Has been approved by

Thesis Committee Supervisor/Chair
_____

Affiliation
_____

Thesis Committee Reader/Examiner
_____

Affiliation
_____

Thesis Committee Reader/Examiner
_____

Affiliation
_____

Thesis Committee Reader/External Examiner
_____

Affiliation
_____

_____ _____ _____ _____

Dept. Chair/Director Date Dean Date

DEDICATION

To my great father; Prof. Mohamed Gamal Abdel-Wahed, source of endless support in my life.

To the soul of my mother; Prof. Fatma Hanafy, whom never left my heart.

My wonderful sisters; Reem and Maryam.

Last and not the least my small family;

My beloved wife; Abeer, whom believe in me all the time; this work is because of you.

To my lovely kids Marwan & Salma; my smile makers in this life, I adore you and I will do my best ever to be proud of your father.

Thanks for all of you.

ACKNOWLEDGEMENTS

I would like to acknowledge ***Dr. Hamza El Dorry; my advisor*** for his supervision and guidance as well as his great efforts in the classes.

Dr. Ahmed Sayed; my co-advisor for his endless support along the research project, his great laboratory guidance, his continuous motivation and his extraordinary support during Biochemistry classes.

Dr. Rania Siam, for her efforts in the Biology department at AUC and accepting me in the Biotechnology program during the early interviews in July 2011.

Dr. Ahmed Mustafa, for his efforts in the M.Sc. Biotechnology Graduate Program and being always a helpful person and very supportive Prof. during our courses.

Dr.Asmaa Amleh, for her efforts during courses and allowing me to do the tissue culture part at her laboratory.

Special thanks to my dear colleagues; ***Mr. Amgad Ouf, Mr. Ahmed Samir, Mr. Mustafa Adel, Mrs. Laila Ziko, and Mrs Salma Shafie*** for their support and efforts to help me achieving this work.

Much gratitude for ***Alfi Foundation*** for financing my studies at AUC.

Many thanks to ***KAUST*** Red Sea spring 2010 expedition for samples collection.

Finally, I would like to thank the whole **Biology department and Biotechnology program** "Really, you have taught me a lot; ***Dr. Ahmed Sayed, Dr. Ahmed Moustafa, Dr. Asma Amleh, Dr. Hamza El- Dorry, Dr. Rania Siam and Dr. Walid Fouad***."

ABSTRACT

Due to the crucial antioxidant role of Thioredoxin (Trx) system in various vital cellular processes; DNA synthesis, oxidative stress defense, protein folding, apoptosis and cell growth, this fundamental system is widely expressed in mostly all life's kingdoms. Thus using metagenomic approaches to characterize novel Trx system in unexplored harsh environment will open the window for understanding the evolution of Trx system and its unique adaptation in extreme habitations. One of the unexplored unique ecosystems is the Red Sea's Atalntis II brine pool, specifically, the lower convective layer (LCL). The exceptional harsh conditions of the LCL; anoxic condition, high temperature around 70°C, high salinity (26%), and high metal content, have a significant contribution for being a unique infrequent ecosystem.

The objective of this study is to characterize a novel Trx isolated from the LCL. Successfully, in the experimental part, Trx was expressed in *E. coli* and purified, where the purified Trx has shown a clear antioxidant activity with a unique thermohalophilicity.

In conclusion, we have characterized a unique antioxidant Trx protein.

TABLE OF CONTENTS

LIST OF TABLES

LIST OF FIGURES

LIST OF ABBREVIATIONS

ATII	Atlantis II
BAC	Bacterial Artificial Chromosome
BLAST	Basic Local Alignment Search Tool
Cys	Cysteine
DTNB	5,5'-DiThio-bis(2-NitroBenzoic acid)
DTT	Dithiothreitol
DNA	Deoxyribonucleic Acid
EDTA	Ethylenediaminetetraacetic acid
E.coli	*Escherichia coli*
Glu	Glutamic acid
HepG2	Hepatic cellular carcinoma cell line
IPTG	Isopropyl-beta-D-thiogalactoside
KAUST	King Abdallah University for Sciences and Technology
LB	Luria-Bertani
LCL	Lower Convective Layer
MTT	[3-(4,5-dimethylthiazol-2-yl)-2,5-diphenyltetrazolium bromide]
NaCl	Sodium Chloride
NADPH	Nicotinamide adenine dinucleotide phosphate co-enzyme
NCBI	National Center of Biotechnology Information
Ni	Nickel
NGS	Next-Generation Sequencing
PCR	Polymerase Chain Reaction
Psu	Practical Salinity Unit
RNA	Ribonucleic Acid
SDS	Sodium Dodecyl Sulfate
Trx	Thioredoxin
TrxATII	Atlantis II Thioredoxin
TrxR	Thioredoxin Reductase
TrxRATII	Atlantis II Thioredoxin Reductase
UCL	Upper Convective Layer
Val	Valine
X-gal	5-bromo-4-chloro-indolyl-β-D-galactopyranoside

Chapter 1: Literature Review

1. Red Sea; The Unique Ecosystem

The Red Sea has different names in different languages; Al Baḥr Al Aḥmar in Arabic, Mare Rubrum in Latin (which means Arabian Gulf or Sinus Arabicus), while in the Greek language known as Erythra Thalassa. Interestingly, the Red Sea has got its name from the changes in color observed in its waters. Typically, the Red Sea has an intense blue-green color; however, it is inhabited by extensive blooms of sea sawdust (*Trichodesmium erythraeum* algae) at the sea surface that upon dying off, turn the color of the sea to a reddish brown color[6]**.** The Red Sea was formed about 5 million years ago due to the split of the African and Arabian plates. It is located between the Asian and African continent, where it is bordered by eight countries; Kingdom of Saudi Arabia, Egypt, Sudan, Jordan, Yemen, Eritrea, Djibouti and Israel as shown in **Figure 1**.

Adopted from http://www.coral-reef-info.com/red-sea-coral-reefs

Figure 1: Map of the Red Sea

The Red Sea is located between the Asian and African continent, where it is bordered by eight countries; Kingdom of Saudi Arabia, Egypt, Sudan, Jordan, Yemen, Eritrea, Djibouti and Israel.

Basically, the Red Sea is a narrow strip of water that extends from Egypt at the southeast for about 2,000 km towards the Bab el-Mandeb Strait that joins with the Gulf of Aden and thereafter with the Arabian Sea. From the geological point of view, the Red Sea separates the coasts of Sudan, Egypt and Eritrea at the west, while the coasts of Saudi Arabia and Yemen at the east [6] .

1.1 Red Sea Oceanography

The surface area of the Red Sea is about 440,000 km^2 with maximum depth of 2.2 km and 2250 km long. The temperature at the surface of the Red Sea is ranging from 28 °C to 34 °C, that's why the Red Sea is considered as one of the warmest seas worldwide. In addition, the Red Sea is characterized by its high salinity, where it is one of the most saltiest water bodies worldwide [6]. Actually, there are three main reasons for being dense and of high salinity; Firstly, the high evaporation rate (net evaporation rate 1.4 – 2 m yr^{-1}) that is coupled with the high temperature of the water's surface. Secondly, absence of substantial rivers that can drain into the Red Sea. Finally, the significant low rainfall rate (about 2.36 inch annually).[7]

1.2 Deep Oceanic Basin

The Red Sea is characterized by having a deep oceanic basin. This deep basin comprises about twenty five brine pools [8], where sequestered hot brines occupy these brine pools. Brine pools can be defined as large isolated depressions filled with water at the seafloor. The impression of a pool down at the seafloor results from the high salinity of the hot brine existing there, leading to a denser environment rather than the neighboring water, showing poor capacity to blend together. And that is why brine pools could be known as submarine lakes. [9]

Basically, the environment at the Red Sea's bottom is exceptionally unique and harsh in terms of oxygen depletion, high salinity, enormously high temperature, and heavy metal enrichment. However, there are significant differences between

the characteristics of the brine pools of the Red Sea. General speaking, the hottest and saltiest brine pools are usually in deep nearby the seafloor [9]. Furthermore, it is believed that the high temperature of the brine pools of the Red Sea is originated from the earth's tectonic activity, where this activity tends to create cracks and fractures at the seafloor sediment, and in turn the deep sea water penetrates these fissures as shown in **Figure 2**. As a result, the penetrated water got heated by the effect of submarine magma and starts to absorb minerals. Finally, the convective currents returns back the heated water to the seabed surface, forming a distinguishing layer of brine, owing to its high density. Stereotypically, the sediments of the brine pools are metal rich; sulfides of iron, copper and zinc, in addition to high value metals as gold, cobalt and silver. [9, 10]

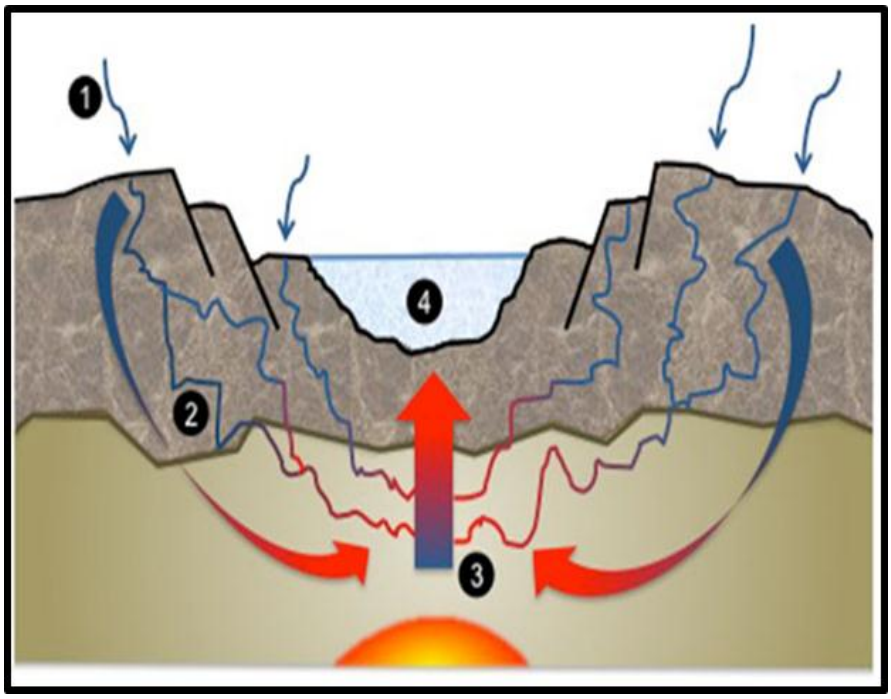

Adopted from http://krse.kaust.edu.sa/spring-2010/research.html

Figure 2: Tectonic Activity and formation of brine pools

(1) The confined tectonic activities (2) lead to the formation of fissures, which in turn allows the penetration of deep-sea water forming brine pools. (3) The submarine magma heats the deep sea water (4) and thus, allows the absorbance of minerals that returned back to the seabed sediment by the action of convective currents [9,10].

2. Atlantis II Deep brine pool

There are twenty five diverse brine pools existing at the bottom of the Red Sea [8]; Atlantis II Deep, Discovery Deep, Chain Deep, Valdivia Deep, Kebrit and other brine pools. Each brine pool has its own characteristics in terms of salinity, temperature and metal enrichment. In 1965, the first two hydrothermal sites within the oceans to be discovered were the Atlantis II Deep and Discovery Deep in the Red Sea, where they are located at 21°20‘N between 2000 and 2250 m depth, additionally, the surface area of Atlantis II Deep and Discovery Deep are about 6 x 13 Km and 4 x 3 Km respectively [11] (**Figure 3**).

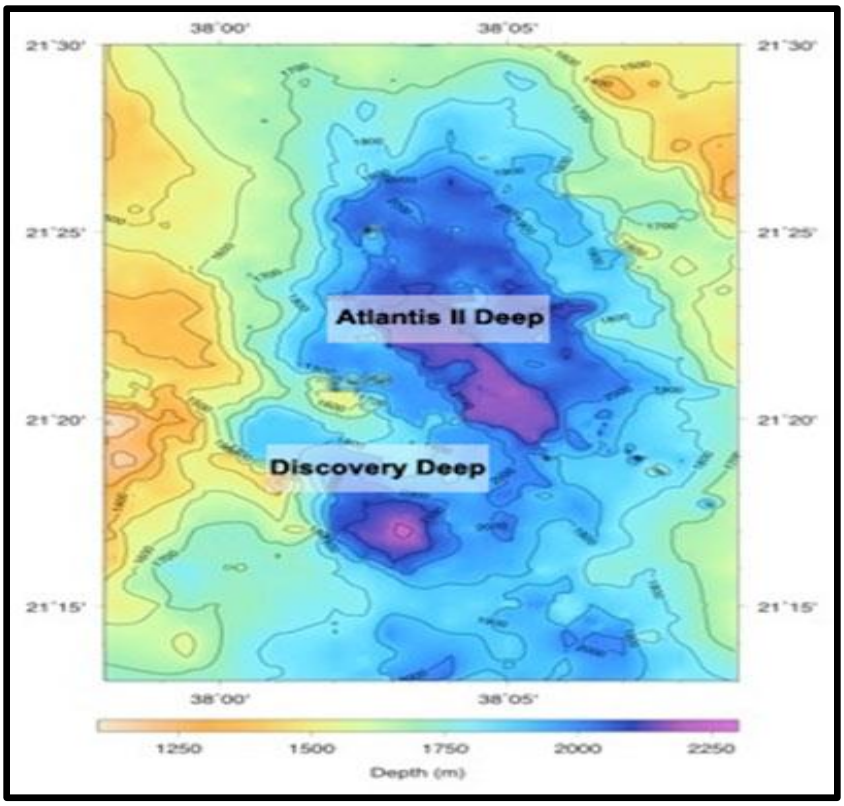

Adopted from http://krse.kaust.edu.sa/spring-2010/research.html

Figure 3: Atlantis II Deep and Discovery Deep brine pools in the Red Sea

The Red Sea map is showing the location of the Atlantis II deep, which is the largest brine pool in the Red Sea till current, and Discovery deep. Basically, both brine pools are located at 21°20‘N between 2000 and 2250 m depth. The bottom color legend is showing the depth of each brine pool in meters[11].

During that time the recorded temperatures were 56°C for Atlantis II Deep and 45°C for Discovery Deep brine pool [11]. Interestingly, from November 1966 to February 1969, the measured temperatures for the uniform vertical layers of the Atlantis II brine pool have showed an obvious increasing pattern, where the temperature of the lower convective layer had increased by 2.7 °C, while the upper convective layer had increased by 5.6 °C [12]. Consequent measurements for the Atlantis II brine pool have demonstrated a continuous increase in temperatures, where in 1997 have reached 67.1 °C and by October 2008 have reached almost 70 °C as per KAUST (King Abdullah University for Science and Technology) Red Sea expedition in fall 2008. [9, 11] That is to say, the temperature of the Atlantis II Deep has increased 14 °C within 43 years, with an approximate rate of 0.3 °C increment per year [11]. **Table 1** is showing temperatures and salinity for different layers of Atlantis II Deep and Discovery Deep.

Table 1: Different parameters for Atlantis II and Discovery Deep brine pools measured in 2008 [11].

	Atlantis II Deep			Discovery Deep	
	Temperature (°C)	Salinity (psu)	Interface depth (m)	Temperature (°C)	Interface depth (m)
LCL	68.28	252	2048	44.99	2059
UCL1	57.32	162	2027		
UCL2	51.25	118	2013		
UCL3	47.98	99	2006		
UCL4	43.53	87	2002		

From the above table, it is clear that, by going down from the water surface to the seabed, the layers of the Atlantis II brine pool are settled as follow: firstly, the upper convective layer (UCL), which is composed of four layers; UCL1, UCL2, UCL3 and UCL4, where UCL4 is at depth of 2002 m while UCL1 is at 2027 m. Secondly, the middle convective layer and finally, the lower convective layer (LCL) at the maximum depth of 2,048 m. Both temperature and salinity increase by going deeper across the layers of the Atlantis II Deep to reach its maximum at the LCL, where temperature is about 68.28 °C and salinity 252 practical salinity unit (psu). On the other hand, the Discovery Deep brine pool is at depth of 2059 m, while its temperature is only 44.99 °C [11]

Practical speaking, Atlantis II brine pool is considered as the biggest brine pool existing in the Red Sea, where its surface area is represented by about 60 km^2. The unique harsh circumstances of the Atlantis II Deep make this environment amongst the most infrequent environments existing on Earth [7]. The Atlantis II brine pool is located at the depth of 2,190 m and segmented into numerous vertical convective layers. Both temperature and salinity increase by going deeper across the layers of the Atlantis II Deep. By going down from the water surface to the seabed, the layers of the Atlantis II brine pool are settled as follow: firstly, the upper convective layer (UCL), which is composed of four layers; UCL1, UCL2, UCL3 and UCL4, where UCL4 is at depth of 2002 m while UCL1 is at 2027 m. Secondly, the middle convective layer and finally, the lower convective layer (LCL) at the maximum depth of 2,190 m [11].

In our study, we are much interested in the lowest layer of the Atlantis II brine pool. The environment of the LCL has unusual blend of tough conditions; extremely high temperature that reaches 68.2°C, salinity of about 26%, which is 7.5 folds more than that of other seas and its pH value is 5.3 [5, 10]. Furthermore, the LCL of Atlantis II Deep is almost oxygen depleted environment (anoxic) and highly enriched with sulfides of iron, zinc, copper and other heavy metals, in addition to high value metals as silver, cobalt and gold [9, 10, 11]. That is why; it is very attractive spot to understand the structural and functional modifications of enzymes and proteins that have been adapted in sake of survival of the microbial communities in these harsh abiotic conditions, in addition to the expectation to discover novel genes, proteins and metabolic pathways that can be conveniently applied in the industry of biotechnology or pharmaceuticals. In this study, we have characterized TrxATII in the LCL.

3. Thioredoxin System

Due to the crucial antioxidant role of thioredoxin system in various vital cellular processes; DNA synthesis, oxidative stress defense, protein folding, apoptosis and cell growth, this fundamental system is widely expressed in mostly all life's kingdoms from Archebacteria to higher eukaryotes [1]. Basically, Thioredoxin system is comprised of three main key players; thioredoxin protein (Trx), thioredoxin reductase enzyme (TrxR) and Nicotinamide adenine dinucleotide phosphate co-enzyme (NADPH) as shown in **Figure 4**. In this antioxidant system, the role of TrxR is to reduce the oxidized inactive state of Trx (comprising a di-sulphide (S-S) bridge) into the reduced active form (comprising thiol (SH) groups) through migration of electrons from NADPH to Trx via TrxR. In turn, the reduced active Trx can maintain the reduced states of different cellular proteins against oxidative stress initiated by different molecules as nitric oxide and hydrogen peroxide [2]. Furthermore, Thioredoxin system is an essential source of hydrogen for numerous reducing enzymes as sulphate reductase, ribonucleotide reductase and sulphoxide reductase [3].

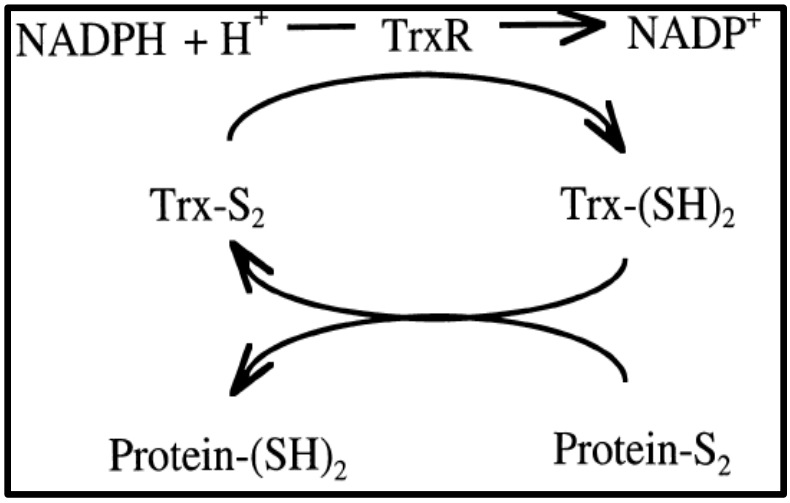

Adopted from Physiological functions of thioredoxin and thioredoxin reductase, S. J. Arner and A. Holmgren, Eur. J. Biochem. 267, 6102-6109 (2000)

Figure 4: Thioredoxin system

The schematic figure illustrates the reduction of the disulfide inactive oxidized form of thioredoxin (Trx-S2), to the active dithiol reduced form of thioredoxin (Trx-(SH) 2), by the action of both thioredoxin reductase (TrxR) and NADPH. Subsequently, Trx-(SH)2 reduces other oxidized disulfides protein, yielding Trx-S2. Moreover, TrxR may have other substrates rather than the homologous Trx to reduce.[2, 3]

3.1 Thioredoxin; The redox protein

Thioredoxin (Trx) is a small monomeric redox protein; about 12,000 Dalton. Trx protein is widely expressed among most species from Archebacteria to eukaryotes and humans [1]. The reason for being highly conserved among wide variety of prokaryotes and eukaryotes is the association of Trx in numerous vital cellular processes and functions, including and not limited to, DNA synthesis, oxidative stress defense, protein folding, apoptosis and cell growth [13]. As a redox protein, Trx reduce other intracellular and extracellular oxidized proteins comprising disulfide bridge through the exchange of cysteine thiol-disulfide bond, where the Trx itself get oxidized forming a disulphide (S-S) bridge as the Cysteine residue oxidized to Cystine residue as shown in **Figure 5**. Further on, the oxidized Trx get reduced again forming thiol (SH) groups by the action of TrxR at the expense of a molecule of NADPH [13].

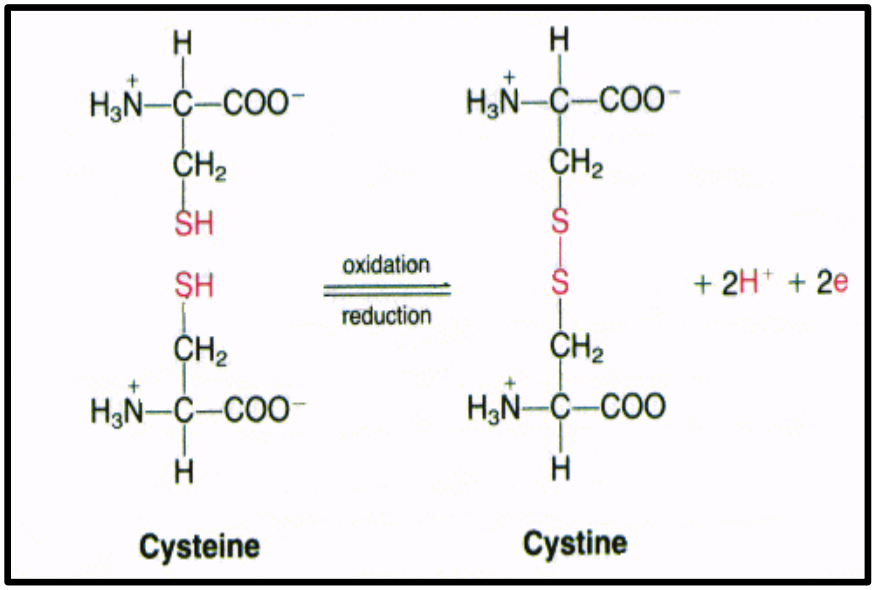

Adopted from http://www.cs.stedwards.edu/chem/Chemistry/CHEM43/CHEM43/Thioredox/FUNCTION.HTML

Figure 5: Disulfide Bridge Exchange

Thioredoxin (Trx) protein is characterized by having a catalytic active motif, which is denoted by two vicinal Cysteines that comprise in-between two other amino acids; Cysteine-Glycine-Proline-Cysteine (Cys-Gly-Pro-Cys). Upon reducing other oxidized proteins, Trx get oxidized, where two Cysteine residues are oxidized to Cystine forming a disulfide bridge through the exchange of cysteine thiol-disulfide bond. [14, 17]

In 1968, the sequence of amino acids of *Escherichia coli* Trx1 was determined[14]. Basically, on the level of amino acids, all thioredoxins are characterized by having a **Trx motif**, where this redox active catalytic motif is denoted by having two vicinal Cysteines and comprise in-between two other amino acids; Cysteine-Glycine-Proline-Cysteine (Cys-Gly-Pro-Cys)[14,15,16]. This active catalytic domain is located near the N-terminal side; C^{32} XX C^{35}. The conserved catalytic site CXXC used to undergo a reversible process of oxidation-reduction via the two vicinal Cysteines [17]**.** In addition to the conserved Trx motif, there is a number of amino acids that are highly conserved among the Trx sequence; Aspartate 26, Alanine 29, Tryptophan 31, Aspartate 61 and Glycine 92 [2] .

Despite of the various functions of thioredoxins (Trxs) - will be discussed in details in the following sections - , all thioredoxins from prokaryotes to eukaryotes display a high homology in sequence to the *E.coli* Trx 1, represented by 27 to 69% identity, which is the well characterized protein[15, 18]. Furthermore, thioredoxins are showing the same global three dimensional structure, where they comprised the same Trx fold. Basically, the Trx fold is composed of a fundamental core of five β-strands that are flanked by four α-helices as shown in **Figure 6** [19]. The Cys-Gly-Pro-Cys conserved domain is positioned on the surface of the Trx protein, exactly at the terminal of the β-strand and at the start of the long α-helix. Around the active catalytic site of Trx, there is a hydrophobic region, which has been proposed to be the central interaction site for other oxidized proteins to be reduced [18, 19]. Using the Nuclear Magnetic Resonance (NMR) spectroscopy, the Trx 3D structure for both forms of *E.coli* Trx; reduced and oxidized have been determined [20]. The overall difference between the two forms of Trx; reduced and oxidized remains elusive, where there is a local conformational change within and round the active disulfide site, in addition to more conformational states in the reduced form of Trx, which is reflected on the altered patterns of Hydrogen bonding[18, 20].

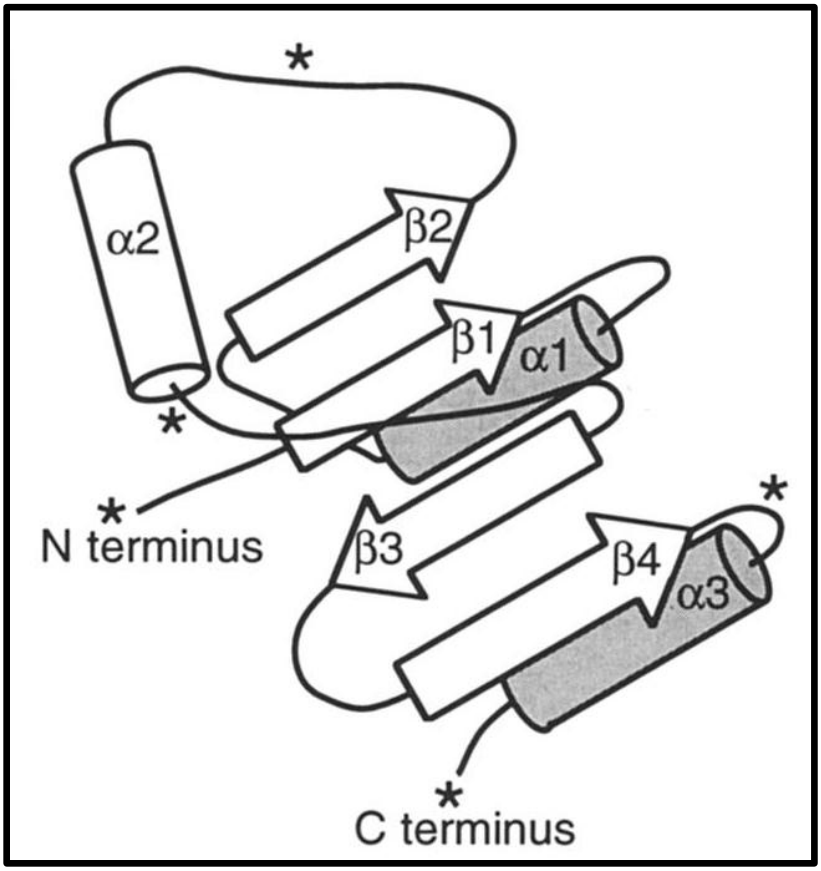

Adopted from Martin, J. Thioredoxin - a fold for all reasons. Structure, 3, 245-250 (1995).

Figure 6: Thioredoxin Fold

The position of the helices in relevance to the central -sheet is demonstrated. The α l and α 3 helices (grey colored), are located behindhand the sheet in this orientation. On the other hand, α 2 helix is located in front of the B-sheet. Moreover, the sites of insertions of other residues are signposted by asterisks [19]

3.2 Thioredoxin System; Prokaryotes versus Mammalians

The mammalian cells are characterized by having a cytosolic thioredoxin (Trx1), cytosolic thioredoxin reductase (TrxR), mitochondrial thioredoxin (Trx2), mitochondrial thioredoxin reductase (TrxR2), membrane bounded Trx, extracellularly Trx and extracellularly truncated Trx (Trx 80) [2] as shown in **Figure 7**.

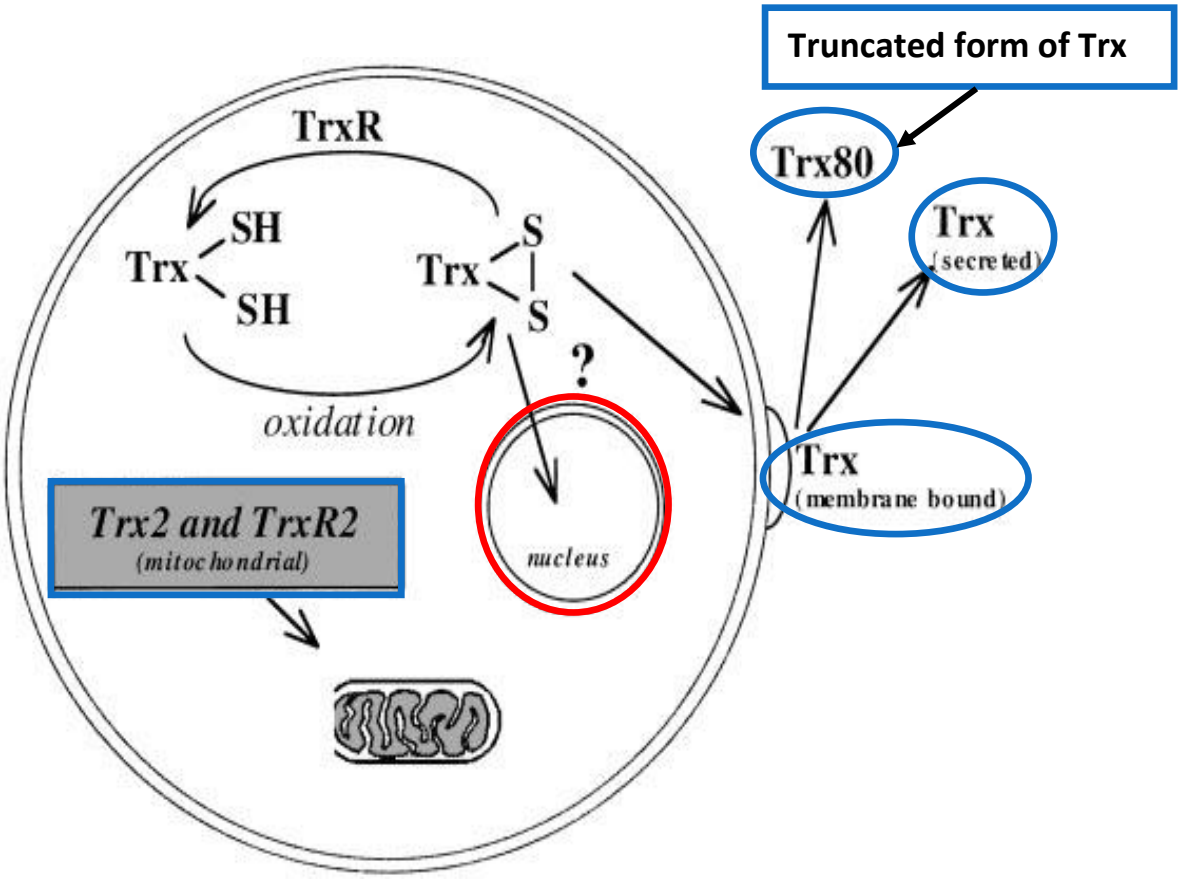

Modified from Arner, E. S. and Holmgren, A. Physiological functions of thioredoxin and thioredoxin reductase. Eur. J. Biochem. 267, 6102–6109 (2000).

Figure 7: Mammalian Thioredoxin System

This Schematic diagram localizes the presence of thioredoxin (Trx) and thioredoxin reductase (TrxR) within the mammalian various cellular compartments; nucleus, cytoplasm, membrane bounded and extra-cellularly as follow [2]:

1- Trx and TrxR within the cytoplasm.
2- Trx and its truncated form (Trx 80) are membrane bounded and extra-cellularly available as well.
3- Mitochondria (Trx2 and TrxR2)

By comparing the Trx system in prokaryotes to high orders eukaryotes, the most significant evolution is in the TrxR, which is a large selenocysteine-enzyme (**Figure 8**) with a broader substrate specificity that shows an obvious variance from those smaller TrxR existing in fungi and all bacteria, where the bacterial TrxR has narrow substrate specificity as it only reduces the bacterial Trx [21]

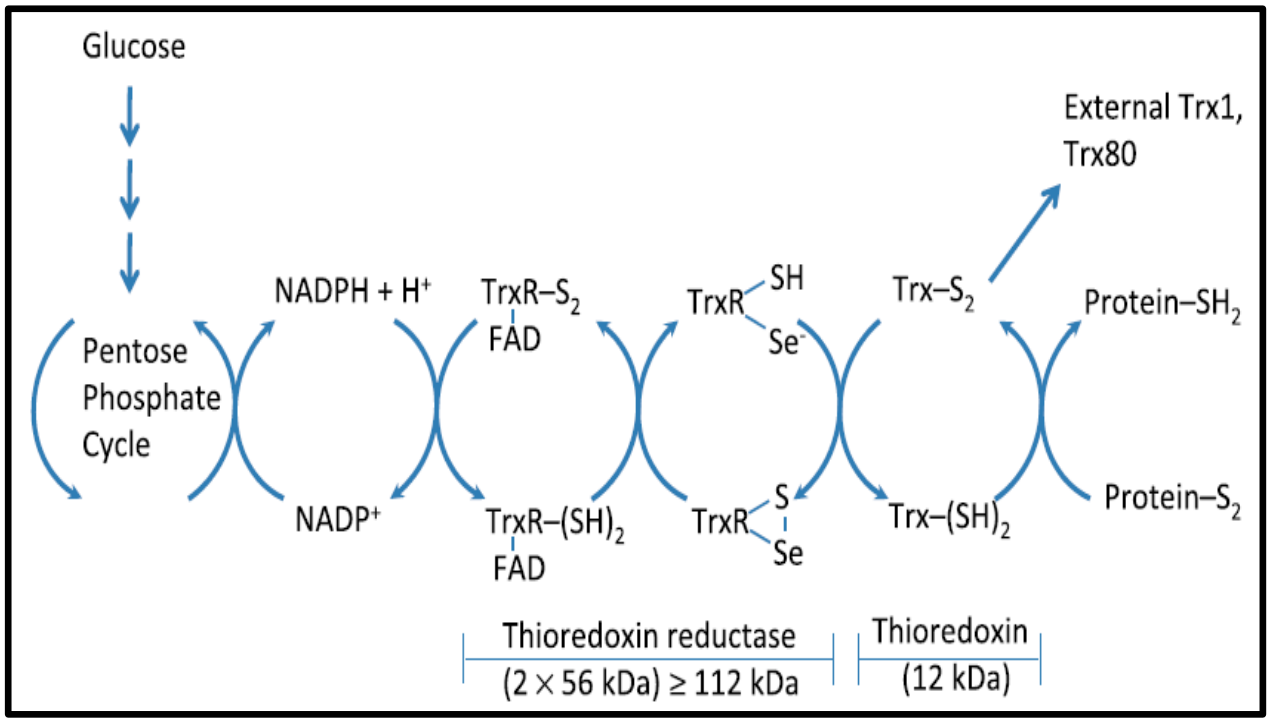

Adopted from Holmgren, A., Lu, J. Thioredoxin and thioredoxin reductase: Current research with special reference to human disease**.** A. Biochem. & Biophys. Res. Comm. 396, 120–124 (2010).

Figure 8: Mammalian Thioredoxin System

The mammalian thioredoxin redox system composed of thioredoxin (Trx), thioredoxin reductase (TrxR), and NADPH. The NADPH is the electron source in the Trx system, which is mainly generated from the pentose phosphate pathway. The oxidized (Trx-S2) is reduced by the TrxR (Seleno-enzyme) and NADPH. Finally, the reduced (Trx-(SH)2) reduces the disulfide bond in various proteins. Interestingly, under the oxidative stress conditions, the thioredoxin secreted into the plasma, where it can be truncated (Trx80) [21]

3.3 Redox mechanism of Thioredoxin

The Cysteine residue at the redox active site located at the N-terminal, where it is characterized by having a low pKa value, that is to say, it will act as the attacking nucleophile that will reduce the disulfides of other proteins. Basically, the oxidoreductase mechanism of Trx comprises two intermediates; a transitory disulfide intermediate as well as a fast thiol-disulfide exchange in a hydrophobic environment [18]. It is a reversible reaction, where Trx either broken or form disulfides based on the redox potential of the substrate. The Trx of *E. coli* (Trx1) is characterized by having a low redox potential (-270 mV), which in turn guarantees that the reduced form of Trx (Trx-(SH)**2**) is the main di-thiol reducing agent at the cytosol [3]. Interestingly, there is a big superfamily of proteins, which that comprise one or more domains of Trx. Those proteins with the Trx fold are existing in all organisms, where they can be clustered in six main classes; Glutathione peroxidases, Thioredoxins, Glutathione transferases, Glutaredoxins, Protein disulfide isomerase and bacterial disulfide oxidoreductase (DsbA) [19, 22]. Actually, the sequence homology among these classes is highly limited with almost no common activity, however, there is a common functional similarity among the following four classes: Protein disulfide isomerases, thioredoxins, DsbA and glutaredoxins, where all of them are redox proteins with active catalytic redox motif; -Cys-X1-X2-Cys- (where X1 and X2 are any non-Cysteine amino acids). Although, the glutathione peroxidases and glutathione transferases classes are missing the active catalytic redox motif, they have a specific interaction with glutathione. A recent addition to the Trx superfamily is the coined PICOT (protein kinase C-interacting cousin of thioredoxin) and the Nucleoredoxin. The coined PICOT which interacts with protein kinase C [23] is a larger cytosolic Trx like protein, which has unknown clear function [24, 25], while the Nucleoredoxin is a nuclear Trx like protein showing an oxido-reductase activity [26].

3.4 Role of Thioredoxin system in different organisms

As being fundamental antioxidant protein expressed in most kingdoms of life, Trx has been revealed in at least a dozen of different systems, which is evidence to its usefulness in nature. Basically, the common physiological function of Trx in most organisms is the essential conserved role as a high-capacity hydrogen donor system for other reductive enzymes in a magnitude faster than those for dithiothreitol (DTT) or glutathione (GSH) [3, 16], with high specified functions in phage T7 DNA replication and assembly of filamentous phage of Escherichia coli phages. Moreover, the identified role for Trx as a thiol redox controller in chloroplast photosynthesis has been also recognized recently in redox regulation of transcription factors and enzymes. Additionally, it was proven that Trx has vital defensive roles against apoptosis and inactivation or aggregation of cytosolic proteins during oxidative stress [2].

The following examples will show the different roles of Trx among most organisms of different life's kingdom; Trx participates in the DNA synthesis by acting as a hydrogen donor for ribonucleotide reductase [3], Trx keeps the intracellular protein disulfides in the reduced active forms [27, 28], additionally, Trx has a fundamental role in signaling pathways as well as defense against oxidative stress as being an electron donor for the thioredoxin peroxidases and peroxiredoxins that catalyze the reduction of Hydrogen peroxide [29]. More detailed examples for the different roles of Trx in numerous organisms are briefed in **Table 2**.

Table 2: Role of thioredoxin in various organisms

Organisms	Thioredoxin Role	Comments
All Organisms	Reduction of protein disulfides	Thioredoxin plays a vital role in reducing intracellular protein disulfides [14, 28]
	DNA synthesis	Thioredoxin is a high capacity hydrogen donor for ribonucleotide reductase [3]
Many Organisms	Reduction of methionine sulfoxide	Thioredoxin is a major hydrogen donor for methionine sulfoxide reductases [84, 85]
	Prevent oxidative stress	Thioredoxin reduce peroxiredoxins that catalyze H2O2 reduction and thus inhibit oxidative stress and apoptosis induction[29, 35, 86]
Bacteria and Yeast	Hydrogen donor for 3'-phosphoadenylsulfate (PAPS) reductase	Assimilation of sulfur by sulfate to sulfite reduction [87, 88]
E. coli Phages (M13, T7, f1)	Plays a vital role in filamentous phage assembly	Exclusively, thioredoxin is the merely host *E. coli* protein required for the assembly and export of phage [31, 89]
	Subunit of T7 DNA polymerase	Required for processivity [90]
Plant	Regulates the enzymatic photosynthesis of chloroplast	Photosynthesis is regulated by light thru ferredoxin [91]
Mammalia	Pregnancy	Synthesis of thioredoxin from cytotrophoblasts takes part in implantation and establishment of pregnancy [92, 93, 94]
	CNS	Thioredoxin secreted from glial cells promotes neuronal survival at ischemia reperfusion [95]
	Birth	Thioredoxin induction prevent hyperoxia at birth[96]
	Regulation of Apoptosis	Reduced thioredoxin makes a complex with ASK1and thereby prevents the downstream signaling for apoptosis [32]
	Redox regulation of transcription factors	Thioredoxin either activates or inhibits different transcription factors are either activated or inhibited by Trx [97]

3.4.1 Thioredoxin role in *E.coli* Phages

An extra function of Trx is to act as a structural component of other enzyme via complex formation. This is obviously recognized in T7 DNA polymerase, where reduced Trx-$(SH)_2$ binds with a highly affinity to the DNA polymerase forming a complex (1 : 1) offering the enzyme a high processivity [30]. Markedly, only the reduced Trx-$(SH)_2$ binds while the oxidized Trx-S_2 is unable to bind despite being closely related in their 3D structures. A comparable structural activity role is presumed for the Trx role in filamentous phage (M13, T7 and f1) assembly, although active site mutants were as efficient as Trx in its wild status, however, the last had to be reduced firstly by Trx reductase for effective functioning in phage assembly [31], and thus creating a significant similar situation as the interaction with T7 DNA polymerase.

3.4.2 Thioredoxin role in mammals

In the same way, the mammalian reduced form of Trx-$(SH)_2$, but not the oxidized form of Trx-S_2, forms an inhibitory complex with the apoptosis pathway; Apoptosis Signaling Kinase 1 (ASK1) [32]. Basically, the mammalian reduced Trx-$(SH)_2$ offers a redox regulation on apoptosis, where apoptosis inhibited under the reduced conditions of the intracellular Trx-$(SH)_2$, that is to say, at the oxidative stress conditions, where apoptosis is activated, the Trx is in the oxidized status. Additionally, this situation meets with the perception of the pivotal role of oxidative stress in inducing apoptosis.

Different transcription factors are regulated by the redox activity of Trx. Subsequently, this offers Trx a dominant role in the thiol redox regulation of critical cell functions by modulation of the expression of specific target genes as illustrated in the schematic diagram (**Figure 9**).

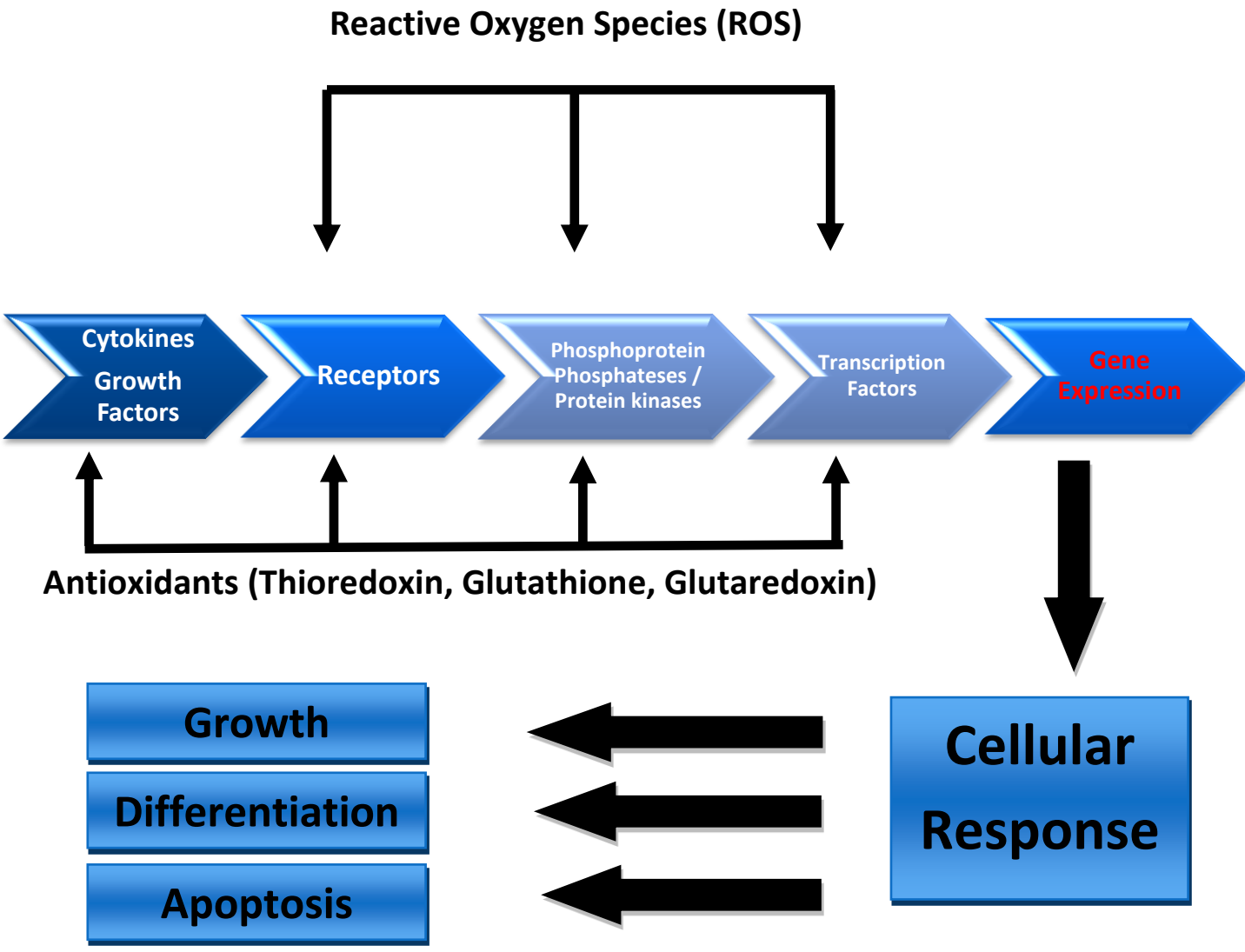

Figure 9: Oxido-reductase regulation of cellular systems

This Schematic diagram is showing the possible redox levels of regulation and their cellular response; growth, differentiation or apoptosis. The oxidoreductase activity is controlled by thioredoxin, glutathione or glutaredoxin systems and. The balance between oxidants and antioxidants control the functioning of proteins directly and regulate the gene expression indirectly[32].

For instance, Trx is crucial for the oxidoreductase regulation of the transcription factor NF-kB [33]; a transcription factor that regulates the expression of several inflammatory genes. Additionally, Trx has a wide-ranging intracellular antioxidant action, where its up-regulation defends against oxidative stress conditions [34]. Another general function for Trx in cell signaling is being an electron donor for the family of thioredoxin peroxiredoxins and peroxidases, where there are six members at least in mammalian cells that reduce oxidizing agents as Hydrogen peroxide [29]. Although both glutathione catalases and peroxidases could reduce Hydrogen peroxide, it was verified that the human thioredoxin peroxidases (human TPxII) when up regulated in cells, they have showed inhibitory effect on apoptosis induction via reducing levels of Hydrogen peroxide. In this manner, there is a thioredoxin regulatory step on apoptosis induction, which is upstream the apoptosis regulator proteins of the Bcl-2 family [35]. Until now, the mechanism of secretion of Trx from mammalian cells is unknown, as it is not depending on a signal peptide [36]. Moreover, the secreted human Trx was found to up regulate the IL-2 receptor with a demonstrated activity for the co-cytokine factor from the T-lymphocytes [37]. Surprisingly, it was recognized that this factor and human Trx are the same protein [38], and thereby it is now obviously clear the multi-tasks of the extracellular human Trx. The secretion of Trx under oxidative damage and inflammation conditions has been detected in both normal and neoplastic cells [36, 39]. From the clinical point of view, plasma levels of Trx are elevated in different cases of patients; rheumatoid arthritis [40], cardiopulmonary bypass operations [41] and in Human immunodeficiency infected cases (HIV/AIDS) [42]. Basically, extracellular Trx has various pro-inflammatory effects via induction of the cytokines release from both monocytes [43] and fibroblasts [40]. Additionally, one of the recent observed activities of Trx, is being a chemotactic protein, that is to say, it induces the migration of T-cells, monocytes and neutrophils with a comparable potency to the chemokines e.g. IL-8 [44]. Mutated residues at the Trx catalytic active motif, which is normally denoted by having two vicinal Cysteines and comprise in-between two other amino acids (Cys-XX-Cys) to Serines caused a loss in chemotactic activity, proposing an obvious demand for the oxidoreductase activity. Furthermore, as being a chemotactic protein, the concentration-dependent activity of Trx is a bell-shaped relationship similar to other chemotactic agents, with a maximum plasma concentration of 25 ng per ml. The

only difference between Trx and other chemokines in being G-protein-independent. Also it was found that Trx might inhibit the action of other chemokines [44]; thus if Trx levels are highly expressed in severe acute inflammations, this could inhibit the cell migration, leading to the increase of infection severity. Besides, the truncated Trx (Trx80), which is found at the surface of monocytes [45], is highly identical to Eosinophilic Cytotoxicity Enhancing Factor (ECEF), which augments the capability of eosinophils to kill the Schistosoma mansoni larvae [46, 47]. To wrap up, it is obviously clear that the mammalian Trx system is a key player that is highly associated with many human diseases as shown in **Figure 10**.

Adopted from Thioredoxin and thioredoxin reductase: Current research with special reference to human disease. A. Holmgren, J. Lu. Biochemical and Biophysical Research Communications 396, 120–124 (2010).

Figure 10: Mammalian thioredoxin system and human diseases

The mammalian Trx system is a key player that is highly associated with many human diseases; cancer, cardiovascular, diabetes, neurodegenerative diseases, virus infection, rheumatoid arthritis and others.

3.4.3 Thioredoxin role in Plants

Interestingly, plants are characterized by having their unique Trx system, where there is a linkage from light to reduction of other disulfide proteins through various chloroplast Trxs and ferrodoxin [48]. Trxs are implemented in a broad spectrum of crucial functions in plants; growth, flowering, photosynthesis and germination as well as development of seeds. Furthermore, plants have extraordinarily different types of Trxs, where they are composed of six well recognized types: Trxs f, Trx m, Trx x, Trx y, Trx h, and Trx o. Basically, each type is located in a different plant cell compartment, where they function in a cascade of processes. For the first time, in 2010 it was discovered that Trx proteins have the capability to move from one cell to another, representing an unusual form of communication between cells in plants.[49]

Furthermore, in plants, the seed is considered as the only tissue with a specific function for the Trx/NADH system. Actually, the wheat grain is rich in proteins comprising disulfide bonds. Glaidens and Glutaenin are the main storage proteins that interact with the Trx redox protein, where these proteins become more liable to proteolysis as a result of Trx reduction in addition to the redox regulation of disulfide inhibitor proteins. Thus, one of the major roles of Trx in plants, is being as an early signal in seed germination.[50]

4. Metagenomic; The Window for Unexplored Organisms

Microorganisms are constantly capturing the scientists' attention due to the fact of being the predominant components of the earth's biota, where they occupy various ecosystems and communities; sea and fresh water, soil, air, etc... with crucial functions, which make them in turn largely contribute to the diversity of genetic material of life [51, 52]. Basically, the genomes of the microorganisms were estimated to be double to triple the combined genomes of animals and plants [53]. Additionally, microorganisms are key players with huge influence on human and animals' health, where the number of microbial cells inhabiting the human body estimated to be about 100 trillion cells (10 folds the human being cells) [54]. Thus, this huge number of microbes inhabiting different

communities is capturing the interest of scientists to reveal their unexplored diversity that could lead to understanding and utilizing new metabolic pathways or novel proteins.

4.1 Metagenomics Approach

The classical way to study different microorganisms was based on the traditional lab culture; solid or liquid media. However, this approach did not succeed except for 1% of the microorganisms, which means losing 99% of them as a result of lacking simulation and mimics of their original environments [52, 55]. Fortunately, the metagenomic approaches have resolved the biased representation of the microorganisms via the direct isolation of the metagenomes from their environmental samples for further characterization via cloning vectors, construction of metagenomic libraries and then sequencing of the genome [52]. And based on that, the Metagenomics term refers to analyzing a variety of genomes isolated from environmental sample. Metagenomics term has different alternatives; environmental genomics, ecogenomics and community genomics [52].

After isolation and processing of the metagenome from its environmental samples, three main pathways can be tracked; Firstly, Direct DNA sequencing, where the isolated DNA is randomly sequenced yielding huge amounts of sequences (about 400 bp read-length) to be subjected to computational analysis to have deeper analysis for the genome of an environmental community. Secondly, 16sRNA phylogenetic analysis that could yield comparative genomics studies and the taxonomical classification. And finally, the functional screening for novel enzymes and proteins' discovery, or sequence based screening to study novel metabolic pathways and genes, where both screenings processed via library construction (**Figure 11**) [55].

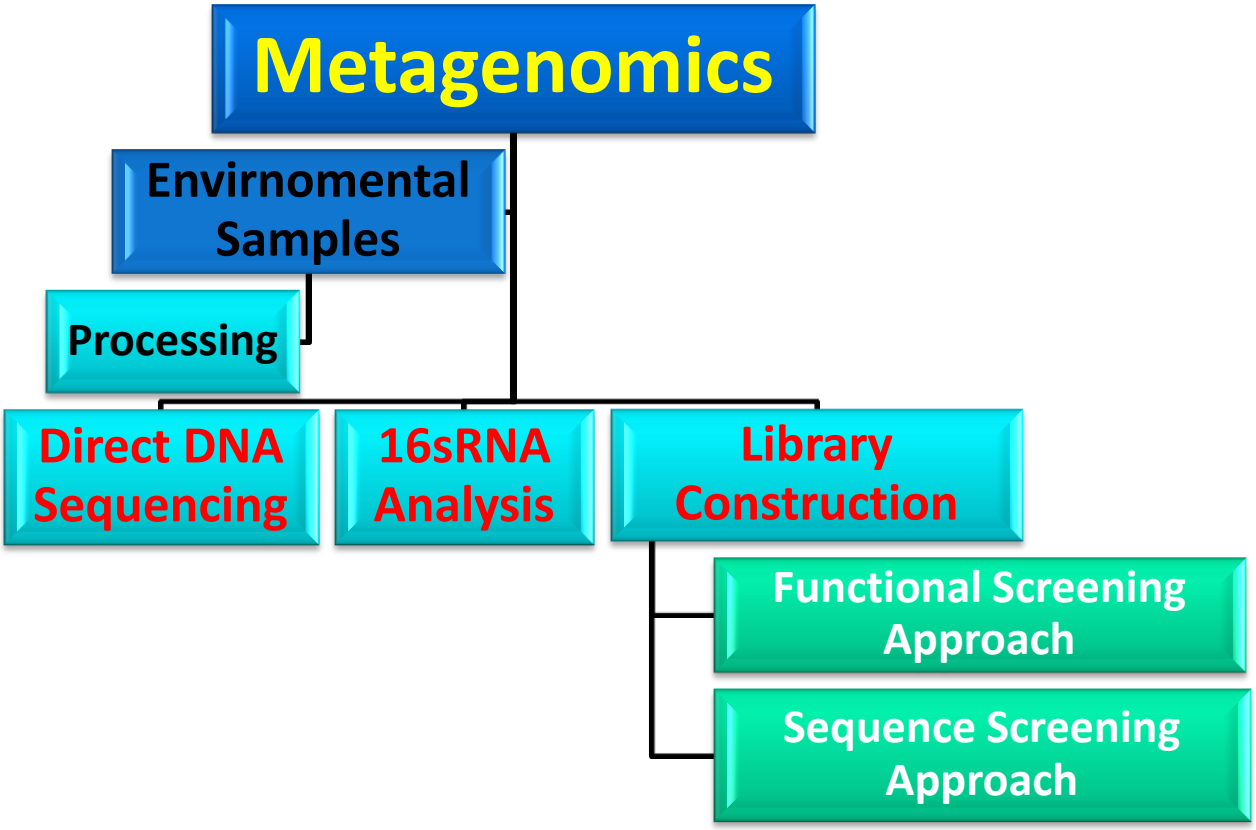

Figure 11: Metagenomics Pathways

After extracting the whole genome directly from their environmental samples and processing, we can proceed in one of the following pathways; Direct DNA sequencing, 16sRNA phylogenetic analysis or library construction (Sequence or Functional analysis) [56].

Basically, the functional screening is based on testing the clones of the metagenomic library on selective media that are enriched with a specific substrate, where target clones can grow. On the other hand, the sequence based screening comprises designing primers for targeting genes of interest [55].

Historically, the first time for the term 'Metagenomics' to be introduced was in 1998 by Jo Handelsman and her colleagues, when they isolated the metagenome of soil microorganisms and cloned in *E.coli* via Bacterial Artificial Chromosomes (BACs) [56]. Furthermore, one of the classical phylogenetic studies was done on environmental samples extracted from the Sargasso Sea, where the whole genome was directly amplified for the entire 16 rRNA genes without culturing that leaded to the identification of new group of bacteria; the SAR11 cluster [57]. However, the idea of direct cloning of DNA from environmental samples without amplification by PCR was formerly proposed in 1985 by Pace, but was applied in 1991, where environmental samples were collected from marine picoplankton community and DNA was isolated and cloned in bacteriophage lambda [58].

4.2 Pyrosequencing technology

Pyrosequencing technology is one of the advancement that supported the Metagenomics approaches in exploring the microbial diversity of any community. It is one of the Next-Generation Sequencing (NGS) methods that have been applied in different metagenomic studies (Schuster, Fitz-Gibbon, Biddle, Brenchley & House, 2008; Roesch et al., 2007; Poinar et al., 2006; Sogin et al., 2006). Pyrosequencing was developed in 1996 by Pal Nyren and Mostafa Ronaghi in Sweden. Basically, it is a DNA sequencing technique (known also as sequencing by synthesis), where it differs from the traditional Sanger method (Chain termination reaction by dideoxynucleotides), in that it counts on the detection of the release of pyrophosphate during incorporation of complementary nucleotides. The pyrosequencing technique tends to amplify the small subunit (SSU) rRNA hypervariable region. In conclusion, there are various advantages for this method; Firstly, although the generated reads from

the pyrosequencing are shorter than that from the Chain Termination Sequencing (traditional Sanger sequencing), where the pyrosequencing reads are about 400 bp in length, while the Sanger sequencing reads approximately 700 bp per read, however the generated pyrosequencing reads are more intensified in magnitude for better coverage and representation. Secondly, pyrosequencing technique is of lower cost and finally, it generates unbiased results toward the predominant species in the community [53].

4.2.1 Pyrosequencing protocol

The pyrosequencing technique relies on synthesizing of the complementary strand for a single helix of unknown DNA by integrating a single base pair at a time and detecting it after each incorporation. The template strand of DNA is immobile, while different solutions of the four possible nucleotides (Adenine, Thymine, Cytosine or Guanine) are consecutively added and then removed. Light is generated only when the complement nucleotide solution fits the first single unpaired base in the DNA template. The identification of the sequence of the DNA template has been allowed by the sequence of the four nucleotides solutions that generate chemiluminescent signals. The pyrosequencing reaction comprises the following; a single stranded DNA template incubated with a sequencing primer with DNA polymerase that incorporates the proper, complementary deoxynucleoside triphosphates (dNTPs) against the DNA template. Consequently, the nucleotides' incorporation generates pyrophosphate (PPi). Additionally, the reaction comprises Adenosine triphosphate (ATP) sulfurylase enzyme that converts the released PPi to ATP in an equal amount in the presence of Adenosine 5´ phosphosulfate (APS). The generated ATP mediates the conversion of luciferin to oxyluciferin that produces quantitatively visible light in presence of luciferase enzyme and apyrase enzyme that degrades the unincorporated nucleotides. Finally, a camera detects the generated light and the received pyrogram is analyzed [59] (**Figure 12**).

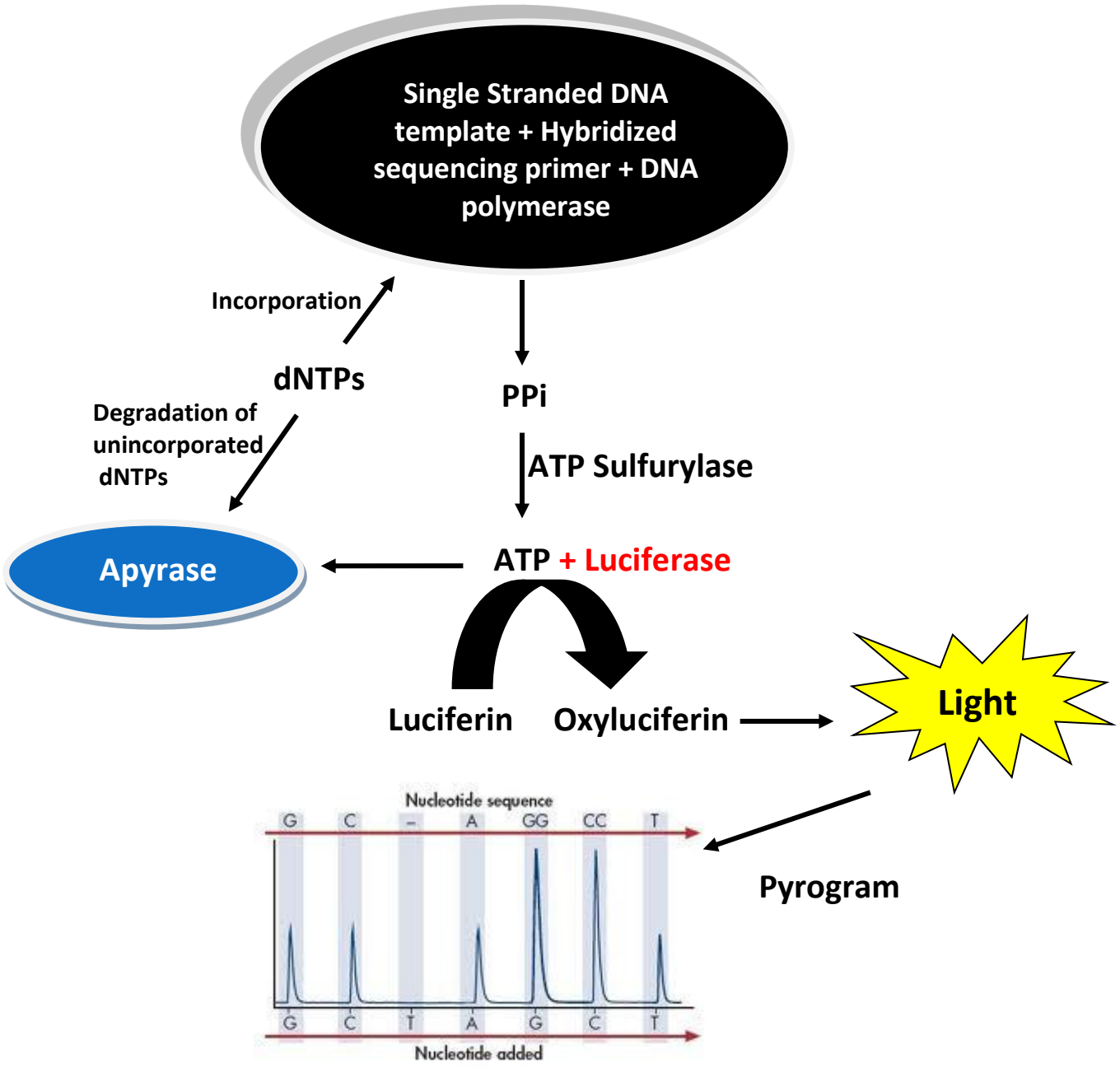

Figure 12: Pyrosequencing technology

4.3 Construction of Metagenomic Libraries

The main objective of constructing a metagenomic library is to facilitate the access to the isolated metagenome from an environmental sample for advanced screening for target genes, biocatalysts, enzymes or any novel proteins. Some safety measures should be followed during constructing a metagenomic library; ensure that the isolated metagenome is well representing the community of the environmental sample so as to avoid any biased representation, the DNA should be intact and not sheared to avoid developing of chimeric products among the smaller fragments of DNA, contamination should be avoided, and finally, in order to prevent any interference with further downstream processes as PCR, the metagenome should be clean and free from inhibitors [52, 60]. To isolate the metagenome from the collected samples via cell lysis, there are two main methods; chemical and physical. The physical method comprises freezing and thawing for the samples several times, followed by sonication, but these steps could cause DNA shearing. On the other hand, the chemical methods that lysis the cells via using SDS is characterized by being much gentler than the traditional physical methods. Thus, a mixed recipe of both methods can be used as per the nature of the sample, where the metagenome was isolated from [52].

The type of the vector that will be used in constructing the library will be decided as per the objective of the study. For instance, if the aim of the study is to characterize single genes, thus we can go for small insert library, where the used cloning vectors are plasmids (inserts size less than 10 kb). On the contrary, if the purpose of the study is to characterize the whole operons or genes' clusters, we have to go for large insert library, where the used cloning vectors could be BACs (insert size range 100-200 kb), or fosmids (insert size range 25-40 kb) or cosmids (insert size 25-35 kb) [61]. Regarding the surrogate host, the most convenient and well established used host is the *E. coli* for various advantages; its ease of transformation, high transformation efficiency and its exemplified genetics [61]. Moreover, for the same DNA amount, the number of

the clones generated from the small insert library are much higher than that of the large insert library (about 10 folds), which allows the efficient screening of all expressed genes, especially those of low levels of expression [61]. In the following section, we will discuss the screening approaches.

4.3.1 Sequence based approach

Usually this approach is followed for phylogenetic analysis, where primers are designed as per the conserved regions or domains of the target protein or gene. PCR is then performed for screening the library and consequently, the whole clone is sequenced to identify the whole gene sequence [52]. One of the privileges of the sequence based approach over the functional based approach that it does not depend on the expression of the cloned gene in its host (*E. coli*); while the functional based approach is depending on the gene expression in the surrogate host [52].

4.3.2 Functional based approach

Fundamentally, the functional screening is based on examining the clones of the metagenomic library on selective or indicator media that are enriched with a specific substrate, where target clones can grow demonstrating a color change or halo zones around target colonies [61]. The main advantage of the functional screening over the sequence screening that it relies on the gene functioning away from its sequence, which in turn open the window of opportunities for discovering novel proteins; enzymes, biocatalysts, receptors or membrane transporters, that might share the same functions with other identified proteins but with other unique gene sequence [62]. However, the main drawback in the functional screening is the mandatory heterologous gene expression of the cloned gene in the surrogate host; which is mostly *E. coli* [4, 52, 61]. Though *E. coli* is the classical surrogate host used in the functional based screening, the risk of failure of heterologous gene expression is valid with high percentage. An example of such failure was demonstrated in a metagenomic

study on the metagenome of 32 prokaryotes, where only 40% of the genes were heterologousely expressed in *E. coli*, while 60% of the genes were missed [61]. Besides, it could be possible that the percentage of the successful heterologous gene expression to be varied and could be lessen than 40 % as per the nature of the environment where the samples have been collected from, for instance, the extreme environments in terms of temperature, salinity, heavy metals, lack of nutrients, etc. By analyzing the reasons behind the failure of heterologous gene expression in *E.coli,* we have to pay attention that the isolated metagenomes from their complex communities are expected to have unusual and unique regulatory factors that are mandatory for the appropriate transcription and translation, while the *E.coli* could lack them. An example for codon usage in *E. coli* is the start codon, which is AUG; the most common start codon (91%), versus other codons that could be preferred as start codons in other organisms or environments [4]. Other reasons that could account for weak or failure of heterologous gene expression are: toxicity of some genes upon expression towards the surrogate host or lack of the required chaperones for folding protein, yielding misfolded proteins [52].

5. Adaptation of Organisms in extreme environment

Various organisms are inhabiting extreme environments; halophiles, thermophiles, acidophiles, alkalophiles, etc..., where they produce unique proteins of exceptional properties and characteristics so as to accommodate with the surrounding environment [63]. In our study, the collected samples were from a thermohalophilic environment; LCL of Atlantis II Deep brine pool in the Red Sea, thus it is expected that our retrieved thioredoixn is of thermophilic and halophilic nature.

5.1 Thermophilic adaptation

Conferring to the optimal functional activity at a wide range of temperatures, bacterial proteins can be categorized into 4 groups; hyperthermophiles (active at more than 80 ºC), thermophiles (active from 45 ºC to 80 ºC), mesophiles (active from 15 ºC to 45 ºC) and finally psychrophiles that

are active from 5 ºC to 10 ºC [64]. Basically, the first two groups; hyperthermophilic and thermophilic, can withstand and properly function at extremely harsh circumstances; high metal content, low nutrients, high salinity, temperature, etc… [64]. The main features of the thermostable proteins are the covalent bonds, extra hydrogen bonds, the rich hydrophobic core and the Van der Waals interactions[65, 66, 67].

5.1.1 Forces influencing protein's stability towards Thermo-Halophilicity

There are a variety of forces and bonds that influence the stability of proteins. Basically, there is a balance between those forces that maintain the native structure of protein versus other forces that could oppose protein's stability [68]. The main contributing force for the protein's stability is the covalent bond, where common electrons can be shared by two molecules. Thioredoxin's active site (Cys-X-X-Cys) is characterized by having two vicinal cysteines, where cysteine amino acid tends to perform disulfide bridge (S-S) upon reducing other amino acids using its sulfhydryl group (SH). The performed disulfide bridge is a strong covalent bond. Thus, the thioredoxin's active site is playing a crucial dual role; maintenance of thioredoxin structural folding as well as the catalytic antioxidant activity of the protein [69, 70]. On the other hand, although Van der Waals forces, electrostatic and hydrophobic interactions do not share electrons among molecules and characterized by being much weaker than covalent bond, they have a role in the conformational stability of the proteins [69, 70].

5.1.2 Role of Salt bridges in protein stabilization

The salt bridge bond is a type of electrostatic interaction, where it is formed between ionized residues of opposite charges. That is to say, salt bridges could be in favor of protein's stability or not for two main reasons; firstly, the performed salt bridge could be of attractive or repulsive nature. Secondly, to perform the electrostatic interaction, re-organization of the conformational structure of protein is mandatory, which in turn could affect protein's stability.

Consequently, salt bridges play different roles in proteins; molecular recognitions, key and lock feature at enzymatic binding sites or protein's stability [68]. The locations of salt bridges within the protein structure are variant; (a) on protein surface, (b) fully buried within protein structure or (c) partially buried (**Figure 13**). Additionally, salt bridges are pH dependent, thus, the presence of salt bridges in proteins is highly influencing the thermo-halophilicity nature of proteins. Finally, it is well established that thermo-halophilic proteins are characterized by being highly thermo-halophilic stable due to their richness in salt bridges within their structures [68].

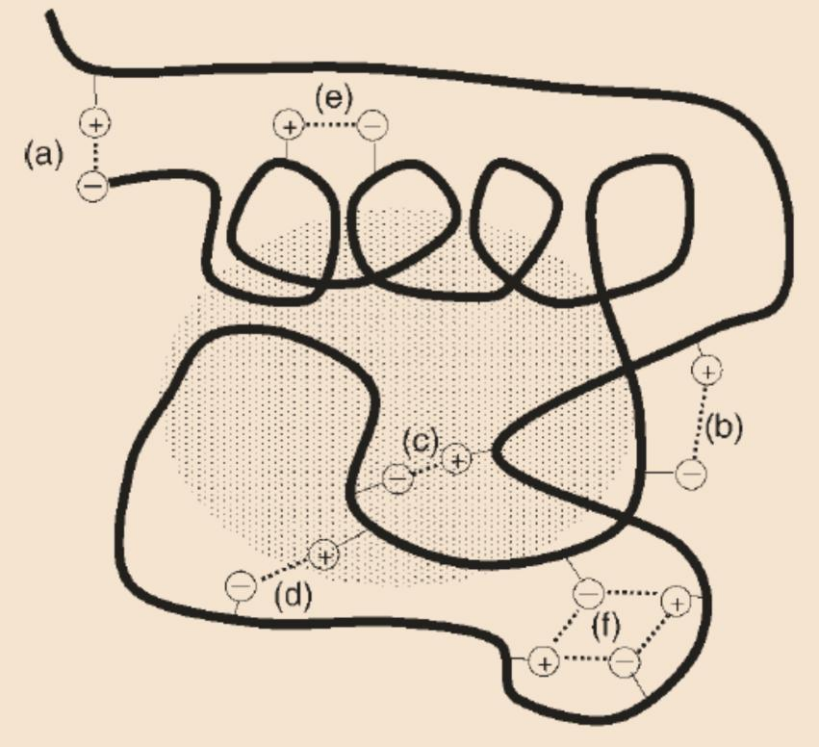

Captured from Bosshard, H.R., D.N. Marti, and I. Jelesarov, Protein stabilization by salt bridges: concepts, experimental approaches and clarification of some misunderstandings. J Mol Recognit, 17(1): 1-16 (2004)

Figure 13: Different locations of salt bridges within protein structure [68]

The figure is showing the probable locations of salt bridges within a protein moiety, where the heavy line is demonstrating a polypeptide chain, while the following points are:
(a) and (b) are representing salt bridges on the surface of protein.
(c) is demonstrating fully buried location in the depth of protein.
(d) is demonstrating partially buried location in the depth of protein
(e) Other charges affecting salt bridges.
(f) Complex salt bridge.

5.2 Halophilic adaptations

Halophilic organisms can exceptionally tolerate harsh salinity conditions, where they can grow in media comprising salts from 0.5 M till 5 M as per their classification; halo-tolerant, moderate halophiles, borderline extreme halophiles and extreme halophiles [71]. Furthermore, halophiles can be defined as microorganisms that are optimally grow at 0.85 M NaCl, with tolerability until 1.7 M NaCl. Basically, the osmotic balance within the halophilic microorganisms and the surrounding environment is maintained via one of two main tactics; (a) Salt out tactic: where osmotic solutes of organic nature as ectoine, L-proline and glycerol are accumulated inside the cytoplasm of halophiles, allowing the cells to flux out salts, without interfering with the activity of cellular proteins. (b) Salt in tactic: where high molar concentration of ions; Chloride and Potassium are accumulated inside the cytoplasm of halophiles, allowing the cellular machinery to be adapted to high concentrations of salts while being active and functioning [72, 73].

6. Thioredoxin Therapeutic Applications

Thioredoxin is a small monomeric redox protein (12 KDa) that ubiquitously exists in human body. It is considered as one of the defensive proteins, which is induced in response to numerous oxidative stress conditions. Adding to its anti-oxidative activity via dithiol-disulfide exchange, thioredoxin has anti-inflammatory and anti-apoptotic activities. The overexpression of thioredoxin in different animal models has been demonstrated to be a key player in the inflammatory disorders and oxidative disorders as well. Interestingly, administration of recombinant thioredoxin has shown anti-inflammatory efficacy in severe acute lung diseases. Furthermore, thioredoxin has shown anti-chemotactic activities for neutrophils as well as inhibitory actions against macrophage migration inhibitory factor (MIF). To sum up, administration of recombinant thioredoxin could have a wide range of potential therapeutic applications in the medical field that should be examined in various animal models [74].

7. Study Objectives and Experimental Plan

The main objective of this study was to identify a novel TrxATII from the LCL of Atlantis II Deep brine pool in the Red Sea. The proper primers have been designed as per the conserved domains of Trx and the full gene was retrieved by performing PCR directly on the 1x metagenome of the LCL, followed by gene sequencing.

The second objective was the TrxATII heterologous protein expression after being cloned in the proper expression vector and transformed into the proper surrogate host (*E.coli* BL21, (DE3)), where the expressed protein was characterized by being His-tagged to allow the protein purification. Additionally, the induction phase of the TrxATII was done by using IPTG, where the expressed TrxATII appeared at its proper size on the SDS-PAGE gel.

The third objective was the purification of TrxATII. The purification procedures was done using Nickel affinity chromatography, where the His-tagged TrxATII was bound to the Ni+ ions, and subsequently, eluted with the proper elution buffer that comprises imidazole of high concentration.

The fourth objective was to assess the activity of the purified thioredoxin. Basically, we have examined the TrxATII antioxidant activity via different assays; Oxidative stress induction assay on HepG2 cell lines (MTT assay), DTNB reduction assay and Insulin reduction assay.

The final objective was to characterize the thermal stability and halotolerance of the purified thioredoxin. To achieve this goal, TrxATII was incubated for a definite time intervals at various salt concentrations and temperatures, followed by measuring the residual activity of the protein. **Figure 14** is showing schematic representation for the experimental plan.

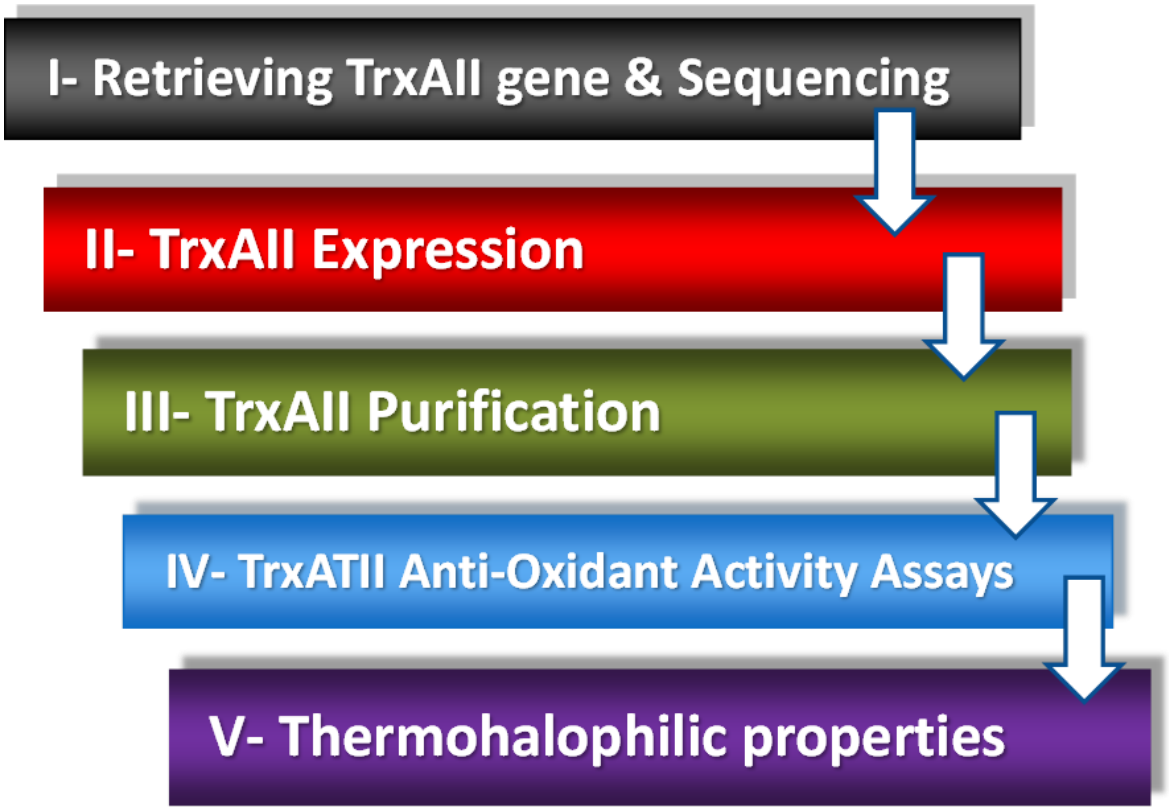

Figure 14: Schematic representation for the experimental plan

Chapter 2: Materials and Methods

1. LCL Samples

All samples that have been used along the study were collected during the expedition of KAUST (King Abdullah University for Science and Technology) at the Red Sea in spring 2010. Moreover, the site where the samples have been collected was the lower convective layer of the Atlantis II deep brine pool; latitudes 21° 13'N and 21° 30'N and longitudes 37° 58'E and 38° 9'E [8]. The total volume of the samples was about 100 liters. Subsequently, the samples were serially filtered via 3 µm, 0.8 µm and 0.1 µm filters. The aim of the serial filtration is to fractionate the prokaryotic community.

2. Amplification of LCL genome

The whole genome of the Lower Convective Layer (LCL) of the Atlantis II brine pool of Red Sea was amplified by Mr. Amged Ouf using REPLI-g Mini Kit (Cat.No.150023, QIAGEN). Basically, the REPLI-g Mini Kit generates a high yield of DNA based on Multiple Displacement Amplification (MDA) technology, where the Phi 29 polymerase (high-fidelity enzyme) is used to amplify complex genome in combination with a denaturation step of gentle alkaline condition to allow a uniform amplification of genomic loci. The kit yields about 10 µg DNA per 50 µl reaction that remains stable in a long term storage conditions. Interestingly, the easy set-up of the reaction and the convenient handling time (about 15 minutes) makes the REPLI-g Mini Kit a reliable method to use in amplifying whole genome in precious samples [75].

2.1 Whole genome amplification Concept

The Multiple Displacement Amplification (MDA) technology is also known as isothermal genome amplification. The MDA technology is based on binding random hexamers to denatured fragments of DNA. Using the high-fidelity enzyme Phi29 polymerase at constant temperature, the strand displacement synthesis occurs, where multiple priming events take place on every displaced strand, which serves as a template that allows the generation of high outcomes and consistent yield of amplified DNA as shown in **Figure 15**.

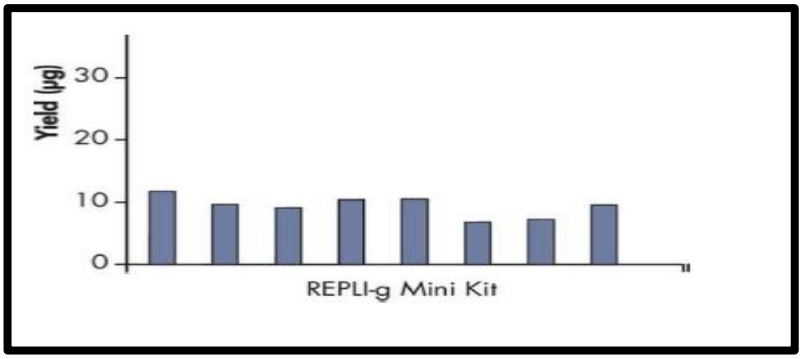

Captured from http://www.qiagen.com/products/catalog/sample-technologies/dna-sample technologies/genomic-dna/repli-g-mini-kit#productdetails

Figure 15: Consistent DNA yields using REPLI-g Mini Kit

Different starting materials comprising genomic DNA have been amplified using REPLI-g Mini Kit, where the yields are ranging from 8 to10 µg.

The high-fidelity enzyme Phi 29 is a DNA polymerase - phage derived enzyme -, with proofreading activity (3'→5' prime exonuclease activity). The Phi29 polymerase is characterized by higher fidelity than *Thermus aquaticus* (Taq) DNA polymerase (about 1000-fold) as shown in **Figure 16**. Additionally, the REPLI-g Mini Kit is supported by a unique buffer system that prevents slippage or stopping of polymerase along amplification procedure via resolving any secondary structures as hairpin loops [75].

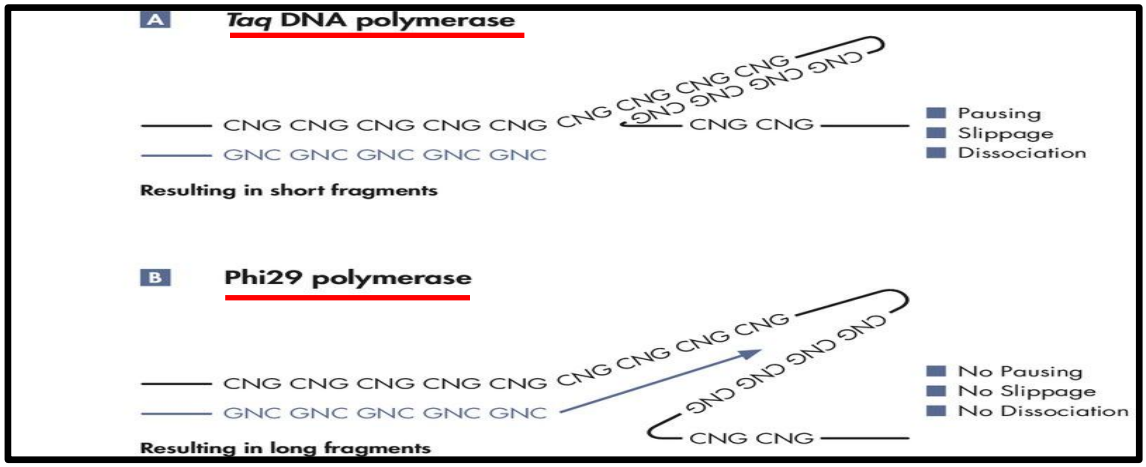

Captured from http://www.qiagen.com/products/catalog/sample-technologies/dna-sample technologies/genomic-dna/repli-g-mini-kit#productdetails

Figure 16: LCL genomic amplification by Phi29 polymerase

[A] Taq polymerase may stop synthesis or detach from the DNA template upon coming across a secondary DNA structure, thus could yield inappropriate DNA amplification and short fragments **[B]** Upon coming across a secondary DNA structure, the Phi29 polymerase displaces the structure as shown allowing high integrity for the amplified genome.

2.2 DNA Denaturation

To proceed in the enzymatic amplification of the LCL genome, gentle alkaline incubation is maintained instead of ordinary harsh conditions; high temperatures incubation or high alkaline incubation. Subsequently, the gentle alkaline incubation allows the uniform denaturation of LCL genome with a minimal DNA fragmentation and the final DNA yield is characterized by high integrity and maximized length of the amplified fragments, which in turn allows the genomic loci and sequences to be represented uniformly without negative results or false positive. The effect of heat denaturation versus alkaline denaturation for genomic DNA in terms of Ct values (threshold cycle) **(Figure 17)**. Basically, the Ct value (threshold cycle) is a relative measure in the PCR reaction for the concentration of target DNA. The Ct value increases with a decreasing amount of template. Thus, the lower the Ct values the better representation of loci [75].

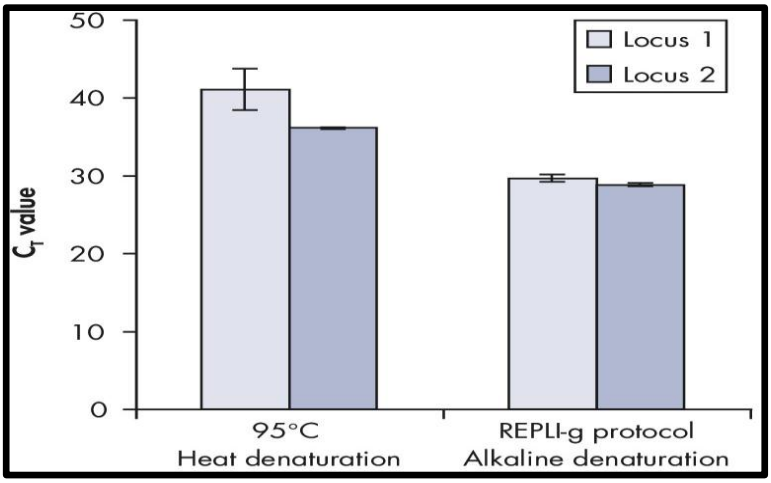

Captured from http://www.qiagen.com/products/catalog/sample-technologies/dna-sample technologies/genomic-dna/repli-g-mini-kit#productdetails

Figure 17: Heat effect versus alkaline denaturation effect on loci representation
10 ng of genomic DNA samples were denatured at 95°C versus gentle alkaline denaturation by REPLI-g Kit. Later on, after amplification, the C_T values (threshold cycle) for 2 loci were calculated and compared between the 2 conditions. It is clear that the C_T values of the amplified loci by the REPLI-g Kit is much lower than that of heat denaturation method, which indicates better representation for the locus with no loss of sequences at these loci.

2.3 Amplification Procedures

The LCL genomic sample is lysed by the addition of the lysis buffer, which has a dual role; Sample lysis and DNA denaturation via its one minute gentle alkaline incubation. Consequently, the denaturation step is stopped by adding the neutralizing buffer, followed by addition of the master mix (including REPLI-g Mini DNA Polymerase), where the multiple displacement amplification reaction proceeds at 30°C overnight (at least 10-15 hours). The procedure of DNA amplification is illustrated in **Figure 18**. Finally, the whole amplified genome can be stored –20°C for a long-term period stable and consistent [75].

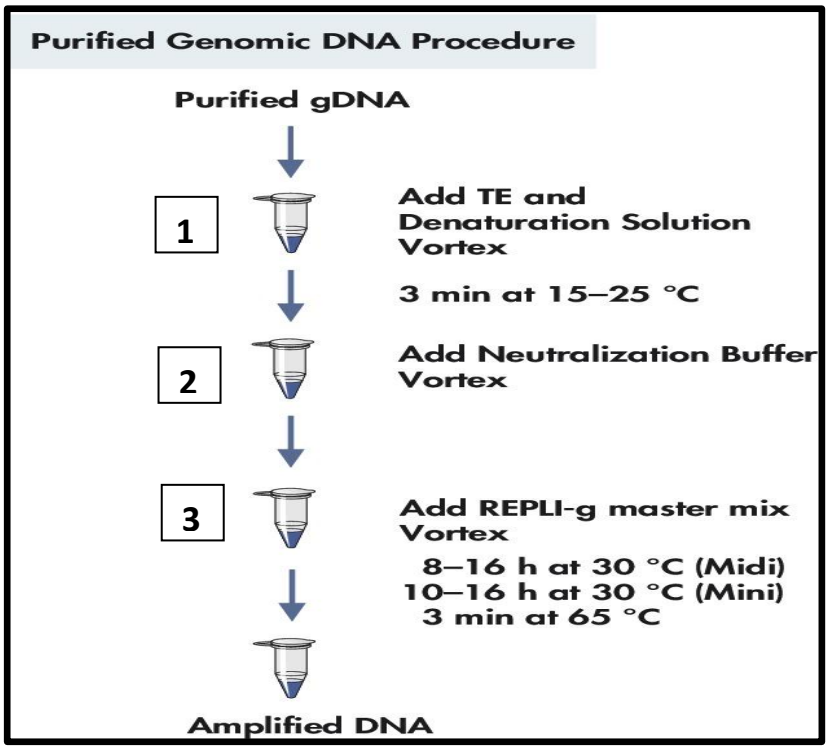

Captured from http://www.qiagen.com/products/catalog/sample-technologies/dna-sample technologies/genomic-dna/repli-g-mini-kit#productdetails

Figure 18: Procedure of the whole genome amplification of the LCL genome by REPLI-g Mini kit

Amplification of the LCL genome comprises 3 main steps:

1- 10 ng of purified LCL genome undergoes gentle alkaline denaturation.
2- Sample neutralization.
3- Incubation at 30°C with REPLI-g master mix.

3. Retrieving TrxATII gene

3.1 DNA isolation

TrxATII gene was retrieved directly from the metagenome of the lower convective layer of the Atlantis II deep brine pool (1x LCL) via PCR reaction. As per the conserved regions of thioredoxin gene, we have designed the primers to retrieve the full gene as follow; forward primer (TrxF) 5'- GGA TCC GTG CAA TCT GAA AGT CGA GAG TC-3' and the reverse primer (TrxR) 5'- AAG CTT TTA TCC ATG AGT GCG TGG ACT AA -3'. Furthermore, the PCR conditions were as follow: initial denaturation at 95^{o}C for 5 minutes, 35 cycles (95^{o}C for 30 seconds, 63^{o}C for 30 seconds and 72^{o}C for 1 minute) and a final elongation stage at 72^{o}C for 7 minutes. The used thermo-stable DNA polymerase was DreamTaq DNA Polymerase (# EP0701, Thermo SCIENTIFIC). Additionally, the used PCR thermal cycler was Veriti 96 wells (Model No.9902, Applied Biosystems).

3.2 Agarose Gel Electrophoresis

Agarose gel electrophoresis is a well-known method in molecular biology, which is used to separate a mixed population of DNA in the agarose matrix. By applying electric field, the negatively charged biomolecules are separated based on their size through the agarose matrix, where the small sized DNA fragments migrated faster downwards the agarose gel [76]. We have used; 0.8% agarose, the running buffer was 1x TBE (Tris/Borate/EDTA) for its good conductivity and less heat productivity, reference molecular weight ladder; Thermo Scientific GeneRuler 1 kb Plus DNA Ladder 75 to 20,000 bp (Ferementas Cat. No.SM1331). We have run the 0.8% agarose gel in Bio Rad electrophoresis chamber (Mini Sub® Cell GT) and finally the separated bands of DNA fragments was viewed using Image Quant 300 (Serial No. 300-06-00130, General Electric).

3.3 Excision and Extraction of TrxATII gene from agarose gel

At the proper size of TrxATII gene (~540 bp), we have excised the DNA fragment from the 0.8% agarose gel with a clean, sharp scalpel. Consequently, to extract and purify the DNA fragment, we have used QIAquick Gel Extraction Kit (Cat. No. 28704) supplied

by Qiagen, where we have followed its protocol. Finally, we have the purified DNA fragment in a 30 µl Buffer (10 mM Tris Cl, pH 8.5).

4. Recombinant TrxATII Clones

4.1 Cloning and Transformation of TrxATII gene

TrxATII gene was then cloned into a high copy number vector. The used plasmid was pGEM®-T Easy (Cat. No. A1360, Promega). Basically, pGEM®-T Easy is a linearized vector with T-overhangs at the insertion site that significantly improve the efficiency of ligation of PCR product with a compatible overhanging. Furthermore, ligation procedure was done according to the manufacturer's instructions. Subsequently, 2 ul of the ligation reaction was used to transform electrocompetent *E. coli* TOP10 cells using MicroPulser™ Electroporation Apparatus (Bio-Rad) as per the instructions of manufacturer. The tube containing transformed *E. coli* TOP10 cells and ligation reaction was incubated with 950µl room-temperature LB broth / Ampicillin (100µg/ml) for 1.5 hours at 37°C with shaking (200 rpm). Finally, 100µl of each transformation culture were plated on LB, Ampicillin (100µg/ml), IPTG (0.5mM) and X-Gal (80µg/ml) agar plates and incubated overnight at 37°C. The features of the pGEM®-T Easy vector are shown in **Figure 19.**

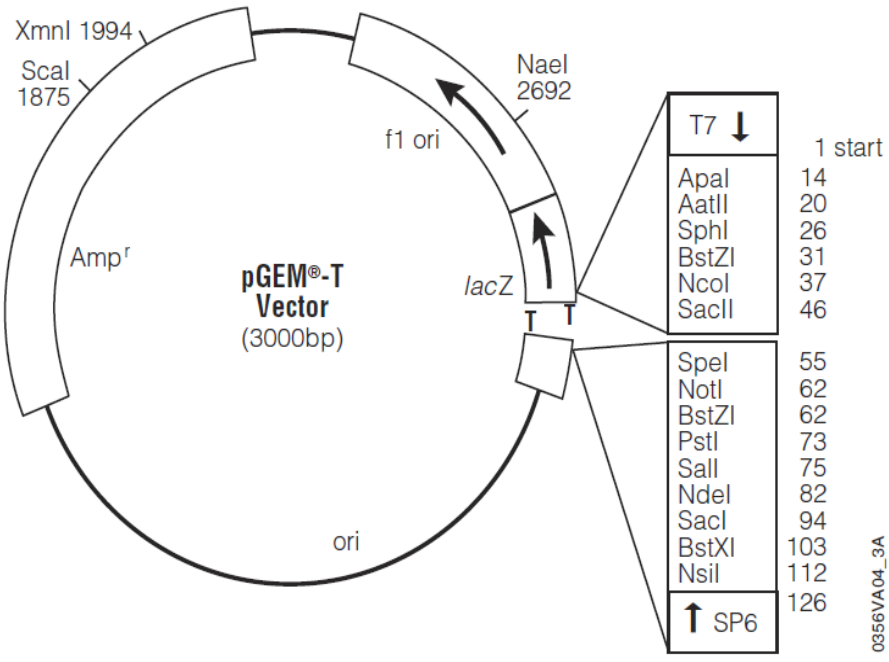

Figure 19: pGEM®-T Vector Map
Captured from the manual of pGEM®-T and pGEM®-T Easy Vector Systems (Part#TM 042, www.promega.com)

4.2 Screening of Recombinant Transformants

The pGEM®-T Easy vector comprises a multi-cloning site within the alpha peptide coding sequence of β-galactosidase enzyme and flanked by T7 and SP6 RNA polymerase promoters. Successful cloning of TrxATII gene into the pGEM®-T Easy vector will interrupt the coding sequence of β-galactosidase enzyme and thus, successful recombinant clones can be recognized by screening of colored colonies on indicator plates (Blue/White screening of recombinants). The white colonies will comprise TrxATII insert at the proper cloning region, while the blue colonies might comprise the TrxATII gene but cloned in-frame with the lacZ gene or might not comprise the insert at all. Twenty white colonies were picked up from indicator plates for gene sequencing.

5. TrxATII gene Sequencing

5.1 Plasmid Extraction

To proceed in gene sequencing, firstly we need to extract the pGEM®-T Easy plasmid comprising the TrxATII gene insert from the recombinant *E. coli* TOP10 cells (White colonies). Out of the indicator plates, twenty white colonies were picked up with autoclaved picks, where each picked colony sub-cultured in a separate falcon tube containing LB broth/Ampicillin (100µg/ml) overnight at 37°C with shaking (200 rpm).

For plasmid extraction, we have used the PureYield™ Plasmid Miniprep System (Cat.No.A1223, Promega), which is designed to extract highly pure plasmid DNA. We have followed the manufacturer's protocol in isolating the twenty plasmids. Finally, we have 30 µl of each plasmid in a separate eppendorf tube and stored at -20°C, where the plasmids stored in 10mM Tris-HCl (pH 8.5) and 0.1mM EDTA buffer. To determine the concentration of the extracted plasmids, we ran them on 0.8% agarose gel electrophoresis.

5.2 Chain Termination Sequencing

To carry out Sanger sequencing (Chain Termination Sequencing), Mr. Amged ouf has used Applied Biosystems 3730xl DNA Analyzer machine using the BigDye® Terminator v3.1 Cycle Sequencing Kit. For each plasmid, two reactions were performed, where each reaction contains: Big dye terminator, 5X Sequencing Buffer, primer

(forward or reverse), DNA template and the volume was completed using water. The used primers were thioredoxin forward (TrxF) and thioredoxin reverse (TrxR). Thermocycler conditions were initial denaturation step at 96^{o}C for 1 minute, 25 cycles (denaturation at 96^{o}C for 10 seconds, annealing at 63^{o}C for 5 seconds and extension at 60^{o}C for 4 minutes). TrxATII gene sample to be sequenced was purified using the Edge-Biosystem Columns, dried and loaded into the 96 well optical plate.

6. Computational Analysis

6.1 TrxATII sequence and alignment analysis

After sequencing the positive TrxATII clones by Applied Biosystems 3730xl DNA Analyzer machine, the generated sequence was BLASTed against non-redundant (nr) protein databases using Basic Local Alignment Search Tool (BLASTP) provided by the National Center for Biotechnology Information (NCBI). Furthermore, the generated sequence was aligned against the first hit; Trx *Prochlorococcus marinus* (accession number WP_002807427.1), using ClustalW version 2.1 [77,78]. Moreover, a multiple alignment was generated for the TrxATII against other members of the Trx super family using ClustalW version 2.1 to detect the conserved active catalytic site.

6.2 3D modeling of TrxATII versus Trx of *Prochlorococcus marinus*

Using the PyMOL Molecular Graphics System (Version 1.3 Schrödinger, LLC), we have made a 3D modeling for the TrxATII versus Trx of *Prochlorococcus marinus*.

6.3 Construction of Phylogenetic tree

A Phylogenetic tree for the TrxATII was constructed using CLUSTALW version 2.1 [77,78] . The generated tree is Neighbour-joining tree including the sequences most similar to the TrxATII sequence.

7. Expression of TrxATII

7.1 Cloning of TrxATII gene in Expression Vector

TrxATII gene was cloned into a high level expression vector with a TA cloning site for efficient cloning. The used expression system was the Champion™ pET SUMO Protein Expression System (Catalog No.K300-01) supplied by invitrogen™. Basically, the Champion™ pET SUMO Protein Expression System utilizes a small ubiquitin-like modifier (SUMO; Smt3 protein of the *Saccharomyces cerevisiae*) that facilitates expression, purification, and generation of native heterologous proteins in the surrogate host; *E. coli*. Additionally, the pET SUMO vector takes the privilege of the bacteriophage T7 RNA polymerase that allows high-level, IPTG-inducible expression of heterologous genes in *E. coli* under the T7 *lac* promoter, plus solubility enhancement of partially insoluble proteins. Moreover, the presence of the N-terminal polyhistidine (6xHis) tag in the pET SUMO expression vector allows purification of the recombinant TrxATII protein against metal-chelating resin (Ni-NTA agarose resin, Cat.No. R901-15, Invitrogen™), where the Ni-NTA resin has high affinity and selectivity for 6xHis-tagged recombinant fusion proteins. The features of the pET SUMO vector are shown in **Figure 20**. Following the manufacturer's protocol, we have cloned TrxATII gene in pET SUMO vector after performing PCR with the previously mentioned conditions. The ligation reaction was incubated at room temperature for 30 minutes then stored at -20°C.

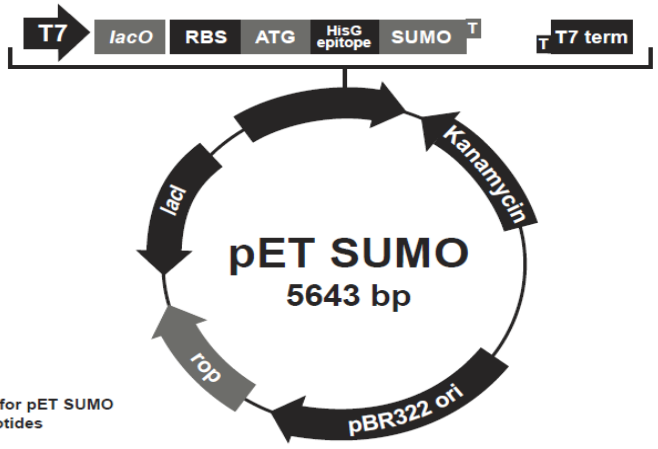

Comments for pET SUMO
5643 nucleotides

T7 promoter: bases 209-225
lac operator (lacO): bases 228-252
Ribosome binding site (RBS): bases 282-288
Initiation ATG: bases 297-299
HisG epitope: bases 309-329
SUMO ORF: bases 360-653
SUMO forward priming site: bases 549-571
TA Cloning site: bases 653-654
T7 reverse priming site: bases 783-802 (C)
T7 terminator: bases 744-872
Kanamycin resistance gene: bases 1431-2246 (C)
pBR322 origin: bases 2342-3015
ROP ORF: bases 3383-3574
lacI ORF: bases 4383-5474 (C)

(C) = complementary strand

Figure 20: pET SUMO® Vector Map
Captured from the manual of pET SUMO Vector (Cat.No.300-01, invitrogen™)

7.2 Transformation of Expression Vector into *E. coli*

The BL21 (DE3) *E. coli* strain (supplied by invitrogen™) is precisely designed for expression of heterologous genes under the T7 promoter. Following the manufacturer's transformation instructions, 2 ul of the ligation reaction was used to transform the chemically competent BL21 (DE3) *E. coli* cells. After that, the tube containing transformed *E. coli* cells and ligation reaction was incubated with 250 µl room-temperature LB broth/kanamycin (50 µg/ml) for 1.5 hours at 37°C with shaking (200 rpm). Finally, 100µl of each transformation culture were streaked on LB and kanamycin (50 µg/ml) agar plates to be incubated overnight at 37°C.

7.3 Analyzing Transformants

To analyze transformants, we performed PCR reaction as the previously mentioned conditions for each transformation culture using the TrxF (Thioredoxin forward primer) and TrxR (Thioredoxin reverse primer). The generated PCR product was run on 0.8% agarose gel electrophoresis to confirm the positive transformants.

7.4 IPTG-inducible Expression of TrxATII

Transformant BL21(DE3) *E. coli* cells comprising the pET SUMO vector with TrxATII gene insert were sub-cultured in LB broth / kanamycin (50 µg/ml) with shaking (200 rpm) and incubated overnight at 37°C. In the following day, in a clean autoclaved 500 ml. flask, 1 ml. of the overnight culture were added to 100 ml. of LB broth/kanamycin (50 µg/ml) and incubated at 37°C with 200 rpm shaking for about 3 hours until reaching optical density (OD) from 0.4 to 0.6 at wavelength (ʎ) 600 nm, where we measured OD using Ultrospec 3100 pro (UV/visible spectrophotometer, Amersham Biosciences). After reaching the desired optical density, we started the induction phase using IPTG (isopropyl β-D-thiogalactoside) of final concentration 0.1 mM, followed by incubation at 37°C with shaking at 200 rpm overnight. By the following day, we have isolated the *E. coli* cell pellets from supernatant via centrifugation for 10 minutes at 5000 rpm using Allegra® X-12R centrifuge (BECKMAN COULTER, USA). Moreover, the *E. coli* cell pellets were collected and dissolved in 1ml. of the binding buffer (250 mM NaH_2PO_4 / 2.5 M NaCl) that will be used later on in the purification of the expressed TrxATII protein. To extract the cell's

proteins out of the cell pellets, we applied 100 watts of sonication power for effective processing using Branson Sonifier 150 machine (Model No.S-150D, USA), where we freezed and thawed the cell pellets for three successive times in -80°C and 42°C respectively and finally we applied sonication for 5 minutes (15 seconds on and 15 seconds off). To collect the total expressed proteins, we centrifuged the sonicated cell pellets at 13,000 rpm for 10 minutes, where we separated the supernatant comprising the whole cell's proteins.

7.5 SDS-Polyacrylamide Gel Electrophoresis (SDS-PAGE)

SDS-PAGE is a well-known molecular biology technique that used to separate proteins from a pool of different proteins based on their molecular weight through the polyacrylamide sieve like matrix. The small sized proteins run faster than larger sized proteins, where each protein represented by a clear separate band. In this technique, proteins reacted with SDS (Sodium dodecylsulfate) forming negative charge complexes, where the amount of SDS that bounds to each protein is approximately proportional to its size [79]. We have analyzed the *E. coli* proteins on 17% SDS gel. To prepare the 17% resolving gel, we have mixed; 3.75 ml 30% Acrylamide/Bisacrylamide (37.5:1), 3 ml Tris-HCl (pH 8.6), 40 ul 20% SDS and 1.2 ml water, then just before casting the gel, we added 48 ul 10% Ammonium per Sulfate (APS) and 12 ul of Tetramethylethylenediamine (TEMED). To prepare the stacking gel, we have mixed 820 ul of 30% Acrylamide/Bisacrylamide (37.5:1), 0.5 ml Tris-HCl (pH 6.9), 20 ul 20% SDS and 2.7 ml water, then just before casting the gel, we added 20 ul 10% Ammonium per Sulfate (APS) and 10 ul of Tetramethylethylenediamine (TEMED). The loading dye recipe was 1% SDS, 10% glycerol, 10 mM Tris-Cl (pH 6.8), 1 mM ethylene diamine tetraacetic acid (EDTA) and 0.05 mgl/ml bromophenol blue. Then, for every 950 ul loading dye, we added 50 ul of 2-mercaptoethanol as a reducing agent. To load the protein samples, we added 6 ul of cell's proteins to 24 ul of loading dye and allow denaturation at 90°C with vigorous shaking for 5 minutes and finally, we loaded 20 ul of denatured protein per SDS gel's well. Furthermore, different samples were collected before and after induction. The used electrophoresis apparatus was Bio-Rad Mini-PROTEAN Tetra Cell, where we ran the cell's proteins till before the end of the gel. For gel staining viewing the protein's

band, we used Commassie Brilliant R-250. The used reference molecular weight ladder was ProSieve®Color Protein Markers (Cat. No.50550, Lonza).

8. Purification of TrxATII

The pET SUMO expression vector is characterized by having N-terminal polyhistidine (6xHis) tag that allows purification of recombinant TrxATII against metal-chelating resin (Ni-NTA agarose resin, Cat.No.R901-15, Invitrogen™), where the Ni-NTA resin has high affinity and selectivity for 6xHis-tagged recombinant fused proteins. Following the instructions of the manufacturer, we purified the *E. coli* whole proteins under the native conditions, where we loaded the whole proteins on Ni-NTA agarose resin after column's equilibration with binding buffer (250 mM NaH_2PO_4 / 2.5 M NaCl) for 3 successive times. Then, the column was gently agitated for 60 minutes to keep the loaded proteins suspended within the resin to allow efficient binding. After resin settlement by gravity, the resin washed with 8 ml native wash buffer (20 mM imidazole/250 mM NaH_2PO_4 / 2.5 M NaCl) for 3 successive times to allow elution of whole *E. coli* proteins except TrxATII protein that fused to polyhistidine (6xHis) tag. Finally, TrxATII protein was eluted into 0.5 ml fractions using native elution buffer (250 mM imidazole/250 mM NaH_2PO_4 / 2.5 M NaCl), via competition against imidazole. Samples of purified TrxATII were taken for SDS-PAGE electrophoresis analysis.

9. Dialysis of TrxATII Fractions

The presence of imidazole within the eluted fractions of TrxATII might affect the protein's activity, thus we removed the imidazole via dialysis. We collected all eluted TrxATII fraction in a dialysis bag, then we allowed imidazole exchange against 1x PBS (Phosphate Buffered Saline) via gentle vortex at +4°C overnight. For preparing 10x PBS, we mixed 80 gm NaCl, 2 gm KCl, 14.4 gm Na_2HPO_4 and 2.4 gm KH_2PO_4 in 1 liter autoclaved water (pH 7.4).

10. Quantification of TrxATII Fractions

After dialysis, we quantified the amount of TrxATII protein using the Thermo Scientific Pierce BCA Protein Assay (Cat.No.23225, Thermo SCIENTIFIC). Basically, this assay combines the reduction of Cu+2 to Cu+1 by protein in a basic medium with the highly sensitive and selective colorimetric detection of the cuprous cation (Cu+1) using a reagent comprising bicinchoninic acid (BCA). Accordingly, a purple-colored product is formed as a result of chelation of two molecules of BCA with one cuprous ion. Interestingly, this purple-colored product exhibits a significant absorbance at 540-590 nm that shows a liner relationship by increasing the protein concentration over a working range from 20µg/ml to 2000µg/ml. Moreover, we followed the manufacturer's protocol to determine unknown concentrations of TrxATII. The used reference protein standard was bovine serum albumin (BSA). Finally, we plotted a standard curve.

11. Redox Activity and Characterization of TrxATII

11.1 Insulin reduction activity assay

Thioredoxins are antioxidant proteins that assist the reduction of other proteins via the exchange of cysteine thiol disulfide. Thus, the standard way to assess the redox activity of Trx protein is the reduction assays. Basically, the insulin molecule consists of two polypeptide chains; A and B chains, where they are linked together via disulfide bridge [80] as shown in **Figure 21**.

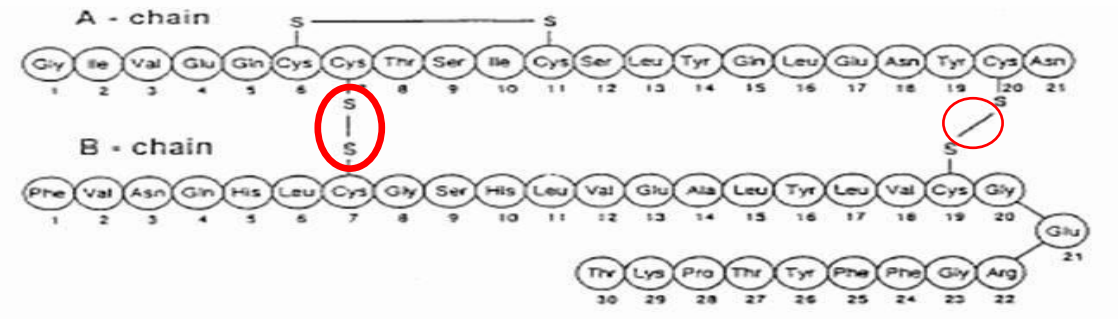

http://dailymed.nlm.nih.gov/dailymed/fda/fdaDrugXsl.cfm?id=7043&type=display

Figure 21: Structure of Human Insulin

Human insulin is composed of two subunit chains A and B. Chain A comprises 21 amino acids, while chain B comprises 30 amino acids. The two chains are bounded by two sulphide bridges enclosed in red circles. Upon reduction, the two chains separated forming thiol groups (SH SH) and insulin aggregates formed, which can be measured spectrophotomerically at 650 nm [78].

The insulin reduction assay is based on the reduction of insulin chain, where its disulfide bridge broken down (S-S to SH SH) in the presence of the active reduced form of thioredoxin that results in the formation of insulin aggregates, which can be measured spectrophotomerically at 650 nm. Moreover, the reduction initiation occurred in the presence of Dithiothreitol (DTT). We have performed the assay in 1 ml reaction as follow; In a clean cuvette, 2mM Ethylenediaminetetraacetic acid (EDTA), 100mM KH_2PO_4, 0.7mg/ml insulin (Human insulin, Cat.No.I0908, Sigma, Denmark), 4µM TrxATII, 0.33mM Dithiothreitol (DTT), and completed the final volume with water to 1 ml.

11.1.1 Thermo-stability

The redox activity of the TrxATII examined in the insulin reduction assay was assayed after incubation of TrxATII at different temperatures (25-80^{o}C).

11.1.2 Halophilicity

The redox activity of the TrxATII examined in the insulin reduction assay was assayed at different NaCl concentrations (0-4 M).

11.2 In Vitro assay of TrxATII antioxidant activity

11.2.1 Cell Culture

Another way to examine the antioxidant activity of thioredoxin protein was to induce oxidative stress conditions on mammalian cell line and then asses the role of thioredoxin as an antioxidant. In this assay, we induced oxidative stress conditions on HepG2; hepatic cancer cell line, where we obtained the cell line from the Holding Company for Biological Products & Vaccines (*VACSERA*) in Egypt. To allow the growth of HepG2 cancer cell line, we have used RPMI 1640 medium (Roswell Park Memorial Institute) with L-Glutamine and 25 mM Hepes (Cat.No.BE12-115F, Lonza, USA) containing 10% Fetal Bovine Serum (FBS) (Cat.No.DE14-701F, Lonza, USA) and 5% penicillin-streptomycin mixture (10,000 units Potassium Penicillin and 10,000 µg Streptomycin Sulfate per ml) (Cat.No.17-602E, Lonza, USA), where the cell line was

incubated at 37 °C in a humidified atmosphere of 95% air and 5% CO_2. The HepG2 cell line reached a confluence stage after 24 hours incubation. Moreover, along the study, we performed 15 passaging (from 35 to 50). To allow the growth of the cell line, passaging was done from T-25 culture flask (25 cm^2) to T-75 culture flask (75 cm^2), where we used to wash the cells gently with sterile 1x Phosphate Buffered Saline (PBS) and then allow trypsinization using trypsin-EDTA (Cat.No.CC-5012, Lonza, USA).

In the seeding phase of the cells, we counted the viable cells via the trypan blue staining, where 10µl of trypan blue was mixed with 10µl of cells and finally we used the haemocytometer to count the viable cells. Furthermore, we seeded the cells in 96 wells micro-plate, polystyrene, flat bottom, clear and sterile (Greiner, Cat.No.EK 25161), where the cell count was fixed along the experiments to be about 20 X 10^3 per well. To allow the seeded cells to attach and form confluent sheath, they were incubated at 37 °C in a humidified atmosphere of 95% air and 5% CO_2 for 24 hours before examining the antioxidant activity of TrxATII protein or inducing oxidative stress by different concentrations of Hydrogen peroxide (H_2O_2) on HepG2 cell line.

11.2.2 MTT Cytotoxicity Assay

The MTT assay is a well-known colorimetric assay, which is used in assessing the viability of cells. This assay is depending on the cellular oxido-reductase enzymes in the mitochondrial cells, where they could be an indicator for the existing viable cells. Basically, the oxido-reductase enzymes are having the ability to reduce the MTT dye [3-(4,5-dimethylthiazol-2-yl)-2,5-diphenyltetrazolium bromide] to the formazan, which is insoluble purple color. The MTT dye characterized by being sensitive to light that is why it should be stored in dark place and the assay should be carried out in dark conditions as well [81]. Thus, to assess the antioxidant role of TrxATII protein, we induced oxidative stress conditions on the HepG2 cancer cell line in presence of thioredoxin and subsequently, we determined the cell viability using the colorimetric MTT assay. Basically, we examined different concentrations of TrxATII (1, 2.5, 5, 10 and 15 µM), where each concentration was incubated with the fully attached HepG2 cells for 1 hour and then exposed to oxidative stress via different concentrations of H_2O_2 (100, 200, 800 and 1600 µM) for further 4 hours. Our control in this experiment was HepG2 cells

incubated only with nourishing medium (RPMI 1640, Lonza, USA). The final volume that was used in the 96 wells micro-plate for any condition; TrxATII, H_2O_2 or nourishing RPMI media was fixed to be 100 µl per each well. After incubating the seeded HepG2 cells with different concentrations of thioredoxin for 1 hour followed by incubation with different concentrations of H_2O_2 for further 4 hours, the old media were removed from all the 96 wells and replaced by 100 µl RPMI 1640 medium and 20 µl MTT dye (Cat.No.20395.01 Serva, Germany) per each well. After that, the 96 wells micro-plate is incubated in dark at 37 °C in a humidified atmosphere of 95% air and 5% CO_2 for 3 hours. Consequently, the RPMI 1640 medium containing MTT dye removed from all 96 wells and replaced by 100 µl DMSO (5mg/ml) to solubilize the purple color precipitate (formazan). Using the FLUOstar OPTIMA microplate reader (BMG LabTech, Germany), the absorbance of formazan was measured at 590 nm. For further confirmation, each examined concentration of TrxATII and H_2O_2 was done in triplicates and the whole set of experiment was done 3 times in 3 different days. Furthermore, to calculate the percentage of viable cells, the absorbance of each sample was divided by the absorbance of the control and multiplied by 100 as follow:

$$\% \text{ of Cell Viability} = \frac{\text{Absorbance of Sample}}{\text{Absorbance of Control}} \text{ X } 100$$

Moreover, to detect the changes in the morphology of the HepG2 cell line along the experiment conditions, we monitored it microscopically. The used microscope was the inverted microscope (Olympus 1X20, USA) under 20x magnification power, where we captured photos for different conditions of the cell line; normal control condition (incubation with RPMI 1640 medium), oxidative stress condition (incubation with different concentrations of H_2O_2) and oxidative stress condition with prior incubation with TrxATII protein.

12. Kinetics of TrxATII

The Trx system as a whole is composed of thioredoxin (Trx), thioredoxin reductase (TrxR), and NADPH that serves as a hydrogen donor. Trx is a small monomeric protein with its typical active site motif (-Cys–XX–Cys-) that catalyzes thiol-disulfide exchange. The oxidized inactive form of Trx (Trx-S_2) is reduced on the expenses of NADPH through the TrxR. Moreover, the reduced active form of Trx (Trx-SH_2) catalyzes the reduction of disulfides in oxidized proteins as follow [1, 2]:

- $Trx\text{-}S_2 + NADPH + H^+ \xrightarrow{TrxR} Trx\text{-}SH_2 + NADP^+$
- $Trx\text{-}SH_2 + Protein - S_2 \longrightarrow Trx\text{-}S_2 + Protein - SH_2$

To obtain the kinetic parameters of Trx system, we have used the DTNB reduction assay. We have calculated the kinetic parameters towards two substrates; TrxATII and DTNB. For the TrxATII; 100mM phosphate buffer at pH 7.5, 2mM EDTA, 1mM DTNB (Cat. No. 20735.02, Serva), TrxATII (0.2-12 µM), 0.1µM *E.coli* TrxR (Cat. No.TR-01, IMCO Corporation Ltd AB) and 200 µM NADPH. For the DTNB; 100 mM phosphate buffer at pH 7.5, 2mM EDTA, DTNB (0.01-1mM), TrxATII (4µM), 0.1µM *E.coli* TrxR, and 200 µM NADPH. The parameters were calculated from the increase in absorbance at 412 nm, where one enzyme unit in the DTNB reduction assay was defined as the NADPH-dependent production of 2 µmol of 2-nitro-5- thiobenzoic acid per minute (ε_{412} = 13.6 $mM^{-1}.cm^{-1}$) [82]. We have applied Michaelis–Menten equation to calculate the Km (µM) and Kcat (S^{-1}), where the Km is the substrate concentration at which the reaction rate is half of Vmax (maximum reaction velocity), while the Kcat (turnover number) measures the number of substrate molecules turned over per enzyme molecule per second [82].

Chapter 3: Results

1. Retrieving TrxATII gene from metagenome of LCL

TrxATII gene was retrieved directly from the metagenome of the LCL via performing PCR with the designed thioredoxin primers on 1x LCL. The PCR product was loaded on 0.8% agarose gel electrophoresis. As shown in **Figure 22**, there is a clear, thick and separated band for the TrxATII gene at its proper expected size; ~ 540 bp. To perform the following experiments on TrxATII gene, we have excised the TrxATII band from the agarose gel and purified it.

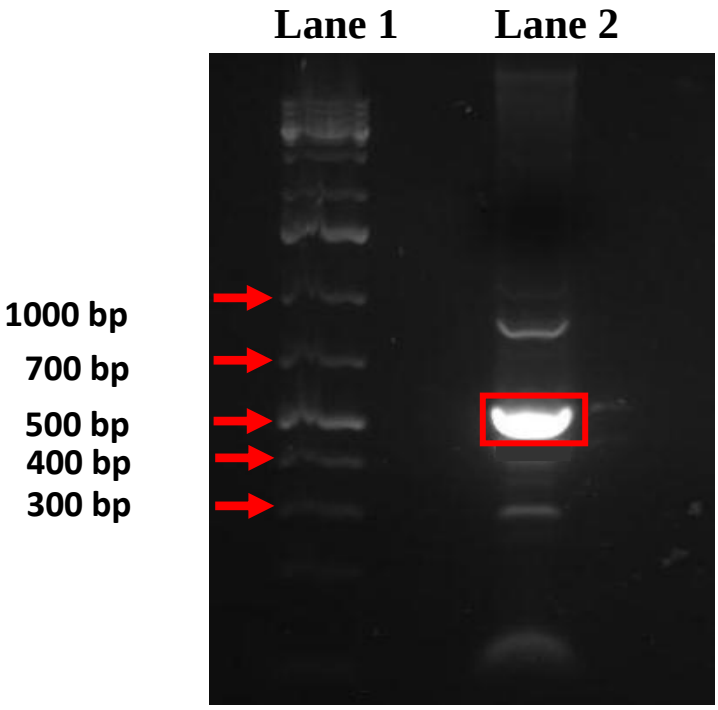

Figure 22: 0.8 % Agarose Gel Electrophoresis for TrxATII gene

Lane 1; Reference molecular weight ladder; Thermo Scientific GeneRuler 1 kb Plus DNA Ladder (Cat. No. # SM1331). Lane 2 is the metagenome of the 1x LCL showing a clear band for TrxATII gene at ~ 540 bp.

2. Recombinant TrxATII Clones (pGEM®-T Easy vector)

Successful cloning of TrxATII gene into the pGEM®-T Easy vector interrupts the coding sequence of β-galactosidase enzyme. As shown in **Figure 23**, successful recombinant clones of *E. coli* Top 10 are recognized by their white colored colonies on the indicator plates [LB, Ampicillin (100µg/ml), IPTG (0.5mM) and X-Gal (80µg/ml) agar plates], where twenty clones were picked up for gene sequencing. On the other hand, unsuccessful cloning of TrxATII gene was represented by the blue colonies.

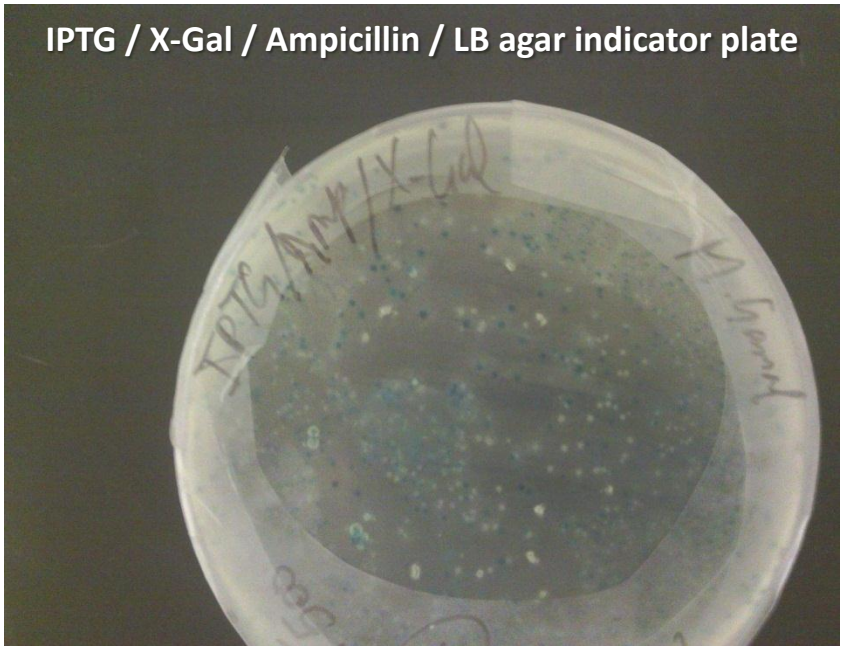

Figure 23: Recombinant TrxATII Clones of Top 10 *E. coli*

Showing recombinant white colonies comprising pGEM vector with thioredoxin insert on indicator plates [LB, Ampicillin (100µg/ml), IPTG (0.5mM) and X-Gal (80µg/ml) agar plates], while blue colonies represent the unsuccessful cloning of TrxATII gene.

3. TrxATII gene Sequencing

3.1 Plasmid Extraction (pGEM®-T Easy Vector)

To sequence the TrxATII gene, we extracted the pGEM®-T Easy plasmid from the picked white colonies, where each picked colony sub-cultured in a separate falcon tube containing LB broth/Ampicillin (100µg/ml) overnight at 37°C with shaking at ~ 200 rpm. For plasmid extraction, we have used the PureYield™ Plasmid Miniprep System (Cat.No.A1223, Promega). As shown in **Figure 24**, the twenty plasmids were analyzed on 0.8% agarose gel electrophoresis showing clear bands at the expected size ~ 3540 bp; 3000 bp for pGEM vector plus 540 bp for TrxATII insert.

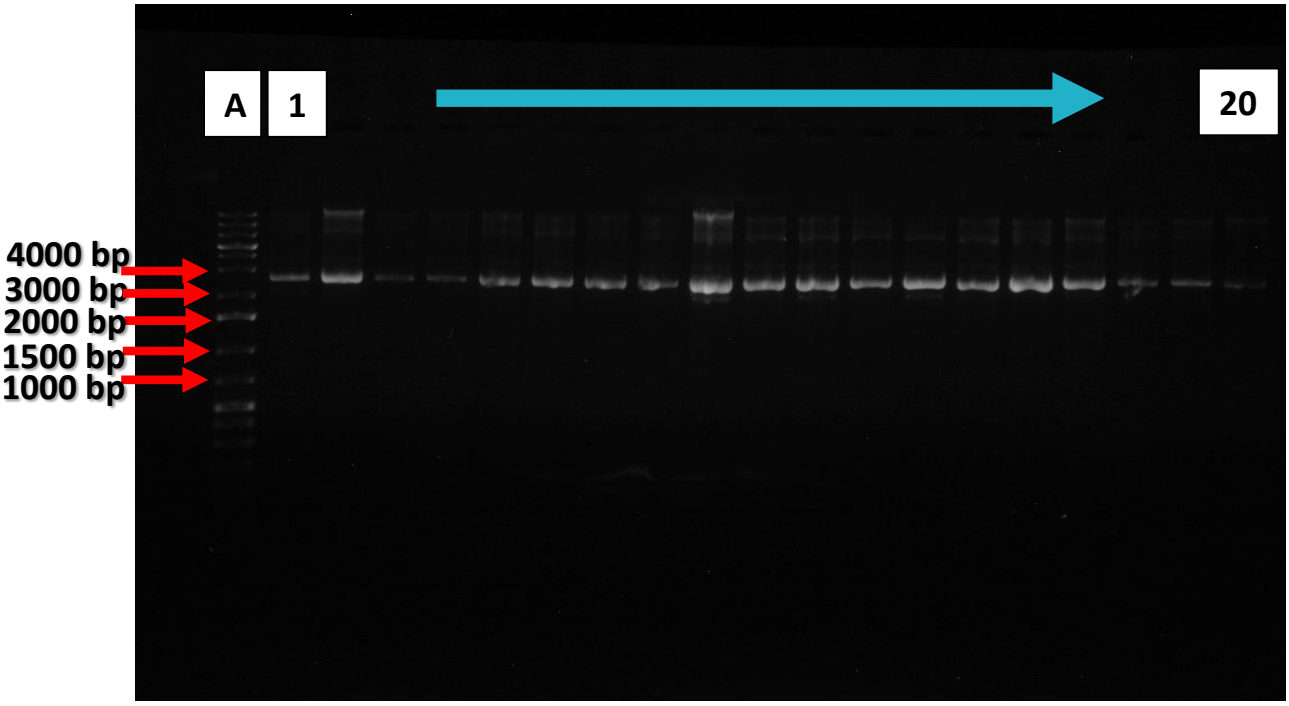

Figure 24: 0.8 % Agarose Gel Electrophoresis for pGEM vector comprising TrxATII gene

Lane A; Reference molecular weight ladder; Thermo Scientific GeneRuler 1 kb Plus DNA Ladder (Cat. No. # SM1331). Lanes from 1 till 20 are showing extracted pGEM T plasmids comprising TrxATII gene at ~ 3540 bp.

For furthermore confirmation, PCR reaction was performed with the previously mentioned conditions on the twenty extracted pGEM plasmids using thioredoxin primers (Forward and Reverse) and analyzed on 0.8% agarose gel electrophoresis as shown in **Figure 25**.

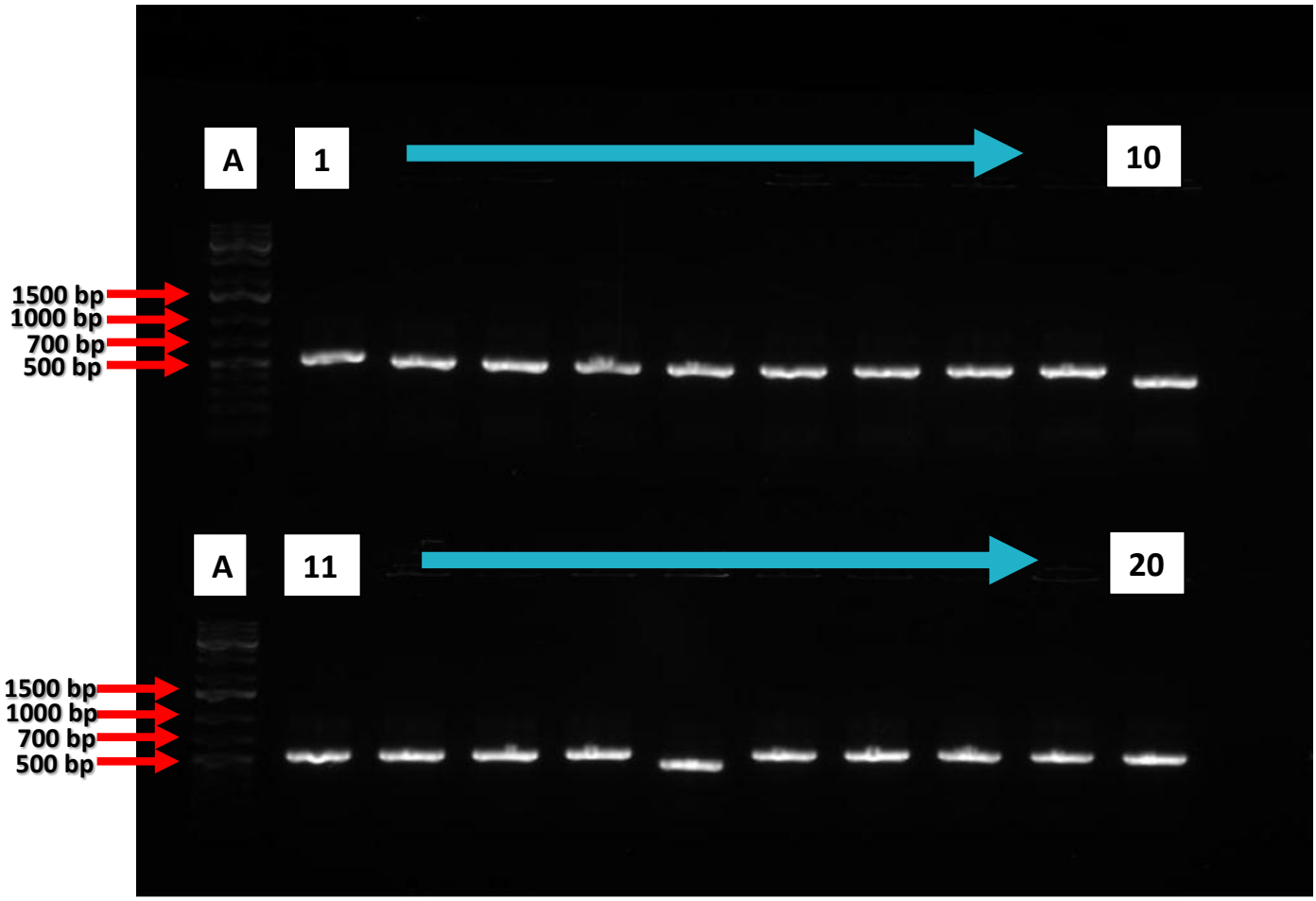

Figure 25: 0.8 % Agarose Gel Electrophoresis for TrxATII gene

Lane A; Reference molecular weight ladder; Thermo Scientific GeneRuler 1 kb Plus DNA Ladder (Cat. No. # SM1331). Lanes from 1 till 20 are showing amplified TrxATII gene from pGEM vector at its proper size ~ 540 bp.

3.2 Sequence analysis of TrxATII

TrxATII sequence that has been generated from Applied Biosystems 3730xl DNA Analyzer machine was BLASTed against non-redundant (nr) protein databases using Basic Local Alignment Search Tool (BLASTP) provided by the National Center for Biotechnology Information (NCBI). The protein sequence of TrxATII is shown in **Figure 26**.

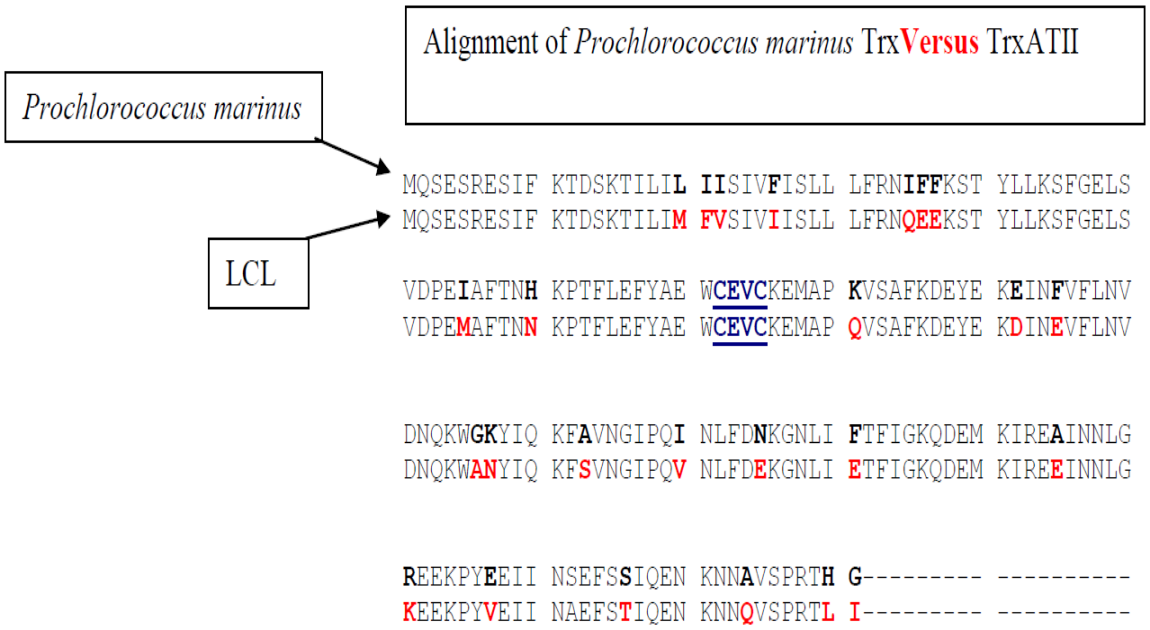

Figure 26: Amino acid sequence of TrxATII Vs *Prochlorococcus marinus* Trx

The figure is showing the TrxATII sequence, where there are 25 amino acid difference (highlighted in red) than the first hit (*Prochlorococcus marinus* Trx). Additionally, the Trx active site ($C^{72:}$ C^{75}) is highlighted in blue color.

Moreover, using ClustalW version 2.1, we have performed a multiple sequence alignment of TrxATII with other members of the Trx super family: *Prochlorococcus marinus, Synechococcus sp, Cyanobium sp, Lyngbya sp.*, where the alignment showed the conserved catalytic active site of Trx Super Family (**Figure 27).**

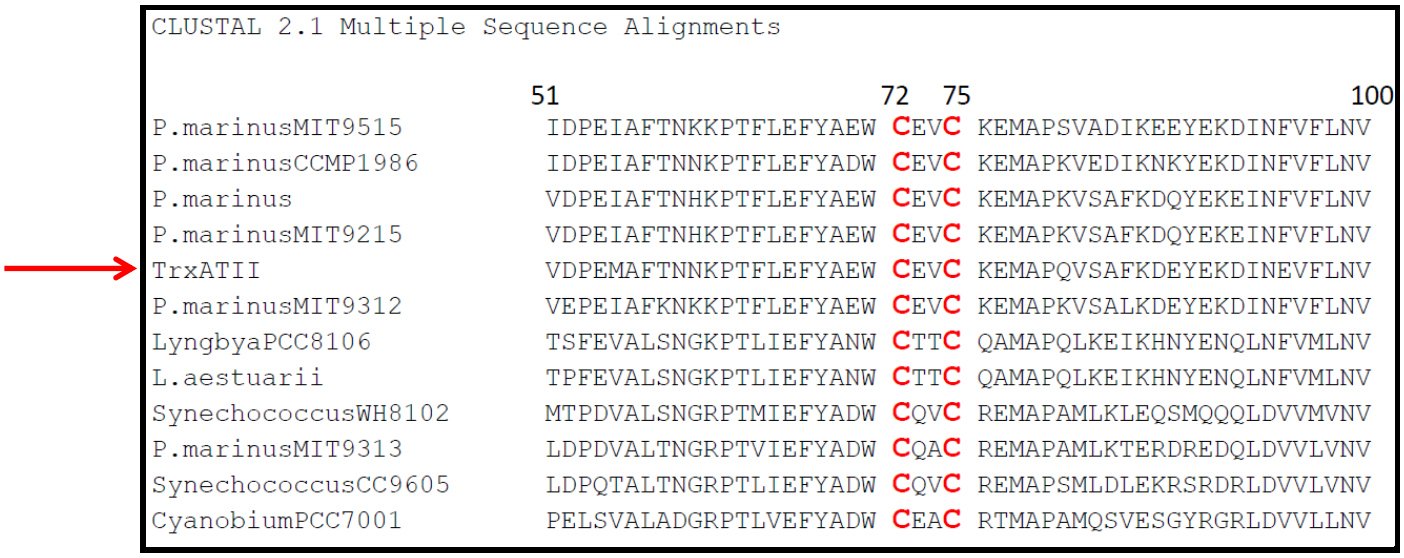

```
CLUSTAL 2.1 Multiple Sequence Alignments

                        51                        72  75                        100
P.marinusMIT9515         IDPEIAFTNKKPTFLEFYAEW CEVC KEMAPSVADIKEEYEKDINFVFLNV
P.marinusCCMP1986        IDPEIAFTNNKPTFLEFYADW CEVC KEMAPKVEDIKNKYEKDINFVFLNV
P.marinus                VDPEIAFTNHKPTFLEFYAEW CEVC KEMAPKVSAFKDQYEKEINFVFLNV
P.marinusMIT9215         VDPEIAFTNHKPTFLEFYAEW CEVC KEMAPKVSAFKDQYEKEINFVFLNV
TrxATII                  VDPEMAFTNNKPTFLEFYAEW CEVC KEMAPQVSAFKDEYEKDINEVFLNV
P.marinusMIT9312         VEPEIAFKNKKPTFLEFYAEW CEVC KEMAPKVSALKDEYEKDINFVFLNV
LyngbyaPCC8106           TSFEVALSNGKPTLIEFYANW CTTC QAMAPQLKEIKHNYENQLNFVMLNV
L.aestuarii              TPFEVALSNGKPTLIEFYANW CTTC QAMAPQLKEIKHNYENQLNFVMLNV
SynechococcusWH8102      MTPDVALSNGRPTMIEFYADW CQVC REMAPAMLKLEQSMQQQLDVVMVNV
P.marinusMIT9313         LDPDVALTNGRPTVIEFYADW CQAC REMAPAMLKTERDREDQLDVVLVNV
SynechococcusCC9605      LDPQTALTNGRPTLIEFYADW CQVC REMAPSMLDLEKRSRDRLDVVLVNV
CyanobiumPCC7001         PELSVALADGRPTLVEFYADW CEAC RTMAPAMQSVESGYRGRLDVVLLNV
```

Figure 27: Conserved Catalytic Active Site of Trx Super Family

Multiple sequence alignment of TrxATII with other members of the Trx super family: *Prochlorococcus marinus, Synechococcus sp, Cyanobium sp, Lyngbya sp.* was performed using ClustalW version 2.1. The alignment shows the conserved catalytic active site of Trx Super Family, where they have two vicinal cysteines (highlighted in red) comprising in between other two amino acids.

Additionally, a pairwise alignment for TrxATII against the first hit; *Prochlorococcus marinus* Trx (accession number WP_002807427.1) was generated**.** Interestingly, the alignment has shown 25 (14%) amino acids difference. Within the 25 amino acids difference, we have noticed that there are 7 acidic residues in TrxATII versus 2 residues in Trx *Prochlorococcus marinus* and 1 basic residue in TrxATII versus 5 residues in *Prochlorococcus marinus* **(Figure 28)**.

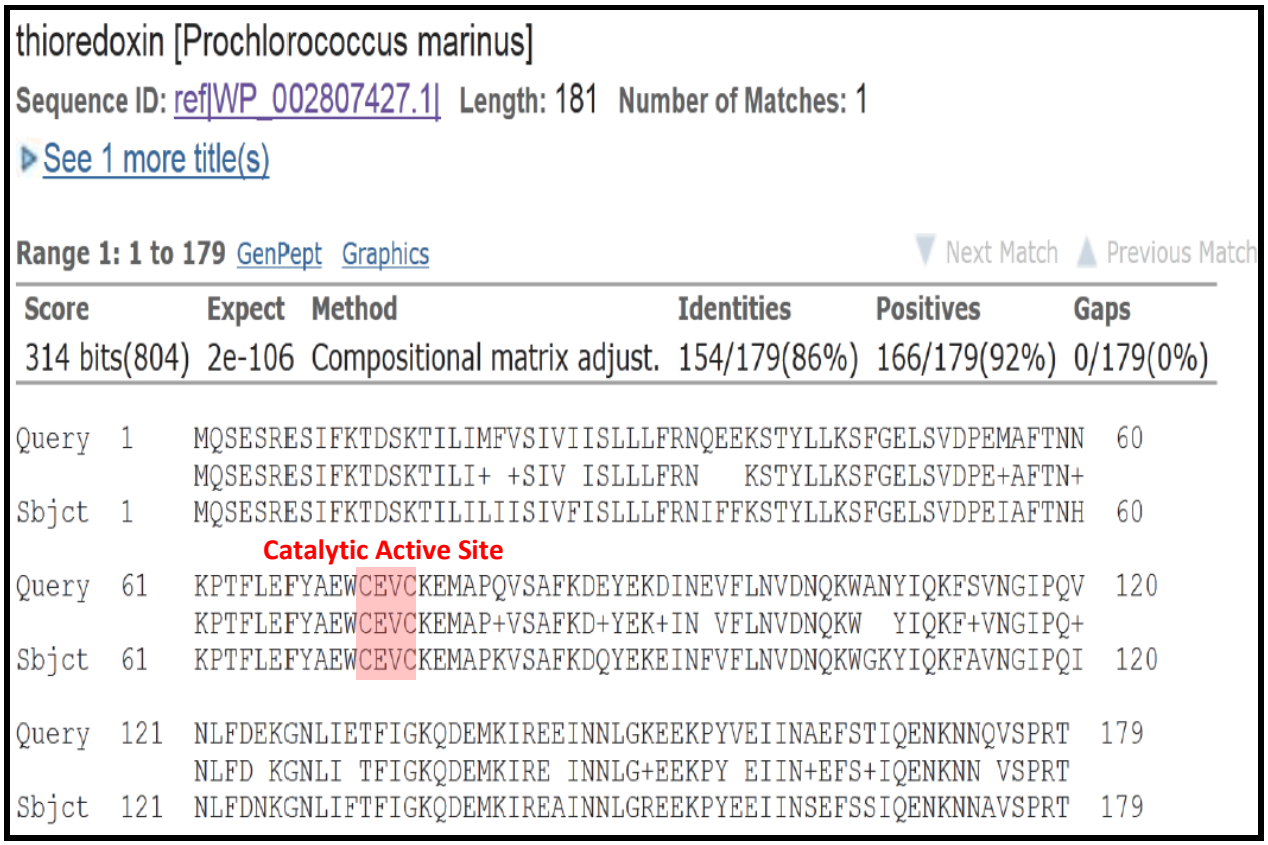

Figure 28: Alignment of TrxATII with best hit

Alignment with the best hit thioredoxin protein from *Prochlorococcus marinus* showed maximum identity 86%, the highest among all

3.3 3D modeling of Trx (ATII versus *Prochlorococcus marinus*)

The 3D modeling of Trx motif has shown the catalytic active site (– Cys^{72} – Glu^{73} – Val^{74} – Cys^{75}–) (**Figure 29).**

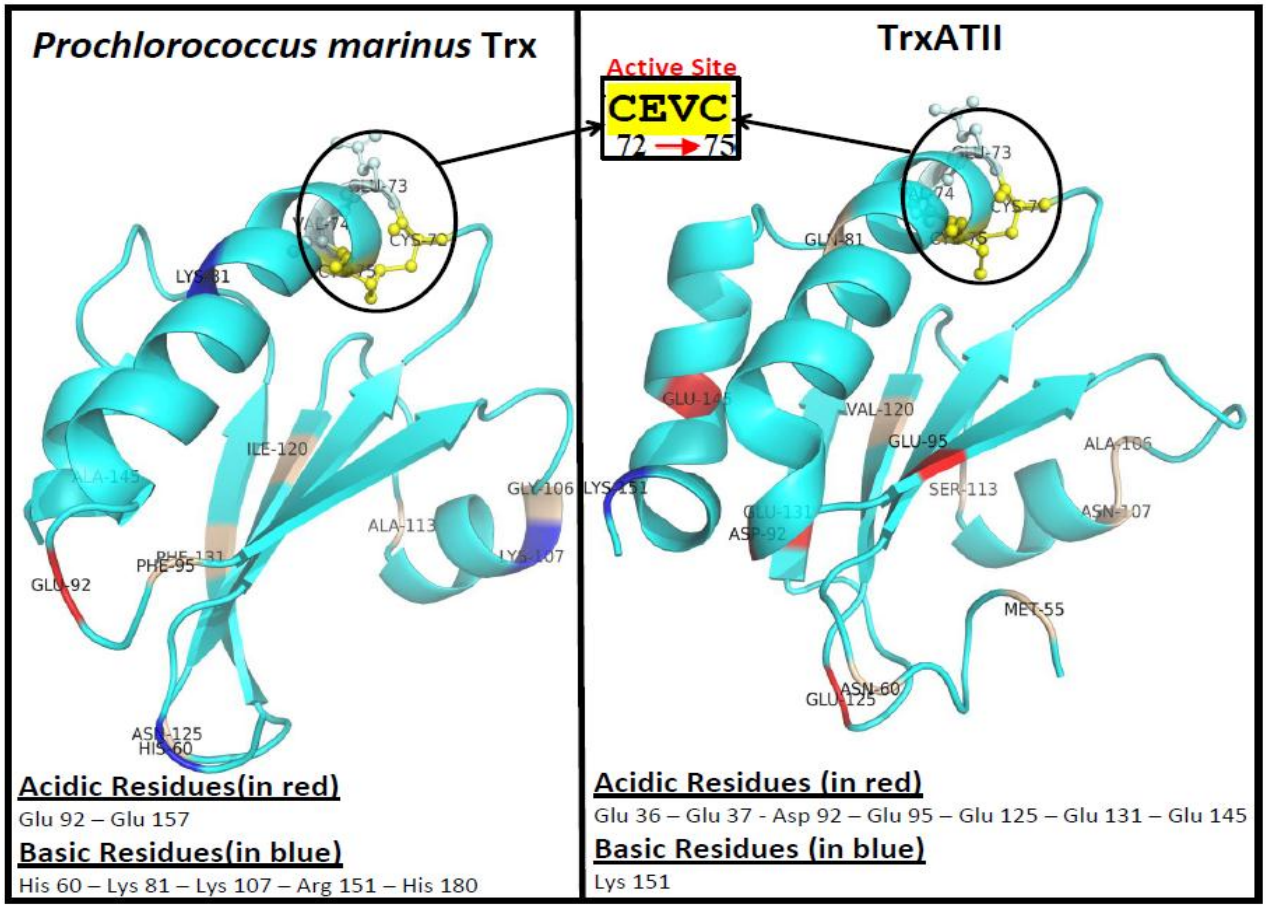

Figure 29: 3D modeling of Trx (ATII versus *Prochlorococcus marinus*)

The 3D modeling is showing the Trx active site (– Cys^{72} – Glu^{73} – Val^{74} – Cys^{75}–) in both ATII and *Prochlorococcus marinus.* Additionally, among the 25 amino acids difference between them, there are 7 acidic residues in TrxATII versus 2 residues in Trx *Prochlorococcus marinus* and 1 basic residue in TrxATII versus 5 residues in *Prochlorococcus marinus.*

3.4 Construction of Phylogenetic tree

The generated phylogenetic tree (**Figure 30)** showed that TrxATII sequence is highly similar to different strains of *Prochlorococcus marinus* Trx. **Table 3** lists the sequence identifiers used to compute the tree. The TrxATII is clustered in the clade of different strains of *Prochlorococcus marinus* Trx, which is evidence for the various stress conditions at the LCL that requires the TrxATII. Moreover, TrxATII modified to accommodate the harsh conditions; thermohalophilicity at the sea bed.

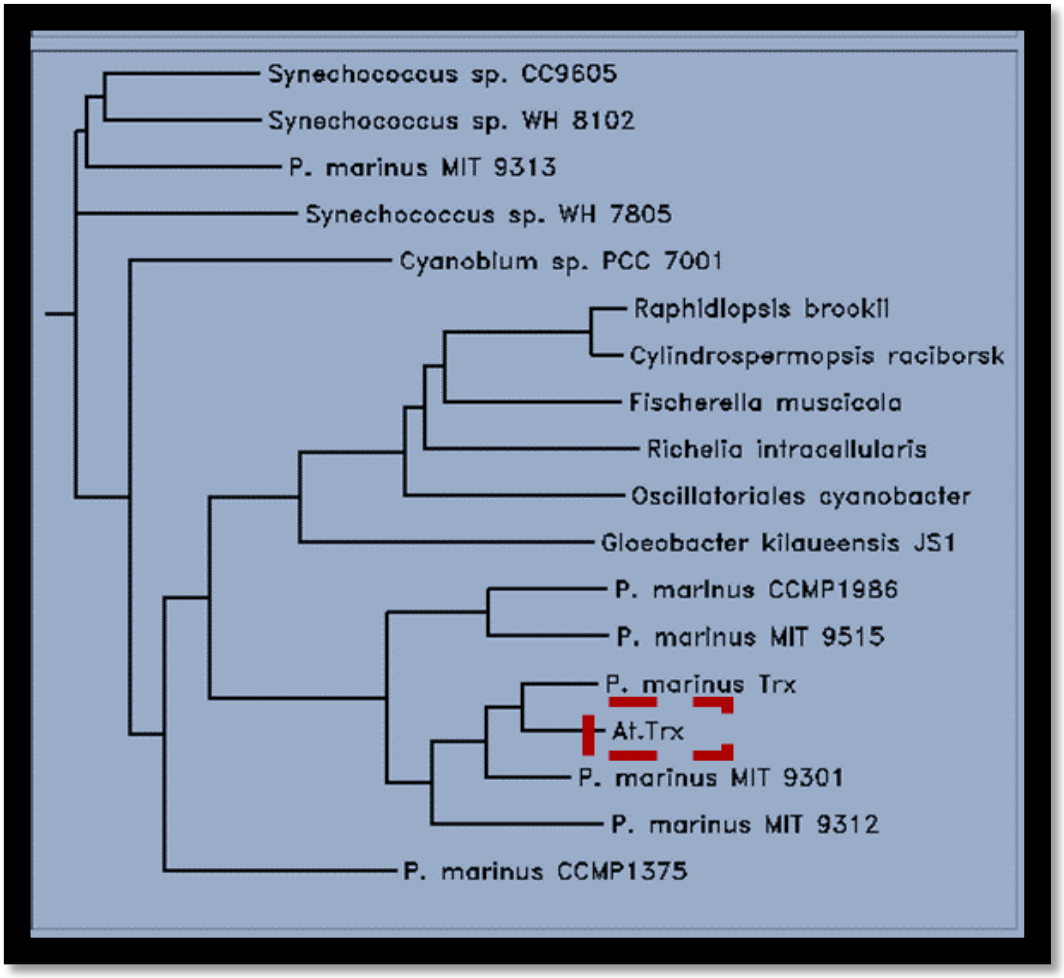

Figure 30: TrxATII Phylogenetic tree

A Phylogenetic tree for the TrxATII was constructed using CLUSTALW version 2.1 [77,78] . The generated tree is Neighbour-joining tree including the sequences most similar to the TrxATII sequence.

Table 3: Organisms used in Phylogenetic tree

Organism	Accession Numbers
Synechococcus sp. CC9605	ref|YP_380605.1|
Synechococcus sp. WH 8102	ref|NP_896375.1|
Prochlorococcus marinus str. MIT 9313	ref|NP_895653.1|
Synechococcus sp. WH 7805	ref|WP_006042318.1|
Cyanobium sp. PCC 7001	ref|WP_006911410.1|
Raphidiopsis brookii	ref|WP_009341404.1|
Cylindrospermopsis raciborskii	ref|WP_006277703.1|
Fischerella muscicola	ref|WP_016866661.1|
Richelia intracellularis	ref|WP_008234229.1|
Oscillatoriales cyanobacterium JSC-12	ref|WP_009556771.1|
Gloeobacter kilaueensis JS1	ref|YP_008713253.1|
Prochlorococcus marinus subsp. pastoris str. CCMP1986	ref|NP_892361.1|
Prochlorococcus marinus str. MIT 9515	ref|YP_001010591.1|
Prochlorococcus marinus	ref|WP_002807427.1|
Prochlorococcus marinus str. MIT 9301	ref|YP_001090489.1|
Prochlorococcus marinus str. MIT 9312	ref|YP_396741.1|
Prochlorococcus marinus subsp. marinus str. CCMP1375	ref|NP_874666.1|

4. Transformed TrxATII clones (pET SUMO® Vector)

Successful cloning of TrxATII gene into the pET SUMO® expression vector, allows the growth of the white colonies of the transformed BL21 (DE3) *E. coli* cells on their indicator plates [LB / Kanamycin (50µg/ml)] as shown in **Figure 31.**

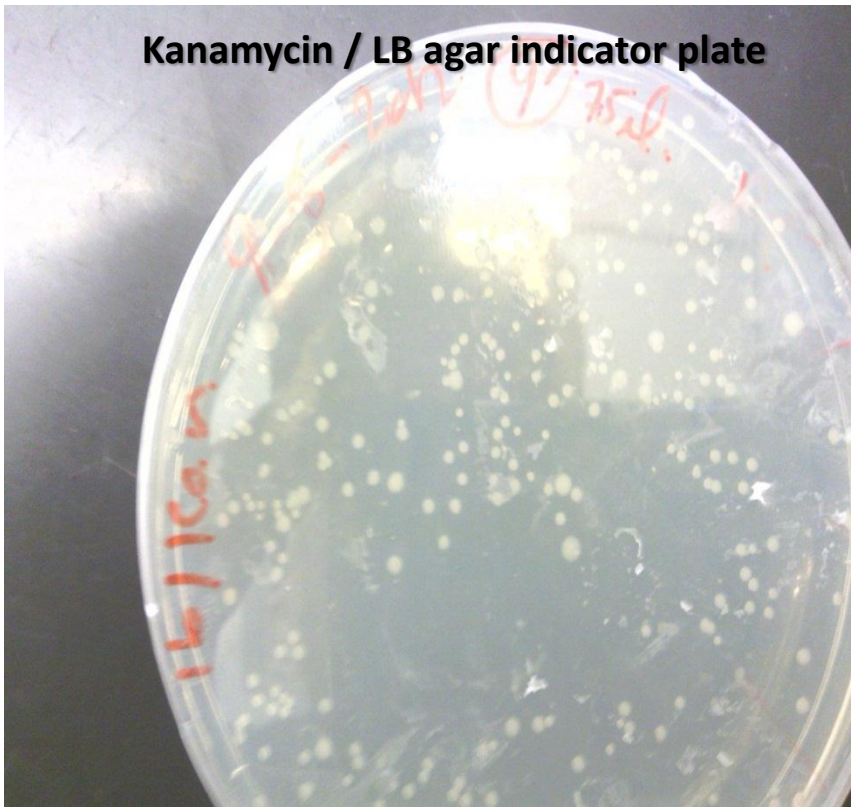

Figure 31: Transformant TrxATII Clones of BL21 (DE3) *E. coli*

The transformed white colonies are spread on the whole plate, comprising pET SUMO vector with TrxATII insert on indicator plates [LB / Kanamycin (50µg/ml)].

4.1 Analyzing Transformants

To analyze the transformed BL21 (DE3) *E. coli*, PCR reaction was performed on five clones, where each picked colony sub-cultured in a separate falcon tube containing LB broth/kanamycin (50µg/ml) overnight at 37°C with shaking at ~ 200 rpm. The PCR conditions performed as previously mentioned using the thioredoxin primers (Forward and Reverse) and analyzed on 0.8% agarose gel electrophoresis. As shown in **Figure 32**, the amplified TrxATII gene band appeared clearly at its proper size ~ 540 bp. in all the picked colonies.

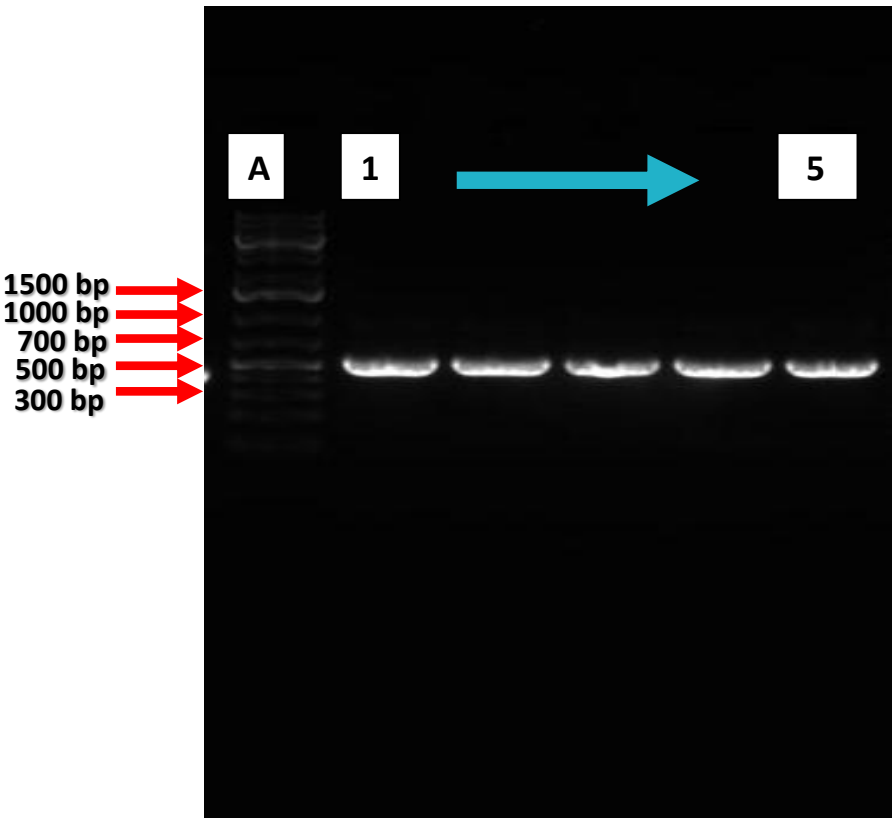

Figure 32: 0.8 % Agarose Gel Electrophoresis for TrxATII gene in pET SUMO® Vector

Lane A; Reference molecular weight ladder; Thermo Scientific GeneRuler 1 kb Plus DNA Ladder (Cat. No. # SM1331). Lanes from 1 till 5 are showing amplified from TrxATII gene from pET SUMO vector at its proper size ~ 540 bp.

5. IPTG-inducible Expression of TrxATII

During the inducible expression of the recombinant TrxATII protein using isopropyl β-D-thiogalactoside (IPTG), 4 samples were collected to be analyzed on the SDS-PAGE electrophoresis. Moreover, the 4 samples were as follow: *E. coli* expressed proteins before IPTG induction phase, *E. coli* expressed proteins after IPTG induction phase, non-induced *E. coli* pellets and induced *E. coli* pellets. As shown in **Figure 33**, both the induced pellets and induced proteins showed more intensified bands for TrxATII protein at its proper size ~ 12 KDa rather than that of the non-induced pellets and proteins.

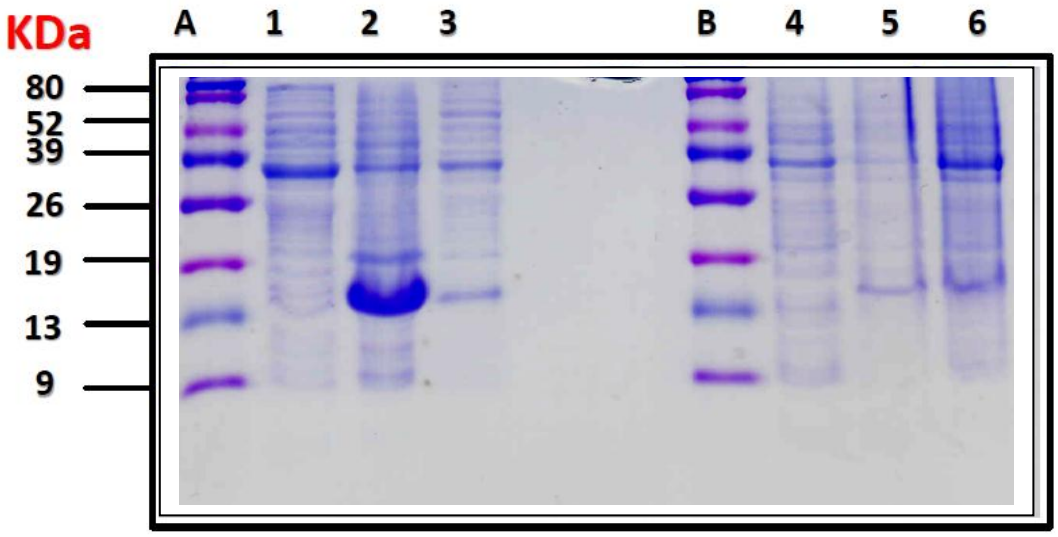

Figure 33: SDS-PAGE Electrophoresis for induced and non-induced TrxATII

Lane A and B show ProSieve®Color Protein Markers (Cat. No.50550, Lonza).
Lane 1 shows *E. coli* non-induced TrxATII overnight.
Lane 2 shows *E. coli* induced TrxATII overnight.
Lane 3 shows *E. coli* induced TrxATII over 2 hours.
Lane 4 shows *E. coli* non-induced pellets.
Lane 5 shows *E. coli* induced pellets over 2 hours.
Lane 6 shows *E. coli* induced pellets overnight.

6. Purified TrxATII fractions

Purification of recombinant TrxATII protein was done against metal-chelating resin (Ni-NTA agarose resin, Cat.No.R901-15, Invitrogen™), where the Ni-NTA resin has high affinity and selectivity for 6xHis-tagged recombinant TrxATII protein. Different samples of purified TrxATII were taken for SDS-PAGE electrophoresis analysis. As shown in **Figure 34**, all *E. coli* proteins were washed out, while different fractions of the recombinant TrxATII protein was eluted and purified.

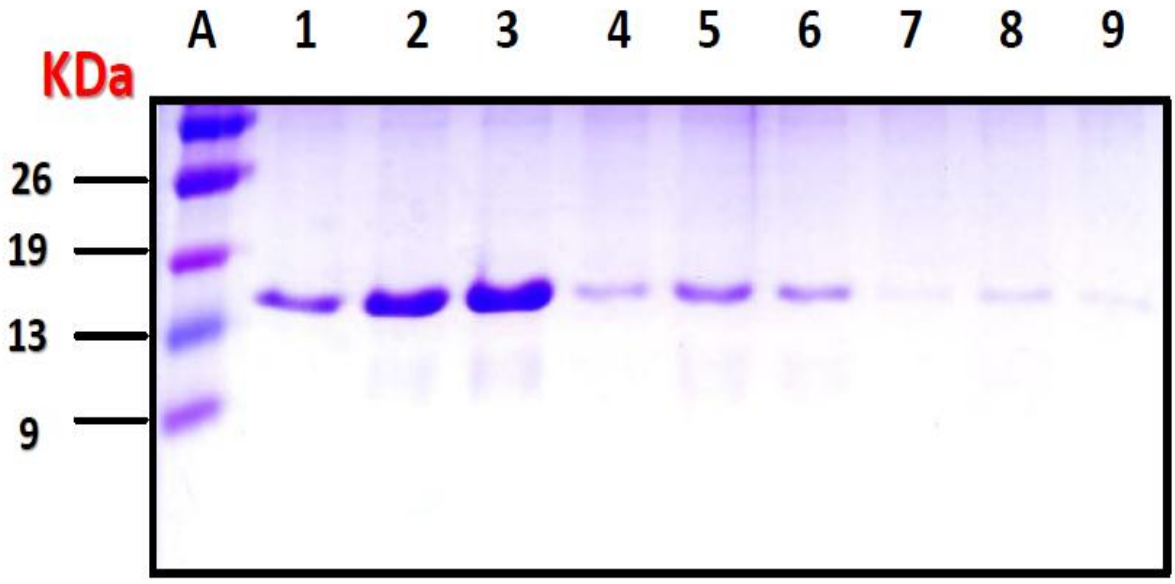

Figure 34: SDS-PAGE Electrophoresis for purified fractions of TrxATII

Lane A shows ProSieve®Color Protein Markers (Cat. No.50550, Lonza), while Lanes from 1 to 9 show purified fractions of TrxATII at ~ 16 KDa.

7. Quantification of TrxATII fractions

After dialysis, we quantified the concentration of TrxATII protein in each eluted fraction using the Thermo Scientific Pierce BCA Protein Assay (Cat.No.23225, Thermo SCIENTIFIC). As shown in **Figure 35**, we have got different concentrations for TrxATII fractions from different induction batches, where the highest concentration was 1303 µl/ml.

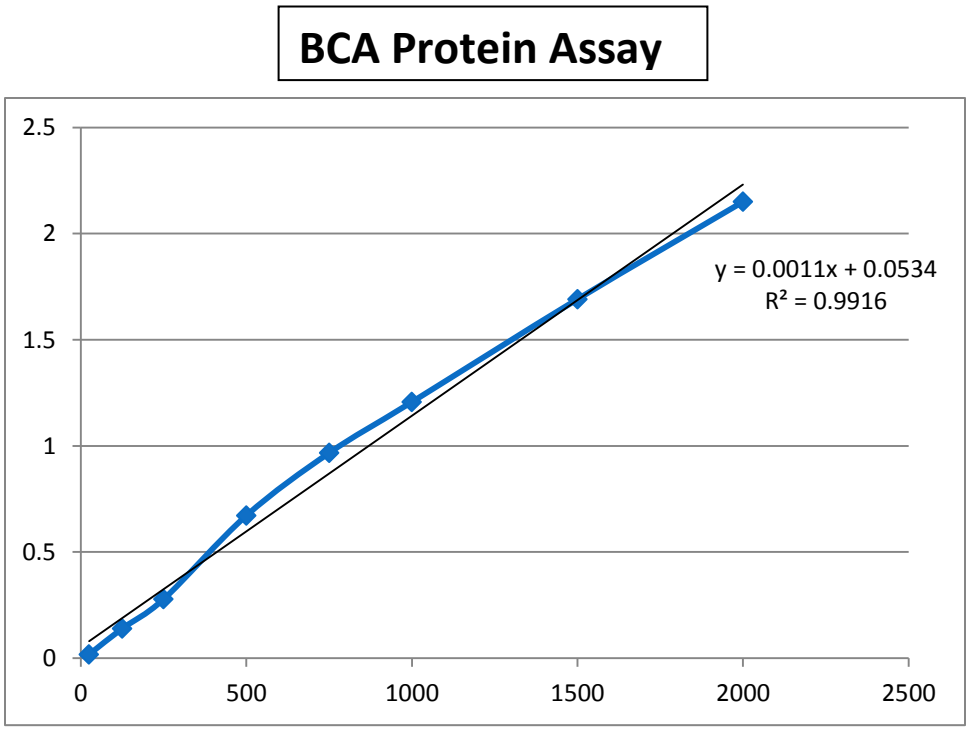

Figure 35: Quantification of TrxATII concentration

Using the Thermo Scientific Pierce BCA Protein Assay kit (Cat.No.23225, Thermo SCIENTIFIC), different concentrations for TrxATII fractions from different induction batches have been quantified after plotting the standard curve of BSA; 1303ug/ml, 216 ug/ml, 168 ug/ml and 125 ug/ml.

8. Cell Culture and MTT Assay

The oxidative stress conditions applied on the cell culture of the cancerous HepG2 cell line after pretreatment with different concentrations of the antioxidant TrxATII protein was maintained to assess the antioxidant role of TrxATII via MTT assay. After, the HepG2 cell line reached a confluence stage (after 24 hours incubation), we induced oxidative stress via different concentrations of H_2O_2 (100, 200, 800 and 1600 μM) for 4 hours. Additionally, we induced oxidative stress condition with the same concentrations of H_2O_2, but after the prior exposure to different TrxATII concentrations (1, 2.5 and 5 μM) for 1 hour. Morphologically under the inverted microscope and 20X magnification power, HepG2 cells show full attachment after 24 hours incubation with RPMI 1640 media as shown in **Figure 36 A**, while the cells detached and became more rounded upon incubation with different concentration of H_2O_2 (100, 200, 800 and 1600 μM) for 4 hours as shown in **Figure 36 B1, C1, D1 and E1**. Moreover, the pre-incubation of the HepG2 cells with TrxATII protein (5 μM) for 1 hour prior oxidative stress induction, shows less detachment with much better survival rather than the oxidative stress conditions only as shown in **Figure 36 B2, C2, D2** and **E2**. Although, we have examined different concentrations of TrxATII protein (1, 2.5, 5μM), the optimum antioxidant concentration that reduced the oxidative stress and showed better cell survival percentage was the 5 μM. Furthermore, in the MTT assay, the exposure of the HepG2 cells to 5μM TrxATII for 1 hour prior the oxidative stress exposure for 4 hours showed survival advantage as shown in **Figure 37.** At 100μM, 200μM, 800μM and 1600μM H2O2, the survival were 87%, 64%, 8% and 3.5% respectively. On the other hand, the pretreatment with 5μM TrxATII improved the survival to 89%, 69%, 10.7% and 8.8 respectively **(Figure 37).**

A

B 1

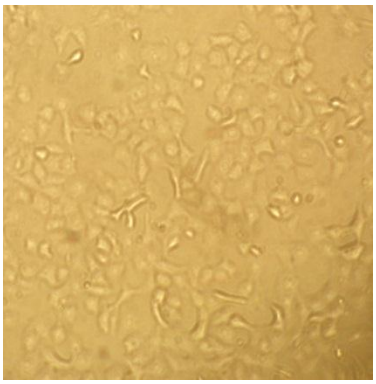

B 2

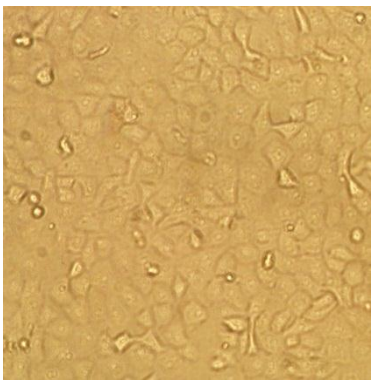

C 1

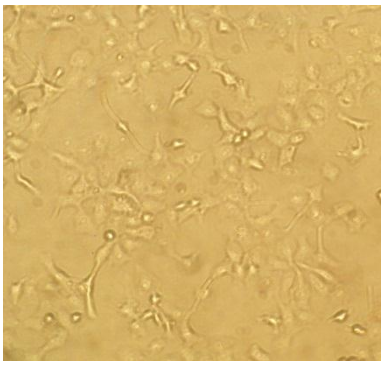

C 2

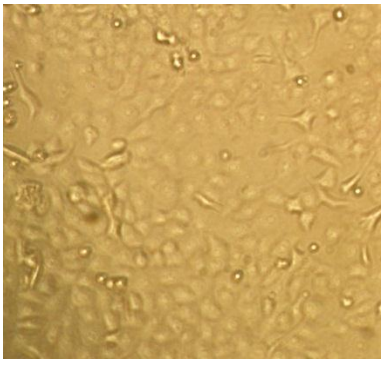

D 1

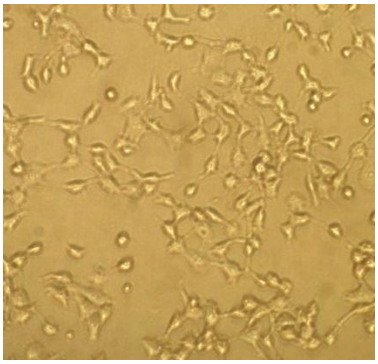

D 2

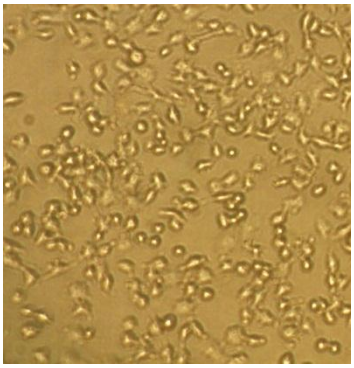

E 1

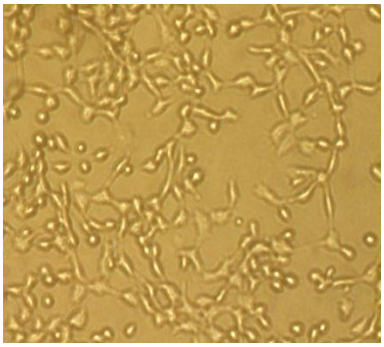

E 2

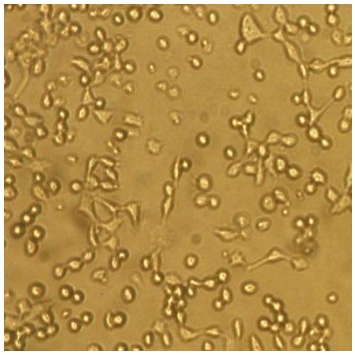

Figure 36: Morphology of HepG2 cells upon induction of oxidative stress conditions using H2O2 (100µM, 200 µM, 800 µM and 1600 µM) in presence and absence of 5µM TrxATII under 20x magnification power.

(A) Confluent sheath of HepG2 cells after 24 hours incubation in RPMI 1640 media.
(B1) HepG2 cells after 4 hours incubation with 100µM H_2O_2
(B2) HepG2 cells after 1 hour exposure to 5µM TrxATII then 4 hours incubation with 100µM H_2O_2
(C1) HepG2 cells after 4 hours incubation with 200µM H_2O_2
(C2) HepG2 cells after 1 hour exposure to 5µM TrxATII then 4 hours incubation with 200µM H_2O_2
(D1) HepG2 cells after 4 hours incubation with 800µM H_2O_2
(D2) HepG2 cells after 1 hour exposure to 5µM TrxATII then 4 hours incubation with 800µM H_2O_2
(E1) HepG2 cells after 4 hours incubation with 1600µM H_2O_2
(E2) HepG2 cells after 1 hour exposure to5µM TrxATII then 4 hours incubation with 1600µM H_2O_2

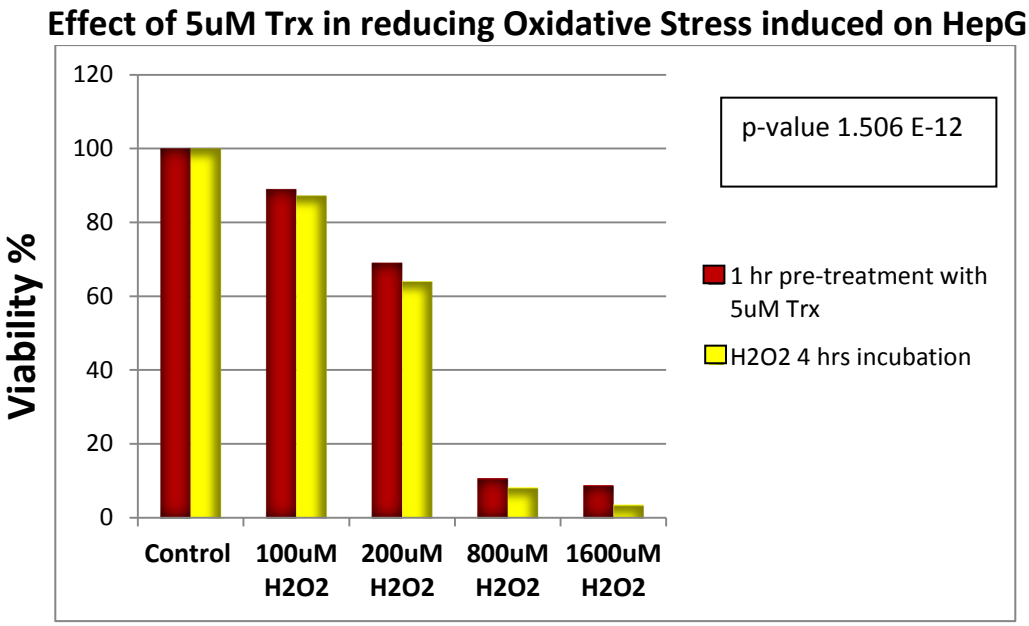

Figure 37: Effect of 5uM TrxATII in reducing Oxidative Stress induced on HepG2

Cell survival of HepG2 cells after exposure to oxidative stress conditions for 4 hrs, as per MTT assay. Left to right: (1) Control untreated HepG2 cells, (2) 100uM H2O2, (3) 200uM H2O2, (4) 800uM H2O2, and (5) 1600uM H2O2. The presented data are mean of three independent experiments, where each concentration is mean of three. The p-value = 1.506 E-12 and the p-value range < 0.001 were computed by ANOVA R© version 2.14.1, a statistical analysis program.

9. Redox Activity and Characterization of TrxATII

9.1 Redox Activity at room temperature

To examine the redox activity of TrxATII, we have performed the insulin reduction assay at room temperature as described in the materials and methods. As shown in **Figure 38**, the absorbance increased rapidly at 650 nm, demonstrating the successful reduction of insulin via disulfide bond exchange with TrxATII.

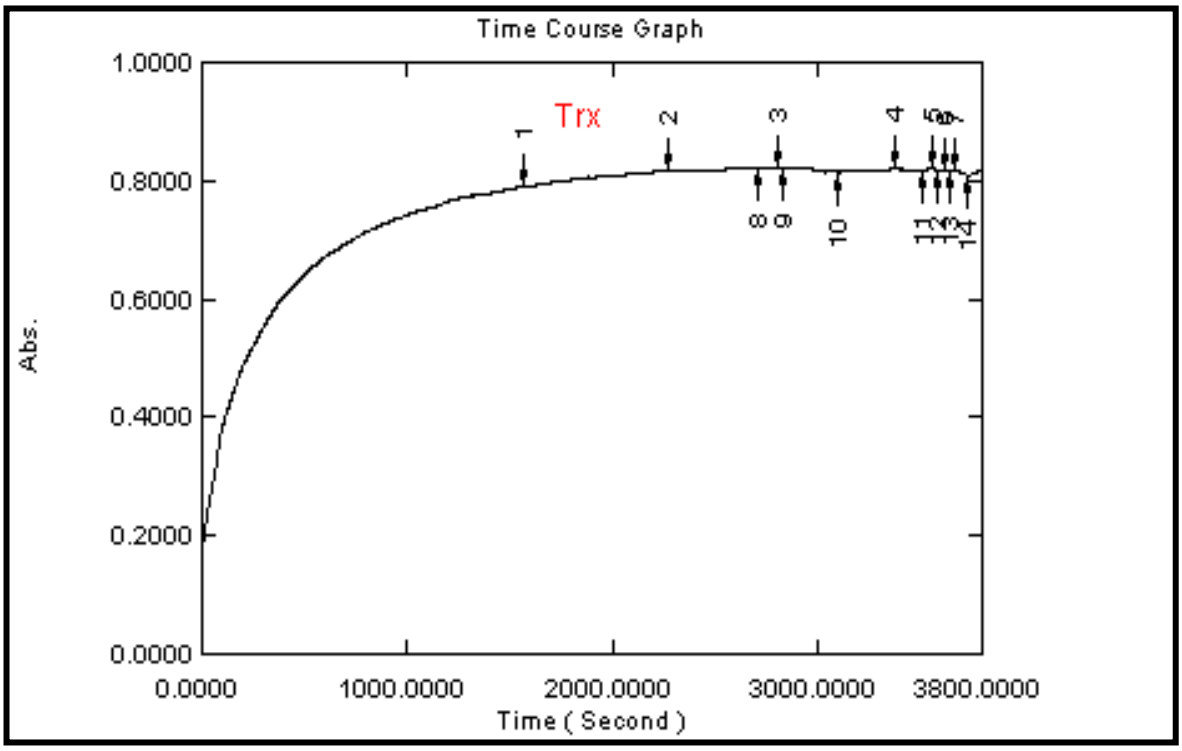

Figure 38: Redox activity of TrxATII at room temperatures

The redox activity of TrxATII was assayed at room temperature via insulin reduction assay, where the aggregation of insulin was measured spectrophotomerically at 650 nm. It is clear that the absorbance increased rapidly until the insulin consumed, then formed a plateau.

9.2 Thermostability

The effect of increasing temperature on the activity of TrxATII was assayed, where Trx was incubated at range of temperatures (25°C to 80°C) for 10 minutes after which the residual activity was assessed by the insulin reduction assay, where the aggregation of insulin was measured spectrophotomerically at 650 nm. As shown in **Figure 39,** the residual activity of TrxATII was 100 %, 100 %, 97.23 %, 90.59 %, 65.57 %, and 10.25% at 25 °C, 37 °C, 50 °C, 60 °C, 70 °C, and 80 °C respectively.

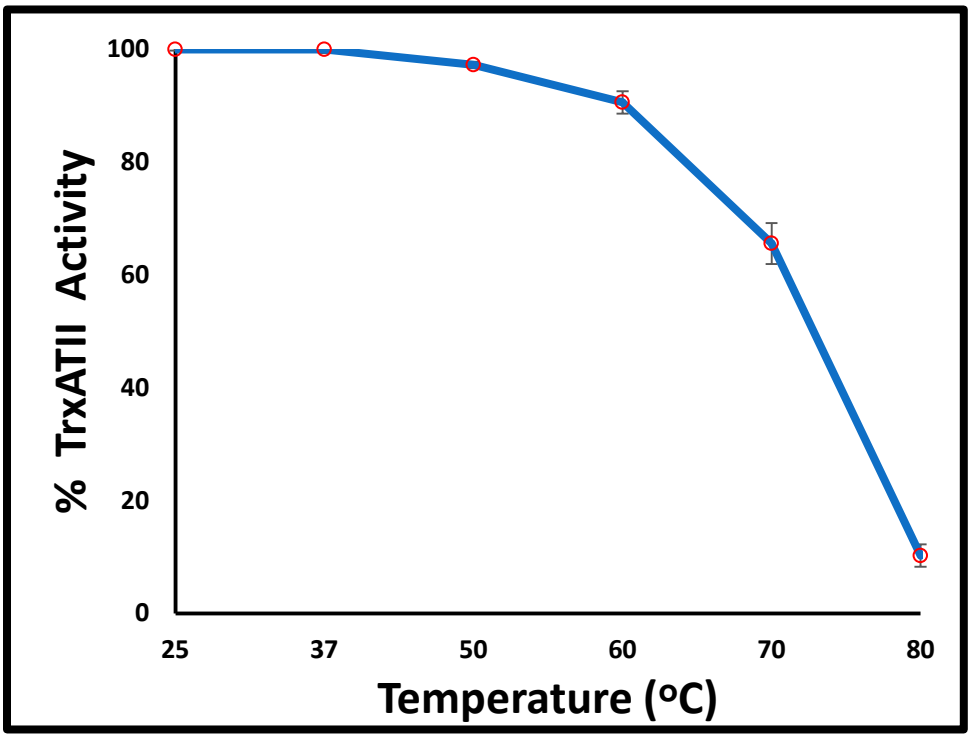

Figure 39: Redox activity of TrxATII at different temperatures (Thermostability)

After incubating thioredoxin at different temperatures (25 °C – 80 °C), the residual activity of thioredoxin was assayed via insulin reduction assay, where the aggregation of insulin was measured spectrophotomerically at 650 nm. It is clear that the residual activity of thioredoxin was 100 %, 100 %, 97.23 %, 90.59 %, 65.57 %, and 10.25 % at 25 °C, 37 °C, 50 °C, 60 °C, 70 °C, and 80 °C respectively.

9.3 Halophilicity

The effect of NaCl concentration on the redox activity of TrxATII was assayed at different molar concentrations of NaCl (0.5M – 4M) using the insulin reduction assay. As Shown in **Figure 40**, the redox activity of TrxATII increased gradually from 6.09 uM/min/mg at 0.5M NaCl to reach its maximum (30.15 uM/min/mg) at 2.5M NaCl, and then shows gradual decrease in redox activity till the lowest activity (0.54 uM/min/mg) at 4M NaCl.

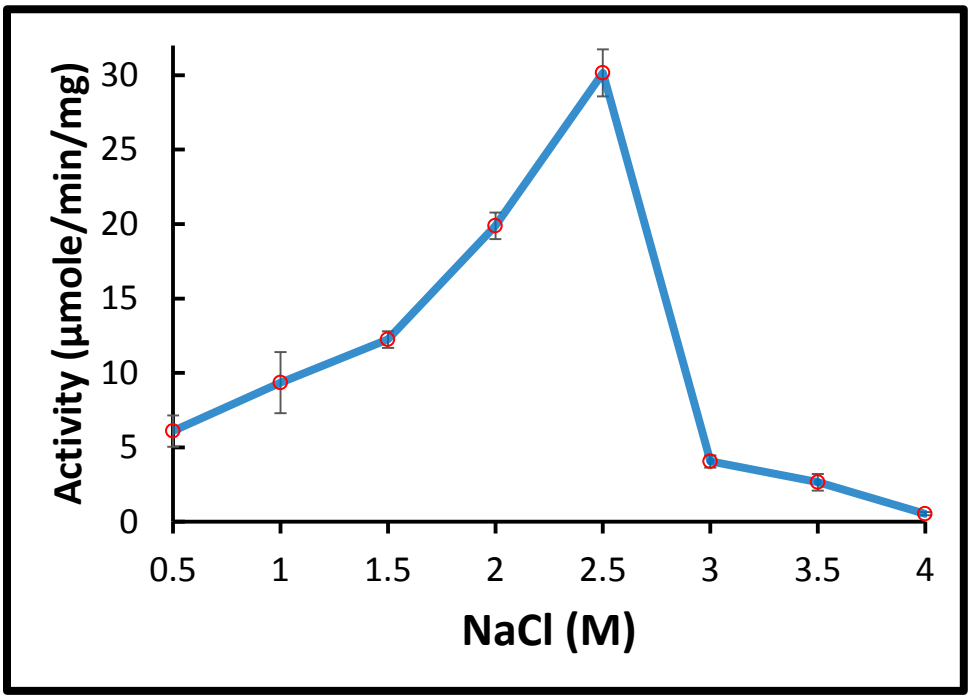

Figure 40: Redox activity of TrxATII at different NaCl molar concentrations (Halophilicity)

The effect of NaCl concentration on the redox activity of TrxATII was assayed at concentrations 0.5M – 4M using the insulin reduction assay. The redox activity of TrxATII increased gradually from 6.09 uM/min/mg at 0.5M NaCl to reach its maximum (30.15 uM/min/mg) at 2.5M NaCl, and then shows gradual decrease in redox activity till the lowest activity (0.54 uM/min/mg) at 4M NaCl.

10. Kinetic parameters of TrxATII

The kinetic parameters were determined (shown in **Table 4**) as described in Materials and Methods. The K_m and K_{cat} for TrxATII was 1.23 µM and 25.74 S^{-1} respectively, while the K_m and K_{cat} for DTNB was 95.72 µM and 15.34 S^{-1} respectively. By comparing our kinetic parameters versus other thermostable Trx system; aerobic hyperthermophilic archaeon *Aeropyrum pernix* K1, the K_m and K_{cat} for Trx was 12.3 µM and 63.2 S^{-1} respectively, while the K_m and K_{cat} for DTNB was 172.4 µM and 9 S^{-1} respectively[83]. Thus, it is clear that the number of *Aeropyrum pernix* Trx molecules turned over per enzyme molecule per second (63.2 S^{-1}) is more than double of that of TrxATII (25.74 S^{-1}). Basically, the reason behind that is the source of TrxR used in our DTNB assay, where it is form *E.coli* source (Cat. No.TR-01, IMCO Corporation Ltd AB) and not from the same environment of TrxATII; Atlantis II brine pool, which could lead to a kind of incompatibility.

Table 4: Kinetics of TrxATII using DTNB assay

Assay	Substrate	K_m (µM)	K_{cat} (S^{-1})
DTNB	**TrxATII** (0.2-12 µM)	1.23	25.74
DTNB	**DTNB** (0.01-1 mM)	95.72	15.34

The kinetic parameters were determined as described in Materials and Methods. The K_m value for TrxATII was determined at 0.2 – 12 µM TrxATII and 1 mM DTNB. Moreover, the K_m value for DTNB was determined at 0.01 – 1 mM DTNB and 4 µM TrxATII.

Chapter 4: Discussion

In this thesis work, we have characterized a novel thermohalophilic antioxidant TrxATII from the metagenome of the Lower Convective Layer (LCL) of the Atlantis II Deep brine pool in the Red Sea. Basically, the Atlantis II Deep is the biggest discovered brine pool in the Red Sea until now, about 6 x 13 Km [11] . The environment of the LCL has unusual blend of tough conditions; extremely high temperature that reaches 68.2°C, salinity of about 26%, which is 7.5 folds more than that of other seas and its pH value is 5.3 [5, 10]. Furthermore, the LCL of Atlantis II Deep is almost oxygen depleted environment (anoxic) and highly enriched with sulfides of iron, zinc, copper and other heavy metals, in addition to high value metals as silver, cobalt and gold [9, 10, 11]. That is why; it is very attractive spot to understand the structural and functional modifications of enzymes and proteins that have been adapted in sake of survival of the microbial communities in these harsh abiotic conditions, in addition to the expectation to discover novel genes, proteins and metabolic pathways that can be conveniently applied in the industry of biotechnology or pharmaceuticals. In this study, we have characterized TrxATII. To the best of our knowledge, this is first attempt to mine for thioredoxin protein from the Atlantis II Deep.

TrxATII gene was retrieved directly from the metagenome of the LCL. For further characterization of TrxATII, we have induced high quantities via sub-cloning into a high copy number vector (pGEM®-T Easy), where we have selected the recombinant clones (White/Blue Screening) to be further analyzed and sequenced to identify the TrxATII. Futhermore, TrxATII similarity search against NCBI non-redundant protein database was done using the BLASTP (2.2.29)[98] (NCBI). The first best hit was thioredoxin protein from *Prochlorococcus marinus* [str. MIT 9202] (thioredoxin family protein) (Accession: WP_002807427.1) with maximum identity 86%, similarity up to 92% and coverage 98% of the query length, (Figure 40). Other hits were from other strains of *Prochlorococcus marinus*; MIT 9215, MIT 301, MIT 312, MIT 515, and AS

9601 as well as other species; *Synechoccus sp* (identity 44%), *Richelia sp* (identity 37%), *Oscillatoriales sp.* (identity 34%), *Lyngbya sp.* (identity 34%), *Cylindrospermopsis sp* (identity 33%),

Moreover, TrxATII protein's sequence showed the thioredoxin motif; two vicinal Cysteines comprising two amino acids in-between (CEVC), with the maximum identity of 86% with *Prochlorococcus marinus* (first hit). Interestingly, the TrxATII amino acid sequence differs from the first hit (Trx of *Prochlorococcus marinus*) by 14 % represented by 25 amino acids that changed the thermo-halophilicity properties of the protein, where the TrxATII has extra 7 acidic residues. Subsequently, upon performing activity assay of TrxATII, it showed redox activity at wide range of temperatures (25^{o}C to 80^{o}C) and at different molar concentrations of NaCl (0.5 – 4 M). In conclusion, it is clear that there is various stress conditions at the LCL of ATII that requires the presence of Trx. Moreover, TrxATII has been modified to accommodate the unique harsh condition at the LCL of Atlantis II brine pool at Red Sea via its thermo-halophilic nature.

This work supports the potentiality of the metagenomic approaches in identifying novel proteins with unique characteristics and potential applications from communities inhabiting extreme environments.

Chapter 5: Conclusion and Future Prospects

In conclusion, we have identified a novel TrxATII protein from the Atlantis II brine pool in the Red Sea. Sequence analysis of TrxATII revealed its difference from other thioredoxins, which has high impact on its thermophilic and halophilic characteristics. We are recommending further characterization of TrxRATII to understand the whole thioredoxin system at the Atlantis II brine pool.

Moreover, there is a room for research that could be conducted to complement this study. Basically, different points should be addressed;

1- Will the combination of the TrxRATII with the TrxATII improve the antioxidant profile of the whole Trx system?

2- During the in vitro assay of the TrxATII on the HepG2 cells, we introduced TrxATII to the cell culture. Does the cloning of both TrxATII gene and TrxRATII within the genome of the cell line improve the antioxidation profile (to implement the whole Trx system from ATII)?

3- If we examined another cell line, will the antioxidation activity of TrxATII be altered?

To wrap up, using recombinant TrxATII could have a wide range of potential therapeutic applications in different oxidative stress conditions as in cancer, which should be examined in various animal models as a potential antioxidant candidate.

References

1. Holmgren, A. Thioredoxin. Annu. Rev. Biochem., 54, 237–271 (1985).
2. Arner, E. S. and Holmgren, A. Physiological functions of thioredoxin and thioredoxin reductase. Eur. J. Biochem. 267, 6102–6109 (2000).
3. Holmgren, A. Thioredoxin and glutaredoxin systems. J. Biol. Chem. 264,13963–13966 (1989).
4. Uchiyama T. & Miyazaki K. Functional metagenomics for enzyme discovery: challenges to efficient screening. Current Opinion in Biotechnology 20, 616–622 (2009).
5. Antunes, A., Ngugi, D.K. & Stingl, U. Microbiology of the Red Sea (and other) deep-sea anoxic brine lakes. Environmental Microbiology Reports 3, 416–433 (2011)
6. http://en.wikipedia.org/wiki/Red_sea
7 . Qian, P.Y. et al. Vertical stratification of microbial communities in the Red Sea revealed by 16S rDNA pyrosequencing. ISME J 5, 507-18 (2010).
8. Ba¨cker H, Schoell M. New deeps with brines and metalliferous sediments in the Red Sea. Nature Phys Sci 240: 153–158 (1972).
9. http://krse.kaust.edu.sa/spring-2010/research.html
10. Bower, A.S. R/V Oceanus Voyage 449-6 Red Sea Atlantis II Deep Complex Area. Woods Hole Oceanog. Instit. Technical Report, WHOI-KAUST-CTR-2009-01 (2009).
11. Stephen A, Amy S, Raymond W., Vertical, horizontal, and temporal changes in temperature in the Atlantis II and Discovery hot brine pools, Red Sea. Elsevier, Deep-Sea Research I 64 118–128 (2012).
12. Brewer, P.G., Wilson, T.R.S., Murray, J.W., Munns, R.G., Densmore, C.D. Hydrographic observations on the Red Sea brines indicate a marked increasein temperature. Nature 231, 37–38 (1971).
13. Karlenius, T and Tonissen, K. Thioredoxin and Cancer: A Role for Thioredoxin in all States of Tumor Oxygenation. Cancers, 2, 209-232 (2010).
14. Holmgren, A. Thioredoxin. The Amino Acid Sequence of the Protein from Escherichia coli B. European J. Biochem. 6 475-484 (1968).
15. Eklund, H., Gleason, F.K. and Holmgren, A. Structural and functional relations among thioredoxins of different species. Proteins, 11, 13 - 28 (1991).
16. Weichsel, A., Gasdaska, J.R., Powis, G. & Montfort, W.R. Crystal structures of reduced, oxidized, and mutated human thioredoxins: evidence for a regulatory homodimer. Structure 4,735-751 (1996).
17. http://pfam.sanger.ac.uk/family/PF00085#tabview=tab0
18. Holmgren, A.Thioredoxin structure and mechanism: conformational changes on oxidation of the active-site sulfhydryls to a disulfide. Structure, 3, 239-243 (1995).
19. Martin, J. Thioredoxin - a fold for all reasons. Structure, 3, 245-250 (1995).
20. Jeng, M.F., Campbell, A.P., Begley, T., Holmgren, A., Case, D.A., Wright, P.E. & Dyson, H.J. High-resolution solution structures of oxidized and reduced Escherichia coli thioredoxin. Structure 2, 853-858, (1994).
21. Holmgren, A., Lu, J. Thioredoxin and thioredoxin reductase: Current research with special reference to human disease. A. Biochem. and Biophys. Res. Comm. 396, 120–124 (2010).
22. Ferrar, D. and Soelin, H. The protein disulphide-isomerase family : unravelling a string of folds. Biochem. J. 339, (1999).
23. Witte, S., Villalba, M., Bi, K., Liu, Y., Isakov, N., and Altman, A.. Inhibition of the c-Jun N- terminal Kinase/AP-1 and NF-kB Pathways by PICOT, a Novel Protein Kinase C-interacting Protein with a Thioredoxin Homology Domain. J. Biol. Chem., 275, 1902–1909, (2000).
24. Vizuete, A., Gustafsson, J., and Spyrou, G. Molecular Cloning and Expression of a cDNA Encoding a Human Thioredoxin-like Protein. Biochem. and Bioph. R. Comm. 243, 284–288 (1998).
25. Lee, K., Murakawa, M., Takahashi, S., Tsubuki, S., Kawashima, S., Sakamaki, K., and Yonehara, S. Purification, Molecular Cloning, and Characterization of TRP32, a Novel Thioredoxin-related Mammalian Protein of 32 kDa. J. Biol. Chem., 273, 19160–19166, (1998).
26. Kurooka, H., Kato,K., Minogushi, S., Takahachi, Y., Ikeda, J., Habu, S., Osawa, N., Buchberg, A, Moriwaki, K., Shisha, H., and Honjo, T. Cloning and Characterization of the Nucleoredoxin Gene That Encodes a Novel Nuclear Protein Related to Thioredoxin. GENOMICS, 39, 331–339 (1997).

27. Holmgren, A. Enzymatic reduction-oxidation of protein disulfides by thioredoxin. Methods Enzymol. 107, 295-300, (1984).
28. Stewart, E., Åslund, F., and Beckwith, J.. Disulfide bond formation in the Escherichia coli cytoplasm: an in vivo role reversal for the thioredoxins. J. EMBO, 17, 5543–5550, (1998).
29. Kang, S., Chae, H., Seo, M., Kim, K., Baines, I., and Rhee, S. Mammalian Peroxiredoxin Isoforms Can Reduce Hydrogen Peroxide Generated in Response to Growth Factors and Tumor Necrosis Factor-α. J. Biol. Chem., 273, 6297–6302, (1998).
30. Huber, H., Tabor, S., and Richardson, C. Escherichia coli Thioredoxin Stabilizes Complexes of Bacteriophage T7 DNA Polymerase and Primed Templates. J. Biol. Chem., 262, 16224-16232 (1987).
31. Russel, M. and Model, P. The Role of Thioredoxin in Filamentous Phage Assembly; CONSTRUCTION, ISOLATION, AND CHARACTERIZATION OF MUTANT THIOREDOXINS. J. Biol. Chem., 261, 14997-15005 (1986).
32. Saitoh, M., Nishitoh, H., Fujii, M., Takeda, K., Tobiume, K., Sawada, Y., Kawabata, M., Miyazono, K. and Ichijo, H. Mammalian thioredoxin is a direct inhibitor of apoptosis signal-regulating kinase (ASK) 1. J. EMBO, 17, 2596–2606, (1998)
33. Hayashi, T., Uno, Y., and Kamoto, T. Oxidoreductive Regulation of Nuclear Factor k B; INVOLVEMENT OF A CELLULAR REDUCING CATALYST THIOREDOXIN. J. Biol. Chem., 268, 11380-11388 (1993).
34. Nakamura, H., Nakamura, K. and Yodoi, J. Redox regulation of cellular activation. Annu. Rev. Immunol., 15, 351-369, (1997).
35. Zhang, P., Liu, B., Kang, S., Seo, M., Rhee, S., and Obeid, L. Thioredoxin Peroxidase Is aNovel Inhibitor of Apoptosis with a Mechanism Distinct from That of Bcl-2. J. Biol. Chem., 272, 30615–30618 (1997).
36. Rubartelli, A., Bajetto, A., Allavena, G., Wollman, E., and Sitia, R.. Secretion of Thioredoxin by Normal and Neoplastic Cells through a Leaderless Secretory Pathway. J. Biol. Chem., 267, 24161-24164 (1992).
37. Wakasugi, N., Tagaya, Y., Wakasugi, H., Mitsui, A., Maeda, M., Yodoi, J., and Tursz, T. Adult T-cell leukemia-derived factor/thioredoxin, produced by both human T-lymphotropic virus typeI-and Epstein-Barr virustransformed lymphocytes, acts as an autocrine growth factor and synergizes with interleukin 1 and interleukin 2. Proc. Nadl. Acad. Sci., 87, 8282-8286, (1990).
38. Gasdaska, P.Y., Oblong, J.E., Cotgreave, I.A. and Powis, G. The predicted amino acid sequence of human thioredoxin is identical to that of the autocrine growth factor human adult T-cell derived factor (ADF): thioredoxin mRNA is elevated in some human tumors. Biochem. Biophys. Acta.,1218,292-296 (1994).
39. Rubartelli, A., Bonifaci, N. and Sitia, R. High Rates of Thioredoxin Secretion Correlate with Growth Arrest in Hepatoma Cells. Cancer Res., 55, 675-680, (1995).
40. Yoshida, S., Katoh, T., Tetsuka, T., Uno, K., Matsui, N. and Okamoto, T. Involvement of Thioredoxin in Rheumatoid Arthritis: Its Costimulatory Roles in the TNF-a-Induced Production of IL-6 and IL-8 from Cultured Synovial Fibroblasts. J. Immunol., 163, 351-358, (1999).
41. Nakamura, H., Vaage, J., Valen, G., Padilla, C.A., BjoÈrnstedt, M. and Holmgren, M. Measurements of plasma glutaredoxin and thioredoxin in healthy volunteers and during open-heart surgery. Free Radic Biol. Med., 24, 1176-1186 (1998).
42. Nakamura, H., Rosa, S., Roederer, M., Anderson, M., Dubs, J., Yodoi, J., Holmgren, A., Herzenberg, L., and Herzenberg, L. Elevation of plasma thioredoxin levels in HIV-infected individuals. Int. Imm., 8, 603-611 (1996).
43. Schenk, H., Vogt, M., DroÈge, W. and Schulze-Osthof, K. Thioredoxin as a potent costimulus of cytokine expression. J. Immunol., 156, 765-771 (1996).
44. Bertini, R., Howard, O., Dong, H., Oppenheim, J., Bizzarri, C., Sergi, R., Caselli, G., Pagliei, S.,Romines, B, Wilshire, J., Mengozzi, M., Nakamura, H., Yodoi, J., Pekkari, K., Gurunath, R., Holmgren, A., Herzenberg, L., Herzenberg, L., and Ghezzi, P. Thioredoxin, a Redox Enzyme Released in Infection and Inflammation, Is a Unique Chemoattractant for Neutrophils, Monocytes, and T Cells. J. Exp. Med., 189, 1783–1789 (1999).
45. Sahaf, B., Soderberg, A., Spyrou, G.,Barral, A., Pekkari, K.,Holmgren, A., and Rosen, A. Thioredoxin Expression and Localization in Human Cell Lines: Detection of Full-Length and Truncated Species. Exp. Cell Res., 236, 181–192, (1997).
46. Silberstein, D., McDonough, S., Minkoff, M, and Balcewicz-Sablinska, M. Human Eosinophil Cytotoxicity-enhancing Factor; EOSINOPHIL-STIMULATING AND DITHIOL REDUCTASE ACTIVITIES OF BIOSYNTHETIC (RECOMBINANT) SPECIES WITH COOH-TERMINAL DELETIONS. J. Biol. Chem., 268, 9138-9142 (1993).
47. Lenzi, H.L., Mednis, A.D. & Dessein, A.J. Activation of human eosinophils by monokines and

lymphokines: source and biochemical characteristics of the eosinophil cytotoxicity-enhancing activity produced by blood mononuclear cells. Cell Immunol. 94, 333-346 (1985).
48. Dai, s., Schwendtmayer, C., Schurmann, P., Ramaswamy, S., Eklund, H. Redox Signaling in Chloroplasts: Cleavage of DisulÞdes by an Iron-Sulfur Cluster. Science, 287, 655, (2000).
49. Meng, L., Wong, J., Feldman, L., Lemaux, P., and Buchanan, B. A membrane-associated thioredoxin required for plant growth moves from cell to cell, suggestive of a role in intercellular communication. PNAS, 107, 3900–3905 (2010).
50. Buchanan, B. Thioredoxin: A Multifunctional Regulatory Protein with a Bright Future in Technology & Medicine. Arch. Biochem. & Biophys. , 257-260 (1994).
51. Whitman, W.B., Coleman, D.C. & Wiebe, W.J. Prokaryotes: the unseen majority. Proc Natl Acad Sci., **95**, 6578-83 (1998)
52. Singh, J., Behal, A., Singla, N., Joshi, A., et al., Metagenomics: Concept, methodology, ecological inference and recent advances. Biotechnology Journal, 4, 480-494 (2009).
53. Huse, S. M., Dethlefsen, L., Huber, J. A., Mark Welch, D., et al., Exploring microbial diversity and taxonomy using SSU rRNA hypervariable tag sequencing. PLoS Genet, 4, e1000255 (2008).
54. Qin, J. et al. A human gut microbial gene catalogue established by metagenomic sequencing. Nature **464**, 59-65 (2010).
55. Sleator, R.D., Shortall, C. & Hill, C. Metagenomics. Letters in applied microbiology **47**, 361-366 (2008).
56. Handelsman, J., Rondon, M. R., Brady, S. F., Clardy, J., Goodman, R. M., Molecular biological access to the chemistry of unknown soil microbes: a new frontier for natural products. Chemistry & biology, 5, R245-R249 (1998).
57.Giovannoni, S.J., Britschgi, T.B., Moyer, C.L. & Field, K.G. Genetic diversity in Sargasso Sea bacterioplankton. Nature **345**, 60-3 (1990).
58.Schmidt, T.M., DeLong, E.F. & Pace, N.R. Analysis of a marine picoplankton community by 16S rRNA gene cloning and sequencing. J Bacteriol **173**, 4371-8 (1991)
59.Nyrén, P. The History of Pyrosequencing. Methods Mol Biology, 373, 1–14 (2007).
60.Schmeisser C., Steele H. & Streit W. R. Metagenomics, biotechnology with non-culturable microbes. Applied Microbiology and Biotechnology **75**, 955–962 (2007).
61.Steele H. L., Jaeger K. E., Daniel R & Streit W. R. Advances in Recovery of Novel Biocatalysts from Metagenomes. Journal of Molecular Microbiology and Biotechnology **16**, 25-37 (2009).
62.Guazzaroni M. E. et al. in Handbook of Hydrocarbon and Lipid Microbiology 2911-2927 (Springer-Verlag Berlin Heidelberg (2010).
63. Fukuchi, S., et al., Unique amino acid composition of proteins in halophilic bacteria. J Mol Biol,. 327(2): 347-57 (2003).
64.Vieille, C. and G.J. Zeikus, Hyperthermophilic enzymes: sources, uses, and molecular mechanisms for thermostability. Microbiol Mol Biol Rev. 65(1):1-43 (2001).
65.Berezovsky, I.N. and E.I. Shakhnovich, Physics and evolution of thermophilic adaptation. Proc Natl Acad Sci U S A.,102(36): 12742-7 (2005).
66.Vetriani, C., et al., Protein thermostability above 100 degreesC: a key role for ionic interactions. Proc Natl Acad Sci U S A, 95(21): 12300-5 (1998).
67.Fukuchi, S. and K. Nishikawa, Protein surface amino acid compositions distinctively differ between thermophilic and mesophilic bacteria. Journal of Molecular Biology, 309(4): 835-843 (2001).
68.Bosshard, H.R., D.N. Marti, and I. Jelesarov, Protein stabilization by salt bridges: concepts, experimental approaches and clarification of some misunderstandings. J Mol Recognit, 17(1): 1-16 (2004).
69.Brandon, C., and J. Tooze, Introduction to Protein Structure. 2nd ed. 1991, New York/London: Garland Publishing Inc.
70.Dressler, D., and H. Potter, Discovering Enzymes. 1991, New York/Oxford: W. H. Freeman, Scientific American Library.
71.Paul, S., Bag, S. K., Das, S., Harvill, E. T., Dutta, C., Molecular signature of hypersaline adaptation: insights from genome and proteome composition of halophilic prokaryotes. Genome Biol, 9, R70 (2008).
72.Oren, A., Microbial life at high salt concentrations: phylogenetic and metabolic diversity. Saline systems, 4, 1-13 (2008).
73.Siglioccolo, A., Paiardini, A., Piscitelli, M., Pascarella, S., Structural adaptation of extreme halophilic proteins through decrease of conserved hydrophobic contact surface. BMC Struct Biol, 11, 50 (2011).

74.Nakamura H, Hoshino Y, Okuyama H, Matsuo Y, Yodoi J. Thioredoxin 1 delivery as new therapeutics. Adv Drug Deliv Rev., 61(4):303-9 (2009).
75.http://www.qiagen.com/products/catalog/sample-technologies/dna-sample-technologies/genomic-dna/repli-g-mini-kit#productdetails
76.Sambrook J, Russel DW (2001). Molecular Cloning: A Laboratory Manual 3rd Ed. Cold Spring Harbor Laboratory Press. Cold Spring Harbor, NY.
77.Higgins, D.G., Bleasby, A.J. and Fuchs, R. (1992) CLUSTAL V: improved software for multiple sequence alignment. Computer Applications in the Biosciences (CABIOS), 8(2):189-191.
78.Thompson J.D., Higgins D.G., Gibson T.J. "CLUSTAL W: improving the sensitivity of progressive multiple sequence alignment through sequence weighting, position-specific gap penalties and weight matrix choice." Nucleic Acids Res. 22:4673- 4680(1994).
79.Rath, Arianna and Glibowicka, Mira and Nadeau, Vincent G. and Chen, Gong and Deber, Charles M. Detergent binding explains anomalous SDS-PAGE migration of membrane proteins". Proceedings of the National Academy of Sciences 106 (6): 1760–1765(2009).
80.Bell GI, Pictet RL, Rutter WJ, Cordell B, Tischer E, Goodman HM. Sequence of the human insulin gene. Nature 284 (5751):26–32 (1980).
81. Mosmann, Tim. Rapid colorimetric assay for cellular growth and survival: application to proliferation and cytotoxicity assays. Journal of Immunological Methods 65 (1–2): 55–63 (1983).
82. Holmgren A, Bjo¨ rnstedt M. Thioredoxin and thioredoxin reductase.Meth Enzymol 252: 199–208 (1995).
83. Sung-Jong Jeon and Kazuhiko Ishikawa. Identification and characterization of thioredoxin and thioredoxin reductase from Aeropyrum pernix K. Eur. J. Biochem. 269, 5423–5430 (2002).
84.Hassouni, M.E., Chambost, J.P., Expert, D., Van Gijsegem, F. & Barras, F. The minimal gene set member msrA, encoding peptide methionine sulfoxide reductase, is a virulence determinant of the plant pathogen Erwinia chrysanthemi. Proc. Natl Acad. Sci. , 96, 887-892 (1999).
85.Brot, N. & Weissbach, H. Biochemistry of methionine sulfoxide residues in proteins. Biofactors, 3, 91-96 (1991).
86.Chae, H.Z., Kang, S.W. & Rhee, S.G. Isoforms of mammalian peroxiredoxin that reduce peroxides in presence of thioredoxin. Methods Enzymol. 300, 219-226 (1999).
87.Lillig, C.H., Prior, A., Schwenn, J.D., A Ê slund, F., Ritz, D., Vlamis-Gardikas, A. & Holmgren, A. New thioredoxins and glutaredoxins as electron donors of 30-phosphoadenylsulfate reductase. J. Biol.Chem. 274, 7695-7698 (1999).
88.Schwenn, J.D., Krone, F.A. & Husmann, K. Yeast PAPS reductase: properties and requirements of the purified enzyme. Arch. Microbiol. 150, 313-319 (1988).
89.Feng, J.N., Model, P. & Russel, M. A trans-envelope protein complex needed for filamentous phage assembly and export. Mol.Microbiol. 34, 745-755 (1999).
90.Huber, H.E., Tabor, S. & Richardson, C.C. Escherichia coli thioredoxin stabilizes complexes of bacteriophage T7 DNA polymerase and primed templates. J. Biol. Chem. 262, 16224-16232 (1987).
91.Buchanan, B.B. Regulation of CO2 assimilation in oxygenic photosynthesis: the ferredoxin/thioredoxin system. Perspective on its discovery, present status, and future development. Arch. Biochem. Biophys. 288, 1-9 (1991).
92.Matsui, M., Oshima, M., Oshima, H., Takaku, K., Maruyama, T., Yodoi, J. & Taketo, M.M. Early embryonic lethality caused by targeted disruption of the mouse thioredoxin gene. Dev. Biol.178, 179-185 (1996).
93.Goto, Y., Noda, Y., Narimoto, K., Umaoka, Y. & Mori, T. Oxidative stress on mouse embryo development in vitro. Free Radic. Biol. Med. 13, 47-53 (1992).
94. Di Trapani, G., Perkins, A. & Clarke, F. Production and secretion of thioredoxin from transformed human trophoblast cells. Mol. Hum. Reprod. 4, 369-375 (1998).
95.Hori, K., Katayama, M., Sato, N., Ishii, K., Waga, S. & Yodoi, J. Neuroprotection by glial cells through adult T cell leukemia-derived factor/human thioredoxin (ADF/TRX). Brain Res. 652, 304-310 (1994).
96.Das, K.C., Guo, X.L. & White, C.W. Induction of thioredoxin and thioredoxin reductase gene expression in lungs of newborn primates by oxygen. Am. J. Physiol. 276, 530-539 (1999).
97.Schenk, H., Klein, M., Erdbrugger, W., Droge, W. & Schulze-Osthoff, K. Distinct effects of thioredoxin and antioxidants on the activation of transcription factors NF-kappa B and AP-1. Proc. Natl Acad. Sci. 91, 1672-1676 (1994).
98. Stephen F. Altschul, Thomas L. Madden, Alejandro A. Schäffer, Jinghui Zhang, Zheng Zhang, Webb Miller, and David J.Lipman, "Gapped BLAST and PSI-BLAST: a new generation of protein database search programs", Nucleic Acids Res. (1997).